The DIONESUS algorithm provides scalable and accurate reconstruction of dynamic phosphoproteomic networks to reveal new drug targets: Supplement

Mark F. Ciaccio, Vincent C. Chen, Richard B. Jones, and Neda Bagheri

May 5, 2015

Extended Notes

List of Figures

1 Supplementary Notes

1.1 Phosphorylation kinetics, together with cell viability, inform modeling of information flow downstream of EGFR.

The first set of perturbations consisted of a panel of growth factors alone and in combination: EGF (200 ng/mL), EGF (200 ng/ml) + Insulin (200 ng/mL), HGF (200 ng/mL), HGF (200 ng/mL) + insulin (200 ng/mL), insulin (200 ng/mL), IGF (200 ng/mL), and media alone control. Phosphorylation abundances were measured at -30 min prior to stimulation, at the time of stimulation (0 min), and 5 and 15 min following stimulation. The fold changes were assessed by dividing each time point by the abundance at -30 min. For a positive control to measure the specificity of stimulation, we quantified the conjugate receptor for each perturbant (EGFR for EGF, c-MET for HGF, Insulin receptor for insulin, and IGFR receptor for IGF). Despite a higher level of EGFR expression relative to the other RTKs, each stimulation showed a strong and unique phosphorylation signature (**Supplementary Figs. 2 and 8a**). EGF stimulation preferentially phosphorylated SRC-family kinase (SFK) substrates, STAT proteins, and PLCγ/calcium associated proteins, but had little change in the AKT/survival pathway. IGF, HGF, and insulin contributed strongly to the activation of the survival pathway. IGF caused an increased activation of p-S6 Ribosomal Protein and p-PKCG(PAN), both known to be important mediators of translational regulation and cell growth.[1] We displayed the data from this set as a clustergram of fold changes in phosphorylation (minus the media-alone results) to show the common and specific subgroups that are regulated by each perturbation. EGF stimulation caused a strong reduction in cell viability(35.1$\pm$3.9% of media control), Insulin and IGF caused a minor decrease (70.2$\pm$1.8% and 78.9$\pm$0.8%), and HGF showed little change (92.0$\pm$9.4%) (**Supplementary Fig. 8b**). Only the combination of HGF and insulin caused an increase in cell viability (110.5$\pm$1.5%) relative to the media control, suggesting additivity of the survival signals downstream of these receptors. Insulin in combination with EGF did not rescue the decrease in cell viability from EGF-alone (33.0$\pm$34.6%), suggesting the predominance of negative mediators of cell viability downstream of EGFR after stimulation with this concentration of growth factor.

We chose the first set of small-molecule inhibitors to block major pathways downstream of the EGF receptor. As shown in the first experiment, the PLCγ proteins, the PI3K pathways, and the SRC-family kinase pathways showed significant phosphorylation after EGF stimulation. The secondary signaling molecules are known to be major binders of the phosphorylated tyrosines on RTKs though their SH2- domains.[2] For these reasons, we hypothesized that these nodes controlled major downstream mediators of the EGF signaling and that their specific inhibition would elucidate the downstream pathways that contribute positively and negatively to cell viability. To test this, we stimulated cells with 200 ng/mL EGF in conjunction with 10 µM PP2 (SRC Family Kinase Inhibitor), 10 µM U73122 (PLCγ1/2 inhibitor), and 10 µM Wortmannin (PI3K inhibitor), along with EGF-only and media-only controls. We added inhibitors 30 minutes before the application of EGF to allow significant inhibitory activity to occur before stimulation and to assess the effect of the inhibitor alone on phosphorylation. The time of application of the inhibitors was designated as -30 mins, while time 0 mins was designated as the time of EGF application. We measured additional time points at 5 and 15 mins after stimulation and assayed for changes in phosphorylation by the MWA (**Supplementary Figs. 3 and 9a**).

We found that PP2 completely attenuated phosphorylation of p-STAT1(Y701), p-PYK(Y402), p-P38(T180/Y182), and p-ERK(T202/Y204). It also decreased survival-associated phosphoproteins such as p-AKT(S473). Both wortmannin and U73122 caused a major decrease in AKT substrates p-GAB2(S159) and p-RAF(S338), and cell-cycle protein p-CDK2(T160). Surprisingly, there was

an increase in the amplitude and duration of p-P38(T180/Y182) and p-JNK(T183/Y182). While 200 ng/mL EGF with wortmannin, and EGF with U73122, caused a decrease in cell viability (28.1±1.3% and 15.1±0.4%, respectively) in comparison to EGF-only (32.9±8.2%), application of PP2 caused a complete attenuation of EGF-stimulated cell death (97.3±10.5%) (**Supplementary Fig. 9b**).

1.1.1 Autocrine signaling alters carcinogenic pathways in A431 cells.

Autocrine signaling has been reported to cause cross-phosphorylation of receptor tyrosine kinases in A431 cells.[3] A panel of sheddase inhibitors (aprotinin, GM6001, and TAPI1) also reported to be effective in surveying autocrine signaling in A431 cells[4] was used in conjunction with EGF stimulation. We hypothesized that sheddases could mediate the EGFR-induced RTK cross-phosphorylation. 1 ug/mL aprotinin (a plasmin and general serine protease inhibitor), 25 µM GM6001 (a broad-range metalloprotease inhibitor), and 100 µM TAPI1 (a TACE inhibitor) were applied before 200 ng/mL EGF stimulation and the phosphorylation kinetics were assayed by MWA (**Supplementary Figs. 4 and 10a**). Aprotinin showed a major increase in phosphorylation of p-INS/IGF1R(Y1134/1135), p-PKCG(PAN)(T514), p-P70S6 Ribosomal Kinase(T421/S422), and p-S6 Ribosomal Protein(S240/244) at 0 min. These proteins match the profile of those stimulated by IGF, suggesting that aprotinin inhibits the cleavage of an IGF binding protein. GM6001 and TAPI1 showed a significant delay in p-INS/IGF1R(Y1134/1135) phosphorylation as well as the reduction in phosphorylation of many known downstream mediators in the IGF-pathway including p-AKT(S473), p-GAB2(S159), and p-RAF(S259). Aprotinin treatment did not cause a change in cell viability (30.24±9.88%) in comparison to 200 ng/mL EGF alone (32.88±8.18%), while GM6001 and TAPI1 showed almost complete loss of cell viability (12.25±8.25% and 2.48±2.48%) (**Supplementary Fig. 10b**). Together, these results suggest that autocrine signaling is a key mediator of cell viability in these cancer cell lines and that phosphorylation profiles of RTK and downstream targets are modified by inhibition of these pathways. Autocrine signaling may be one means by which a cancer cell overexpressing EGFR can activate multiple pathways leading to carcinogenic behavior.

1.1.2 Distinct antioxidants demonstrate positive and negative influences on A431 cell viability.

Reactive Oxygen Species (ROS) and its inhibition of phosphatase activity has been shown to be important in EGF-induced RTK cross-phosphorylation in A431 cells.[5] To survey the contribution of ROS, A431 cells were treated with the antioxidant panel, 100 µM Epigallactocatechin Gallate (EGCG),10 µM Caffeic Acid Phenylethyl Ester (CAPE), and 30 mM N-acetylcysteine (N-ac) 30 minutes prior to EGF stimulation (**Supplementary Figs. 5 and 11a**). All antioxidants that caused a common down-regulation of the PI3K/AKT pathway included p-INS/IGFR(Y1134/1135), suggesting that much of the impact of ROS is mediated through this receptor. EGCG specifically caused A431 cells to become insensitive to EGF stimulation. EGCG also caused significant and specific increase in the phosphorylation of P38, JNK, and IGFR, with a total loss of cell viability (**Supplementary Fig. 11b**). Since EGCG had zero viability and a phosphorylation profile divorced from other perturbations, it was excluded from the final PLSR analysis. In addition to suppressing the AKT-pathway, CAPE caused a specific decrease in the phosphorylation of p-CDK2(T160) with a strong decrease in cell viability (3.60±3.20%). N-ac caused a decrease in the survival pathway but an increase in the MEK/ERK pathway, resulting in a net increase in cell viability (58.21±15.15%) in comparison to EGF alone (37.52±20.72%). In summary, antioxidants decreased the AKT pathway, but they had variable effects on other cell pathways and increased or decreased viability of the

cancer cells, suggesting that antioxidant effect alone is probably insufficient as a general treatment in this cancer model.

1.1.3 Reactive oxygen species affects cell receptor cross-phosphorylation.

Stimulation of A431 cells was reported to cause inactivation of protein-tyrosine phosphatase 1B through the release of reactive oxygen species.[6] We therefore chose the fourth and fifth panels of inhibitors to study how ROS release affects cross-phosphorylation (**Supplementary Figs. 6,7,12,13**). Studies have shown expression of NADPH Oxidase in A431 cells and its stimulation by EGF to produce ROS[5]. Therefore, two concentrations (10 µM and 25 µM) of the NADPH oxidase inhibitor, Diphenyleneiodonium chloride (DPI), were used, along with an inhibitor of the regulatory subunit of the NADPH oxidase complex, inhibitor of RAC1 (2 ng/mL Clostridium Toxin B), and a PTP1B inhibitor, 25 µM EMBPTP1B1. As SHP2 is an SH2-domain containing phosphatase relating to the highest fold change after EGF stimulation [7], the SHP2 inhibitor, at 20 µM PHPS1, was used after EGF stimulation to observe its contribution to phosphokinetics and cell viability. Both concentrations of DPI showed no change in cell viability (10 µM = 31.69±9.74%; 25 µM = 26.35±3.85%) from EGF alone (29.36±3.77%). However, Clostridium Toxin demonstrated a decrease in viability (15.29±2.98%). The PTP1B inhibitor resulted in a slight decrease in cell viability (30.12±3.16%), whereas the SHP2 inhibitor showed a major decrease in cell viability (4.50±4.17%) with a very large increase in the fold change of STAT1 phosphorylation, suggesting that this phosphatase is a major mediator of the pro-apoptotic STAT1 phosphorylation and a possible target in a subset of cancers. Finally, the cells were stimulated with the SRC-inhibitor, PP2, at a lower concentration (200 nM) than in Inhibitor Set 1 to show greater specificity to the SRC Family Kinases. Again, we confirmed that this condition increased cell viability (44.29±3.60%), over EGF-stimulation alone, demonstrating that a subset of phosphosites downstream of Src-family kinases negatively contribute to cell viability in this cancer model.

References

[1] Dufner, A. & Thomas, G. Ribosomal s6 kinase signaling and the control of translation. Experimental Cell Research **253**, 100–109 (1999). URL `http://www.sciencedirect.com/science/article/pii/S0014482799946839`.

[2] Jones, R. B., Gordus, A., Krall, J. A. & MacBeath, G. A quantitative protein interaction network for the ErbB receptors using protein microarrays. Nature **439**, 168ï£¡174 (2006). URL `http://www.ncbi.nlm.nih.gov/pubmed/16273093`. PMID: 16273093.

[3] Shvartsman, S. Y. et al. Autocrine loops with positive feedback enable context-dependent cell signaling. American Journal of Physiology - Cell Physiology **282**, C545 –C559 (2002). URL `http://ajpcell.physiology.org/content/282/3/C545.abstract`.

[4] Roztocil, E., Nicholl, S. M. & Davies, M. G. Insulin-induced epidermal growth factor activation in vascular smooth muscle cells is ADAM-dependent. Surgery **144**, 245–251 (2008). URL `http://www.sciencedirect.com/science/article/pii/S0039606008001864`.

[5] Lou, Y. et al. Redox regulation of the protein tyrosine phosphatase PTP1B in cancer cells. The FEBS Journal **275**, 69âĂŞ88 (2008). URL `http://www.ncbi.nlm.nih.gov/pubmed/18067579`. PMID: 18067579.

[6] Lee, S., Kwon, K., Kim, S. & Rhee, S. G. Reversible inactivation of Protein-Tyrosine phosphatase 1B in a431 cells stimulated with epidermal growth factor. Journal of Biological Chemistry **273**, 15366–15372 (1998). URL `http://www.jbc.org/content/273/25/15366`.

[7] Ciaccio, M. F., Wagner, J. P., Chuu, C., Lauffenburger, D. A. & Jones, R. B. Systems analysis of EGF receptor signaling dynamics with microwestern arrays. Nature Methods **7**, 148–155 (2010). URL `http://www.ncbi.nlm.nih.gov/pubmed/20101245`. PMID: 20101245.

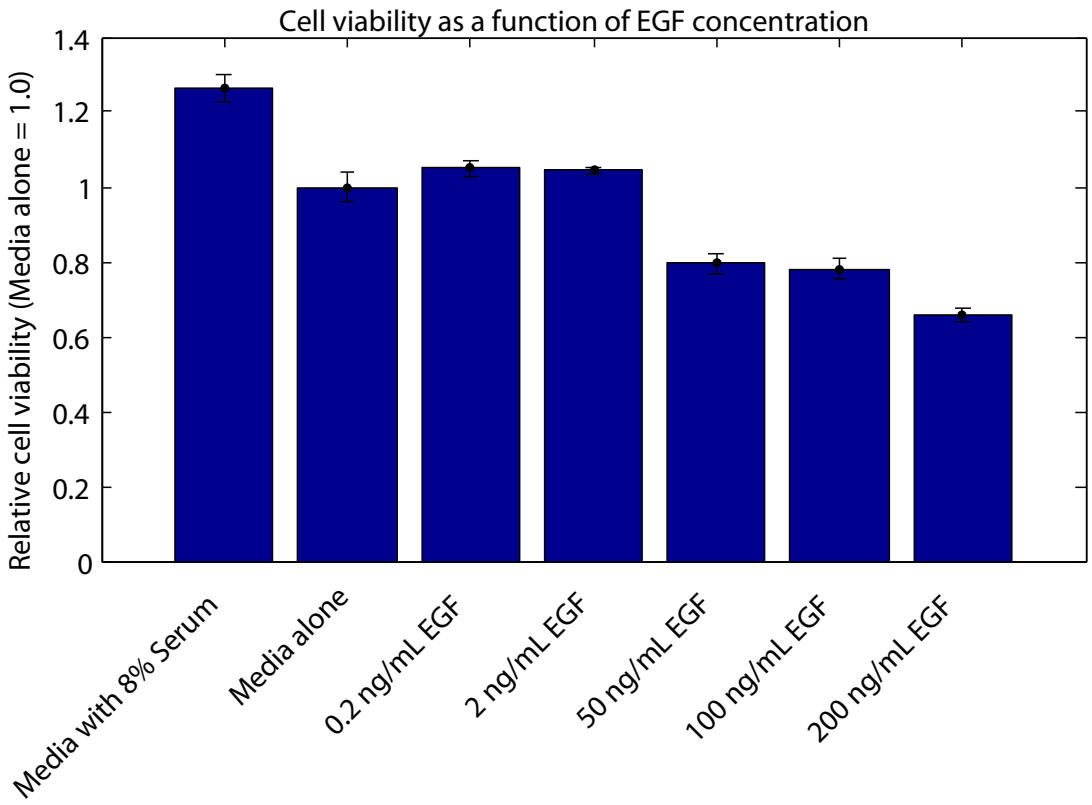

Figure 1: *Viability as a function of EGF concentration in A431 cells. Low concentrations increase cell viability in A431 cells after 24 hrs relative to media-alone stimulation while high concentrations of EGF induce a loss of cell viability.*

.

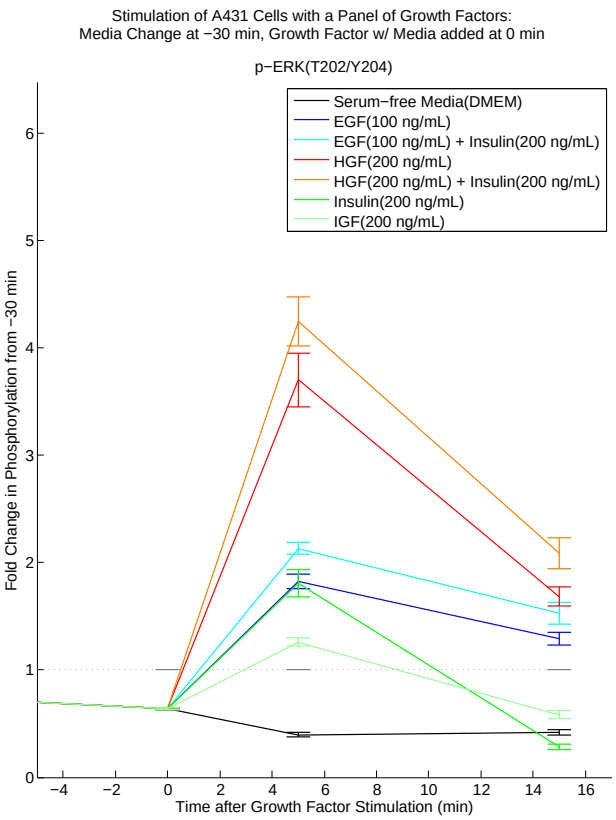

Figure 2: *Serial graphs of phosphorylation kinetics for Panel 1 of growth factors. Subsequent serial graphs are shown on the next 5 pages, where the x-axis reflects time (in minutes) and the y-axis reflects fold change relative to -30 minutes (A fold change of 1 reflects no change from -30 minutes)*

.

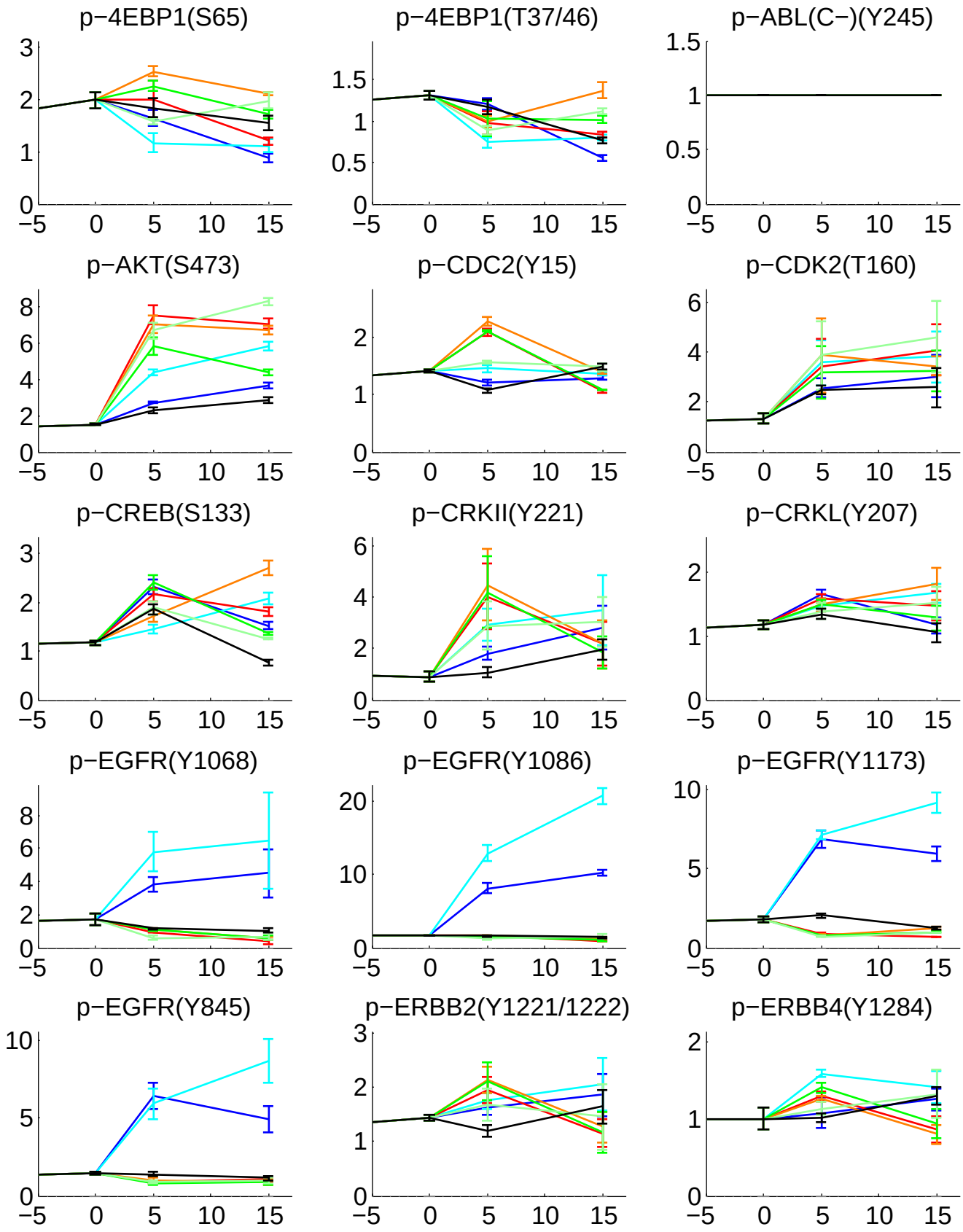
p−4EBP1(S65)
p−4EBP1(T37/46)
p−ABL(C−)(Y245)
p−AKT(S473)
p−CDC2(Y15)
p−CDK2(T160)
p−CREB(S133)
p−CRKII(Y221)
p−CRKL(Y207)
p−EGFR(Y1068)
p−EGFR(Y1086)
p−EGFR(Y1173)
p−EGFR(Y845)
p−ERBB2(Y1221/1222)
p−ERBB4(Y1284)

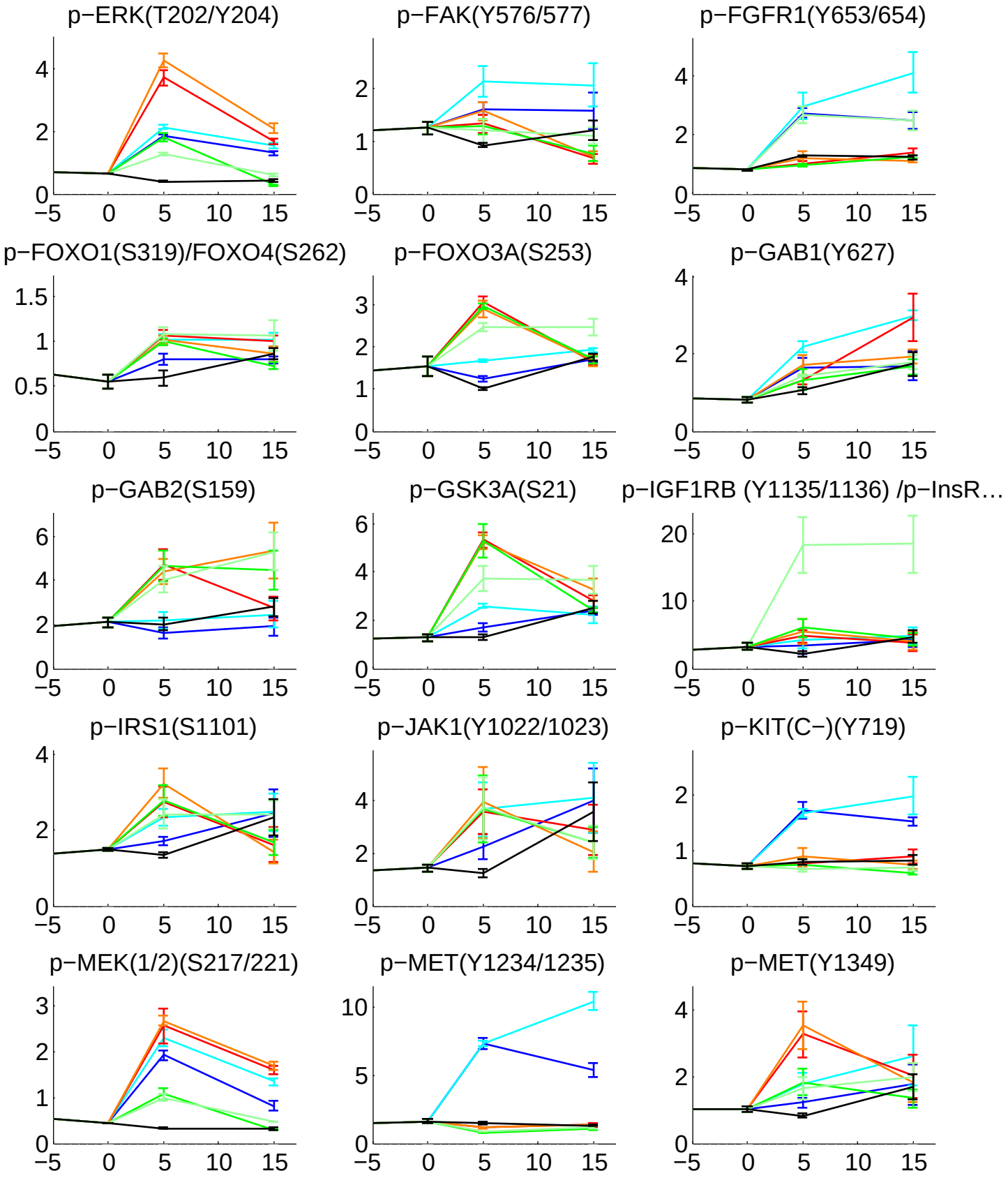
p−ERK(T202/Y204)
p−FAK(Y576/577)
p−FGFR1(Y653/654)
p−FOXO1(S319)/FOXO4(S262)
p−FOXO3A(S253)
p−GAB1(Y627)
p−GAB2(S159)
p−GSK3A(S21)
p−IGF1RB (Y1135/1136) /p−InsR…
p−IRS1(S1101)
p−JAK1(Y1022/1023)
p−KIT(C−)(Y719)
p−MEK(1/2)(S217/221)
p−MET(Y1234/1235)
p−MET(Y1349)

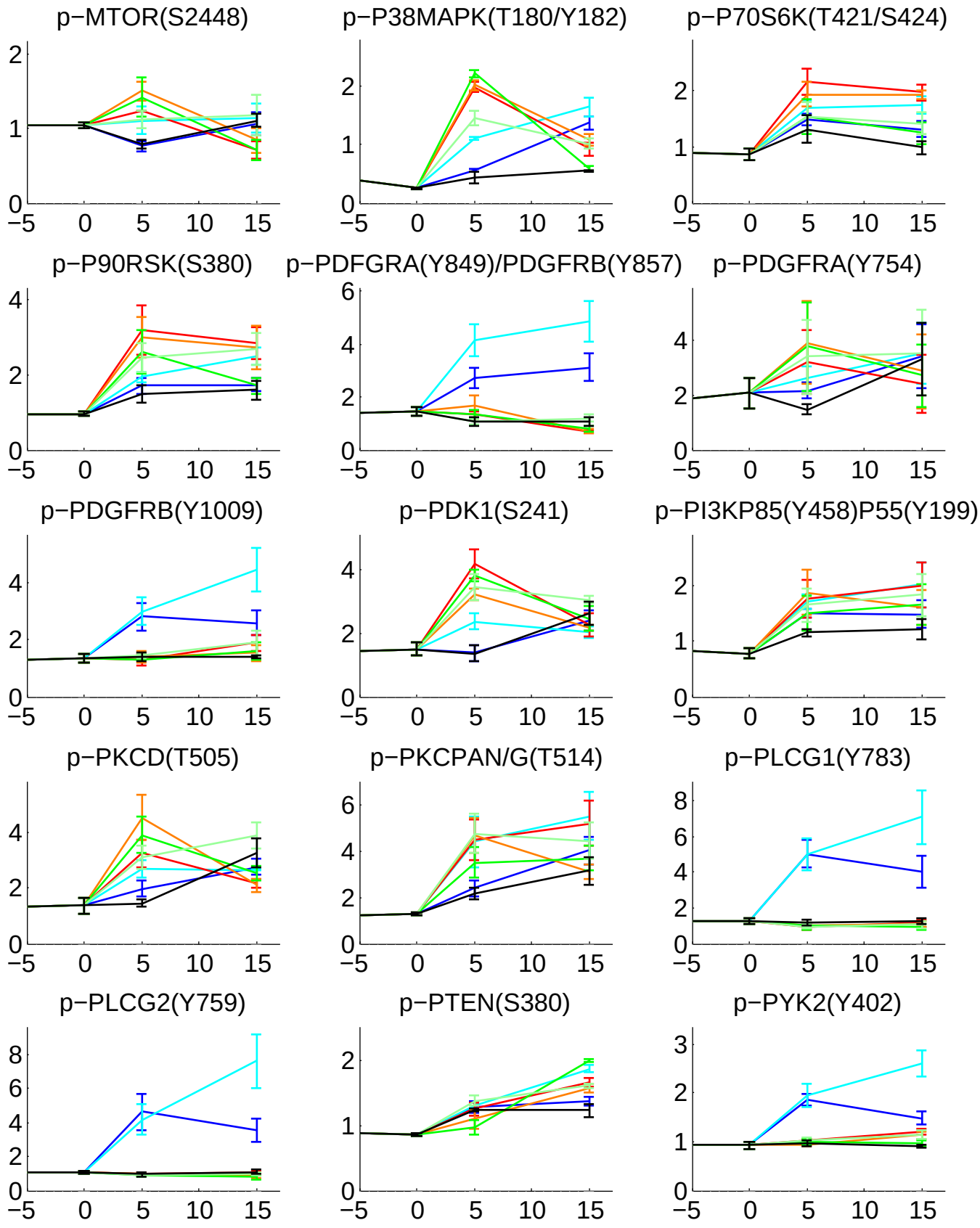
p−MTOR(S2448)
p−P38MAPK(T180/Y182)
p−P70S6K(T421/S424)
p−P90RSK(S380)
p−PDFGRA(Y849)/PDGFRB(Y857)
p−PDGFRA(Y754)
p−PDGFRB(Y1009)
p−PDK1(S241)
p−PI3KP85(Y458)P55(Y199)
p−PKCD(T505)
p−PKCPAN/G(T514)
p−PLCG1(Y783)
p−PLCG2(Y759)
p−PTEN(S380)
p−PYK2(Y402)

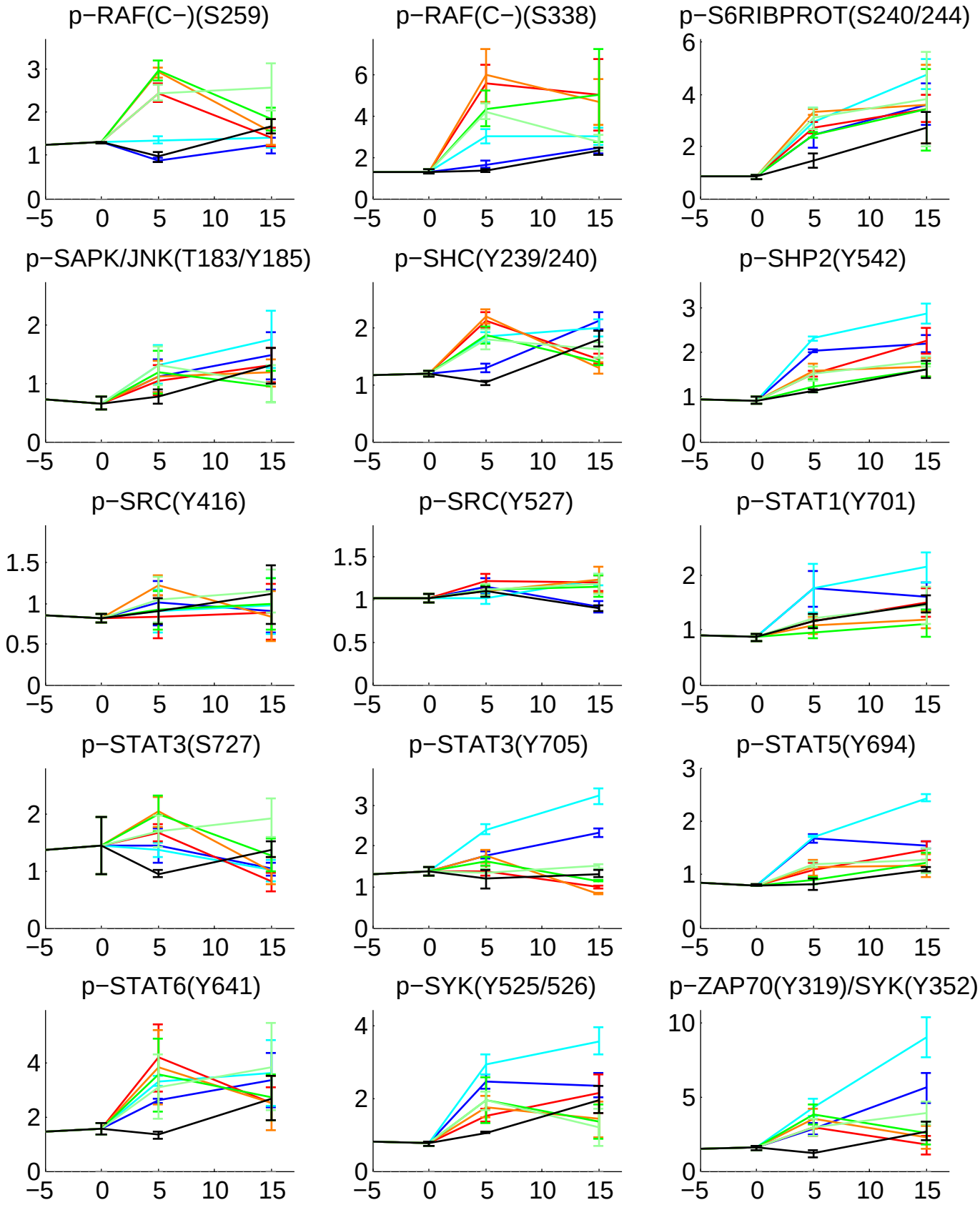
p−RAF(C−)(S259)
p−RAF(C−)(S338)
p−S6RIBPROT(S240/244)
p−SAPK/JNK(T183/Y185)
p−SHC(Y239/240)
p−SHP2(Y542)
p−SRC(Y416)
p−SRC(Y527)
p−STAT1(Y701)
p−STAT3(S727)
p−STAT3(Y705)
p−STAT5(Y694)
p−STAT6(Y641)
p−SYK(Y525/526)
p−ZAP70(Y319)/SYK(Y352)

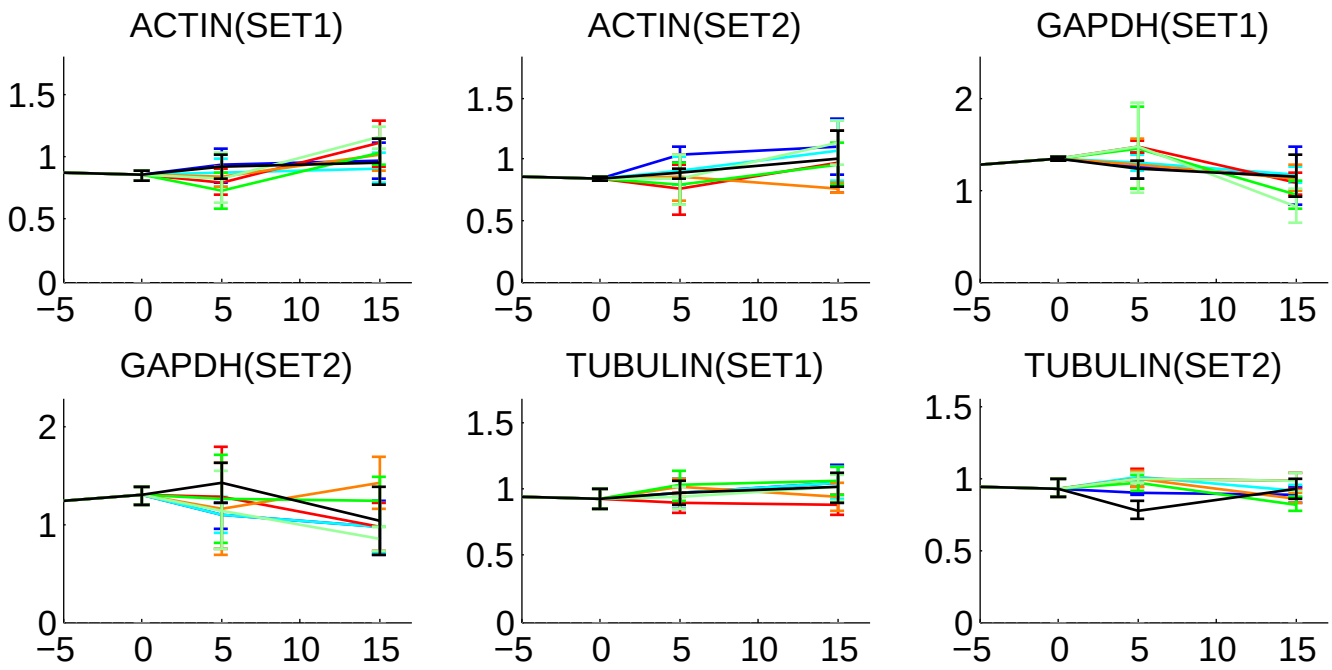
ACTIN(SET1)
ACTIN(SET2)
GAPDH(SET1)
GAPDH(SET2)
TUBULIN(SET1)
TUBULIN(SET2)
0
0.5
1
1.5
2
−5
0
5
10
15

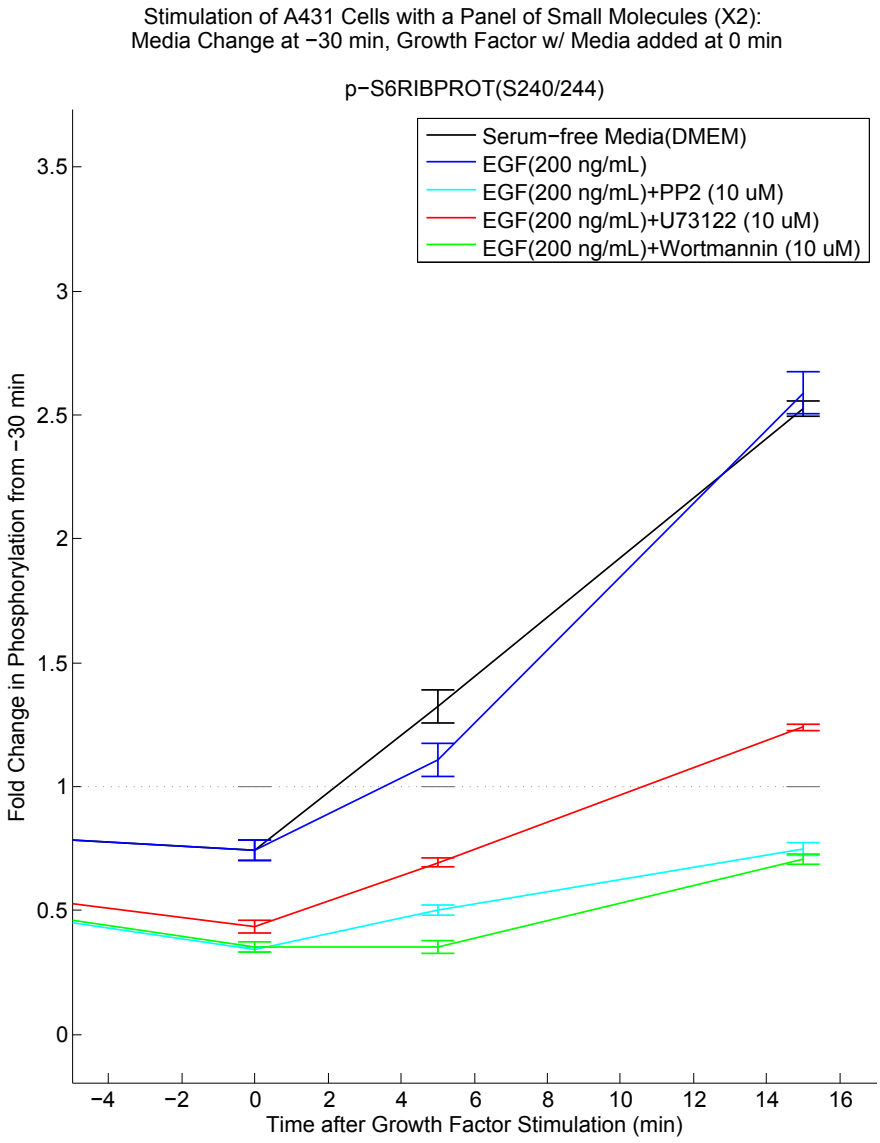

Figure 3: *Serial graphs of phosphorylation kinetics for Panel 2 of small molecules. Subsequent serial graphs are shown on the next 5 pages, where the x-axis reflects time (in minutes) and the y-axis reflects fold change relative to -30 minutes (A fold change of 1 reflects no change from -30 minutes).*

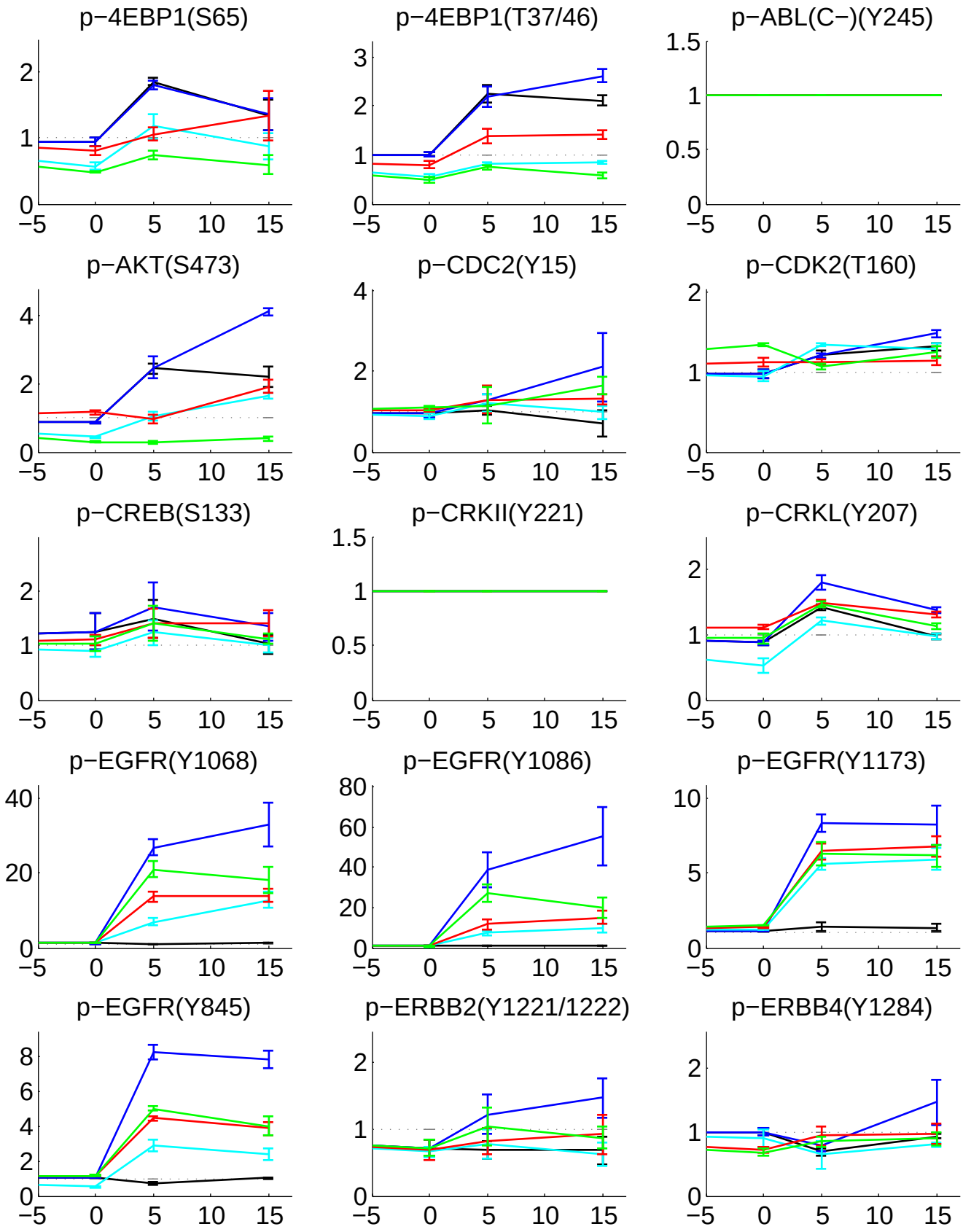
p−4EBP1(S65)
p−4EBP1(T37/46)
p−ABL(C−)(Y245)
p−AKT(S473)
p−CDC2(Y15)
p−CDK2(T160)
p−CREB(S133)
p−CRKII(Y221)
p−CRKL(Y207)
p−EGFR(Y1068)
p−EGFR(Y1086)
p−EGFR(Y1173)
p−EGFR(Y845)
p−ERBB2(Y1221/1222)
p−ERBB4(Y1284)

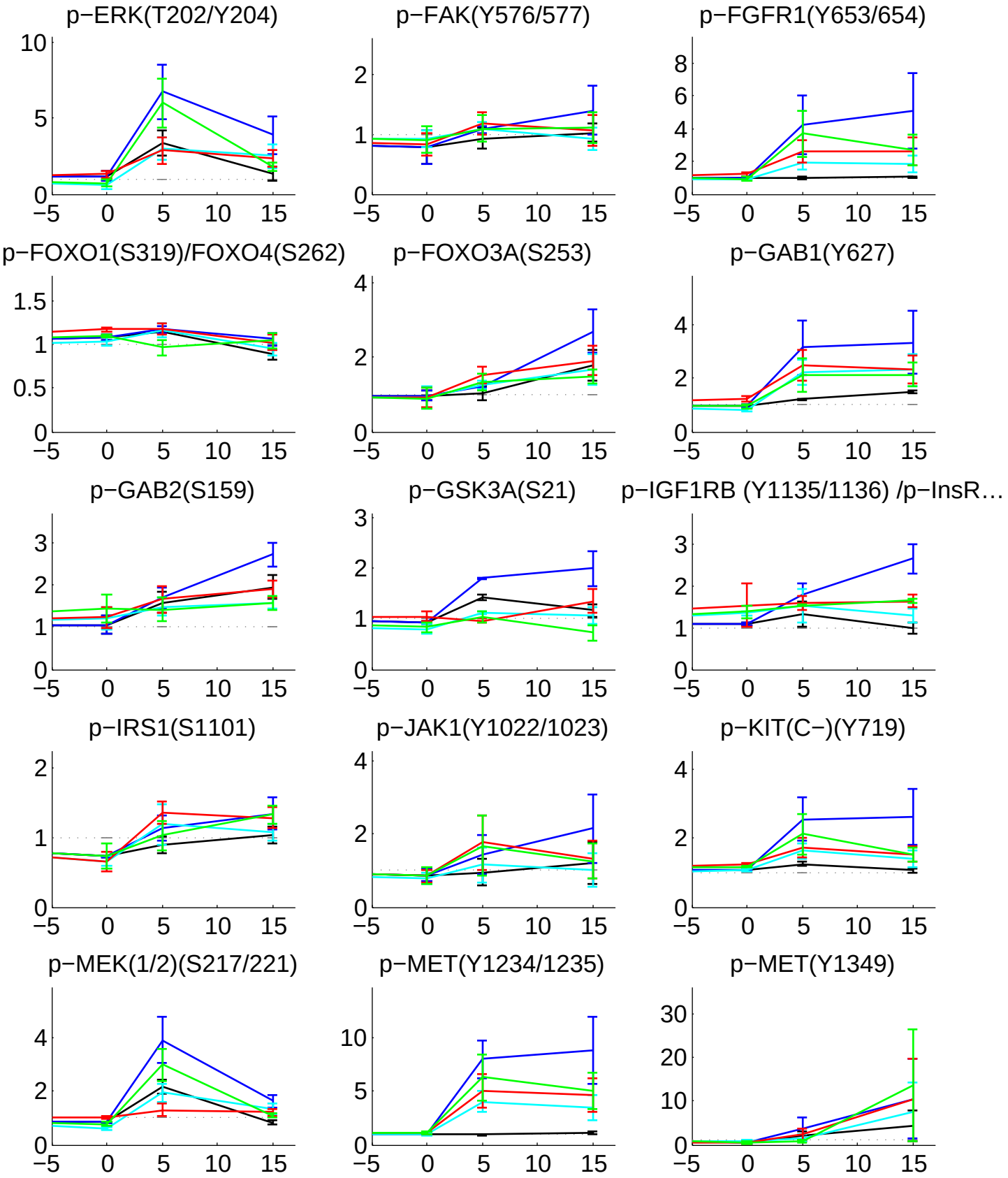
p−ERK(T202/Y204)
p−FAK(Y576/577)
p−FGFR1(Y653/654)
p−FOXO1(S319)/FOXO4(S262)
p−FOXO3A(S253)
p−GAB1(Y627)
p−GAB2(S159)
p−GSK3A(S21)
p−IGF1RB (Y1135/1136) /p−InsR…
p−IRS1(S1101)
p−JAK1(Y1022/1023)
p−KIT(C−)(Y719)
p−MEK(1/2)(S217/221)
p−MET(Y1234/1235)
p−MET(Y1349)

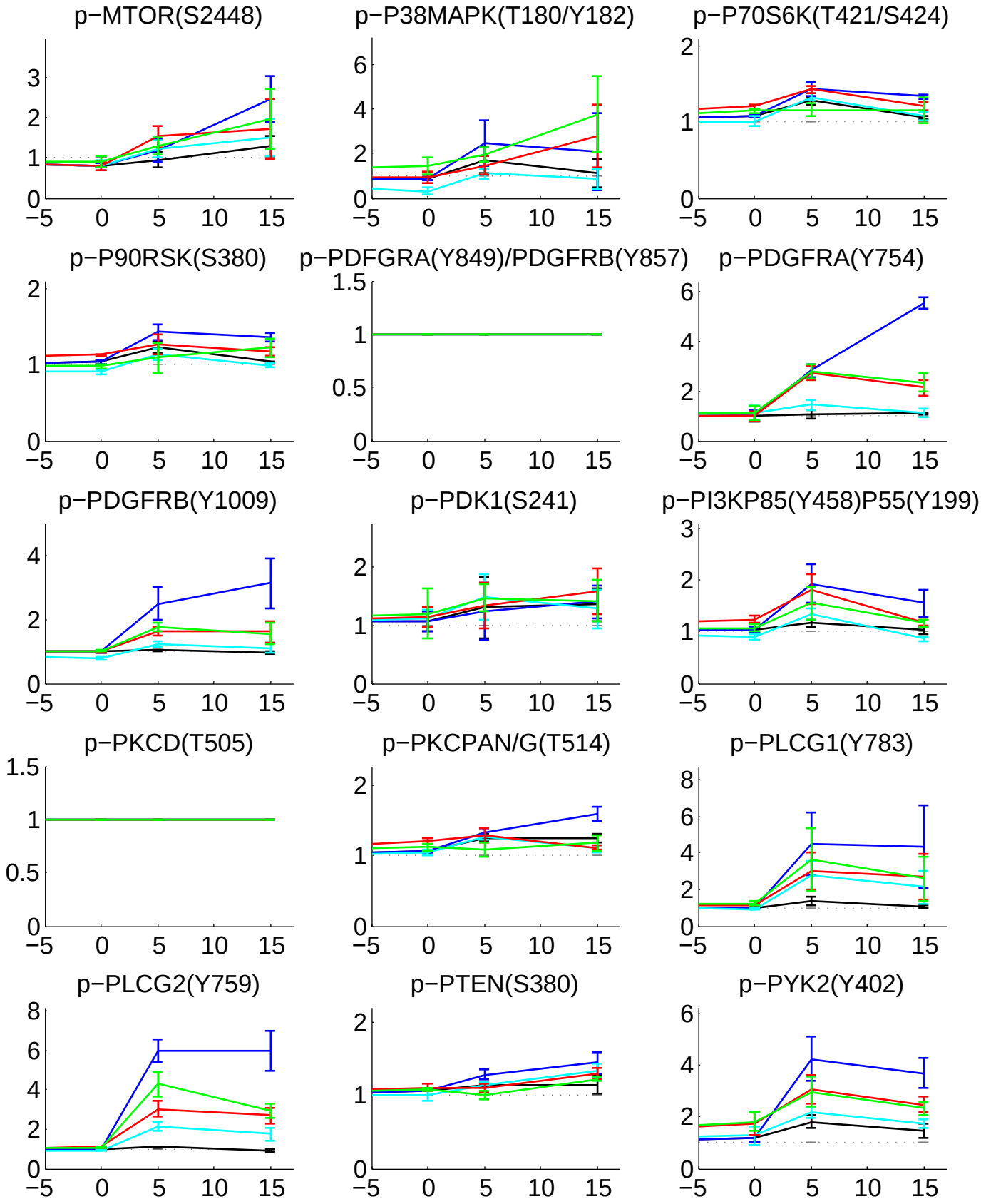
p−MTOR(S2448)
p−P38MAPK(T180/Y182)
p−P70S6K(T421/S424)
p−P90RSK(S380)
p−PDFGRA(Y849)/PDGFRB(Y857)
p−PDGFRA(Y754)
p−PDGFRB(Y1009)
p−PDK1(S241)
p−PI3KP85(Y458)P55(Y199)
p−PKCD(T505)
p−PKCPAN/G(T514)
p−PLCG1(Y783)
p−PLCG2(Y759)
p−PTEN(S380)
p−PYK2(Y402)

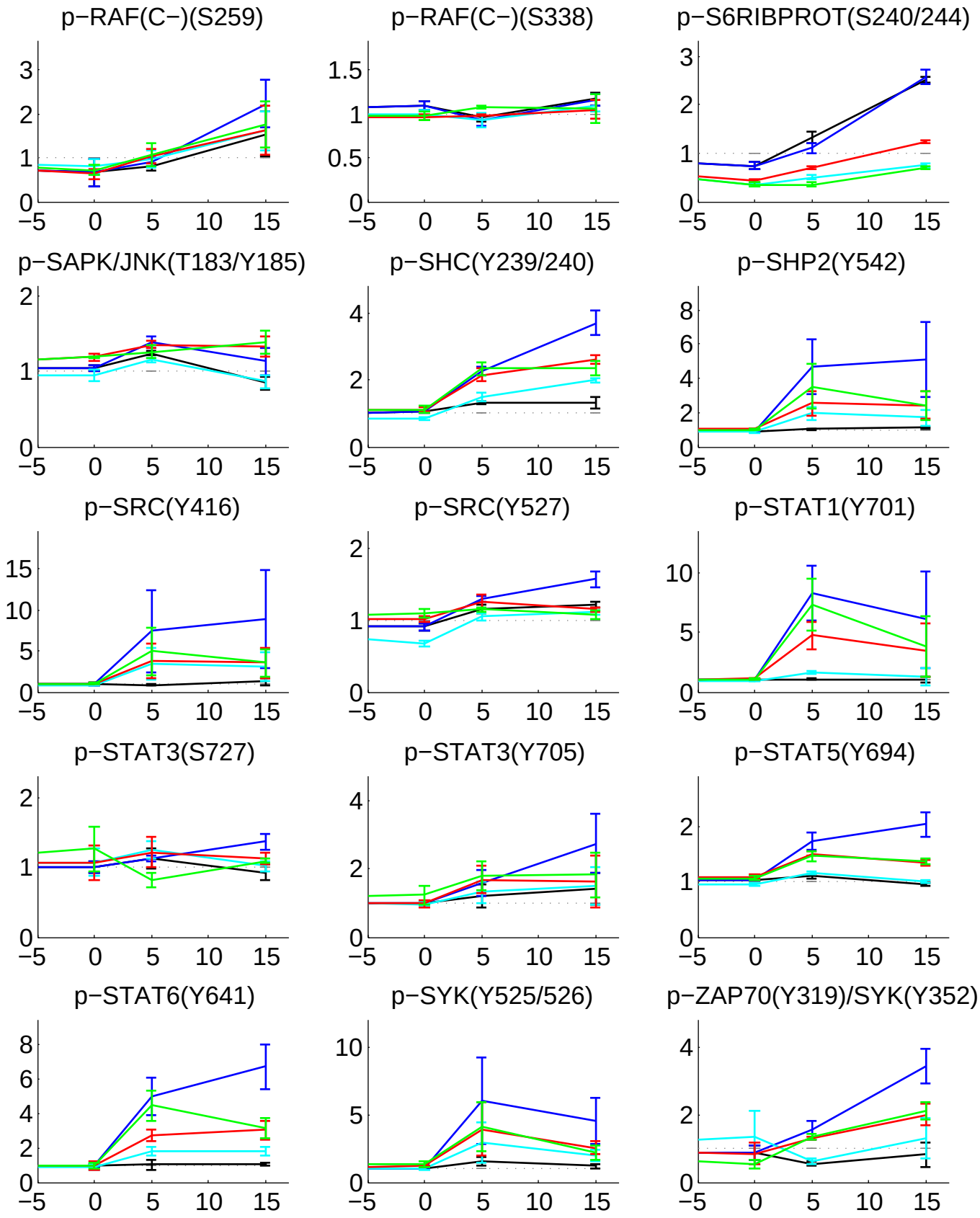
p−RAF(C−)(S259)
p−RAF(C−)(S338)
p−S6RIBPROT(S240/244)
p−SAPK/JNK(T183/Y185)
p−SHC(Y239/240)
p−SHP2(Y542)
p−SRC(Y416)
p−SRC(Y527)
p−STAT1(Y701)
p−STAT3(S727)
p−STAT3(Y705)
p−STAT5(Y694)
p−STAT6(Y641)
p−SYK(Y525/526)
p−ZAP70(Y319)/SYK(Y352)

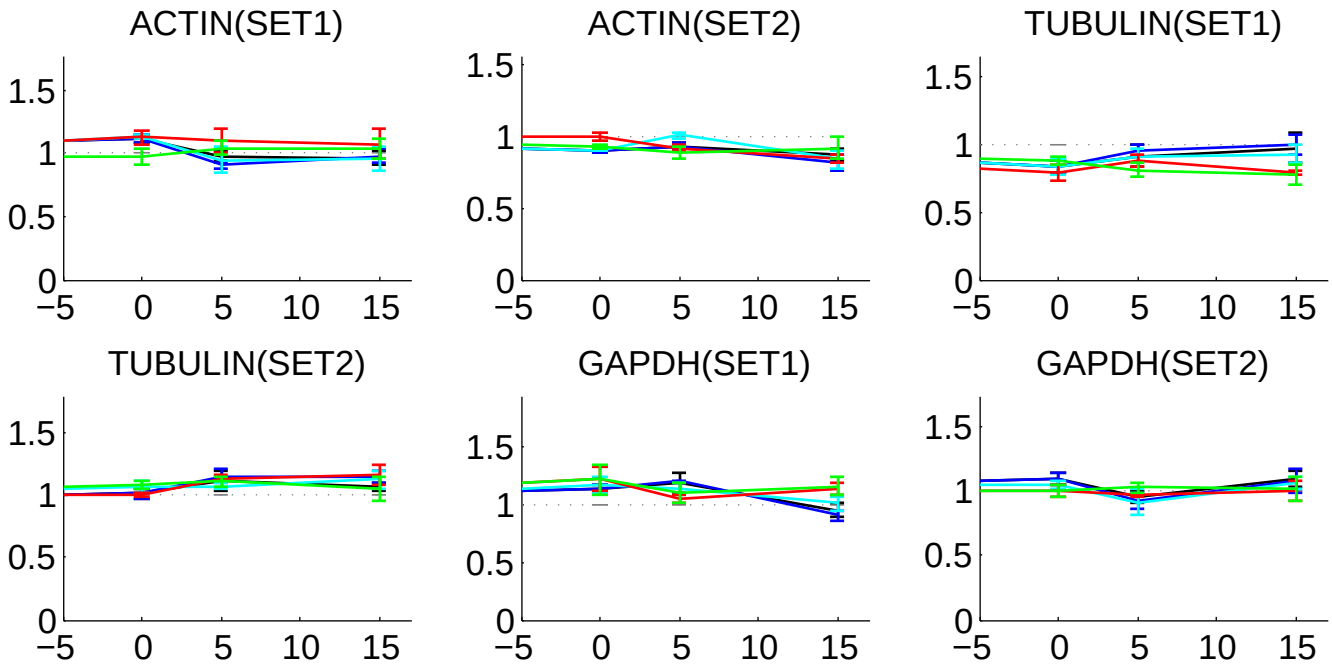
ACTIN(SET1)
ACTIN(SET2)
TUBULIN(SET1)
TUBULIN(SET2)
GAPDH(SET1)
GAPDH(SET2)
1.5
1
0.5
0
−5
0
5
10
15

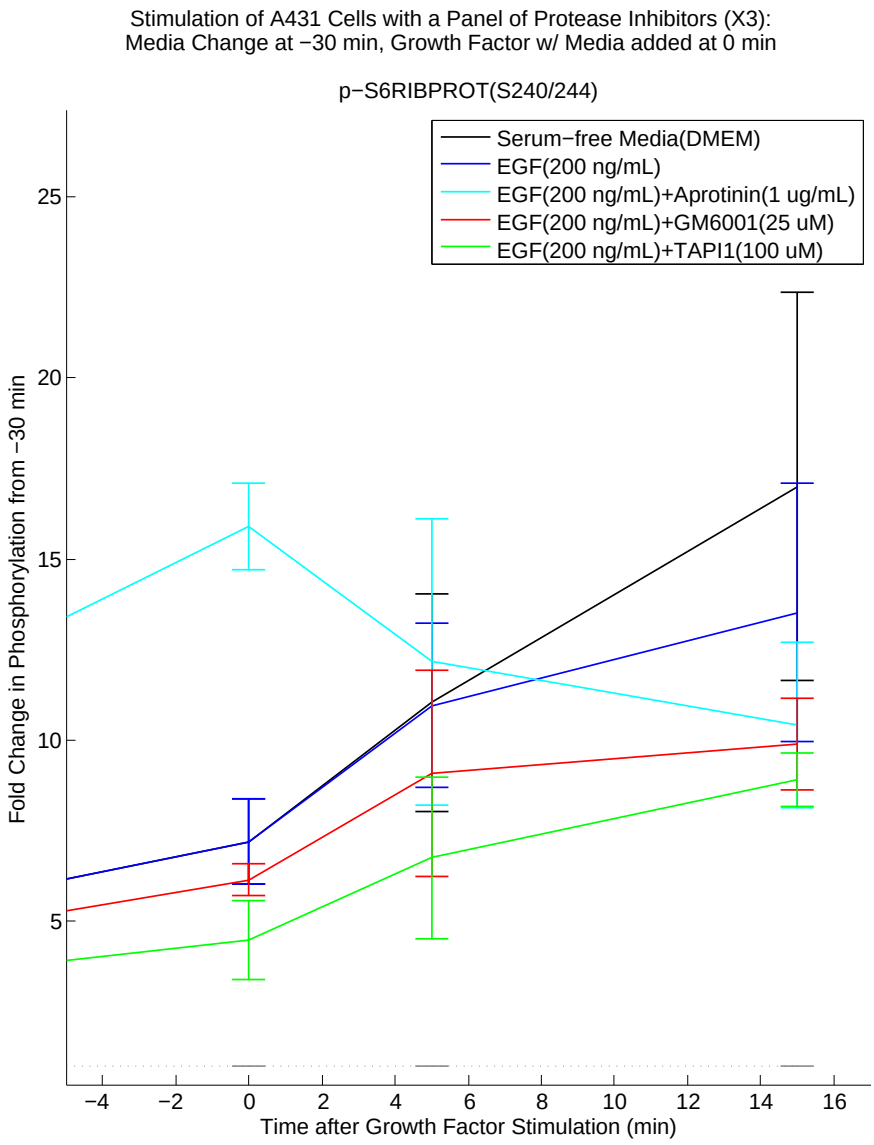

Figure 4: *Serial graphs of phosphorylation kinetics for Panel 3 of small molecules. Subsequent serial graphs are shown on the next 5 pages, where the x-axis reflects time (in minutes) and the y-axis reflects fold change relative to -30 minutes (A fold change of 1 reflects no change from -30 minutes).*

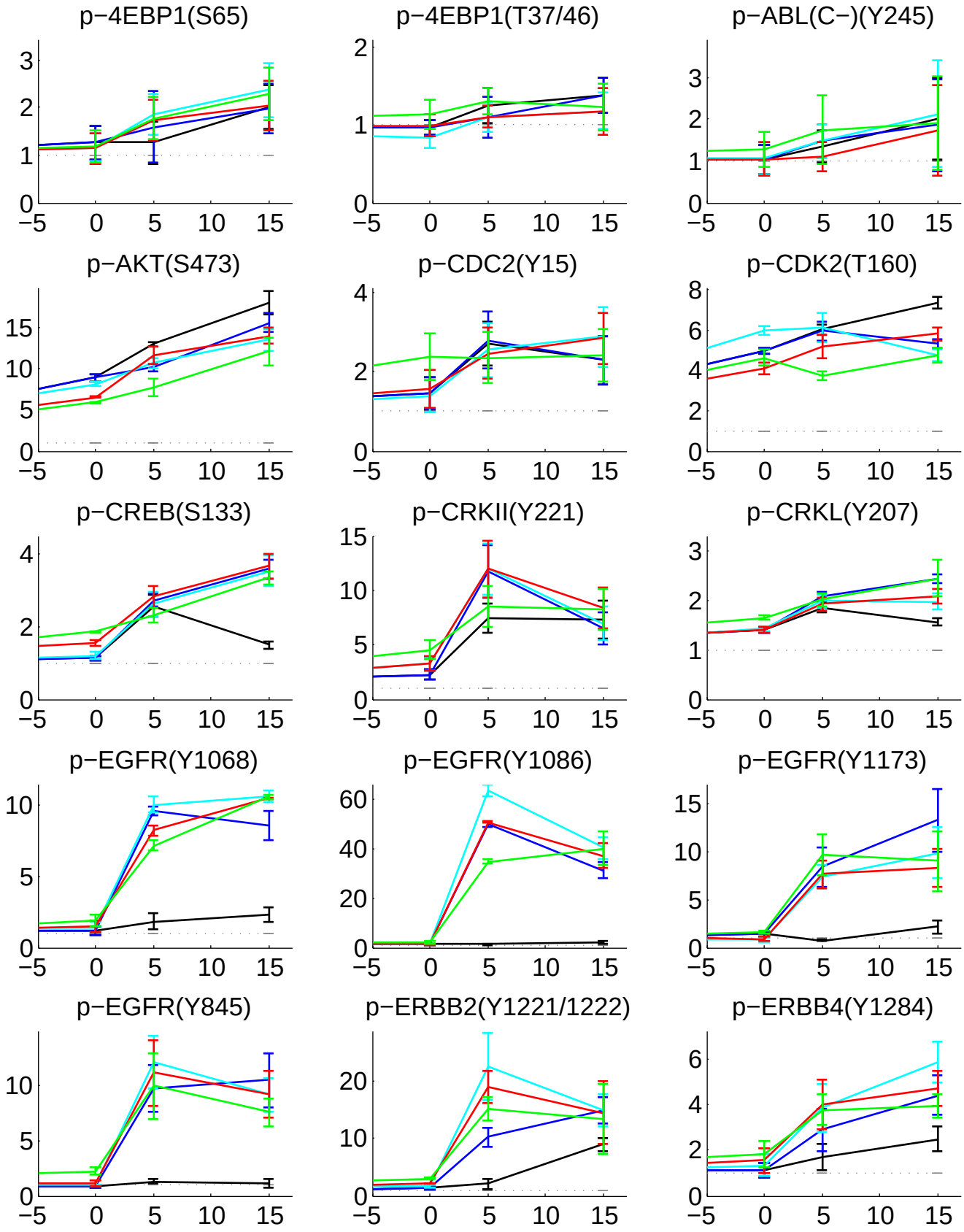
p−4EBP1(S65)
p−4EBP1(T37/46)
p−ABL(C−)(Y245)
p−AKT(S473)
p−CDC2(Y15)
p−CDK2(T160)
p−CREB(S133)
p−CRKII(Y221)
p−CRKL(Y207)
p−EGFR(Y1068)
p−EGFR(Y1086)
p−EGFR(Y1173)
p−EGFR(Y845)
p−ERBB2(Y1221/1222)
p−ERBB4(Y1284)

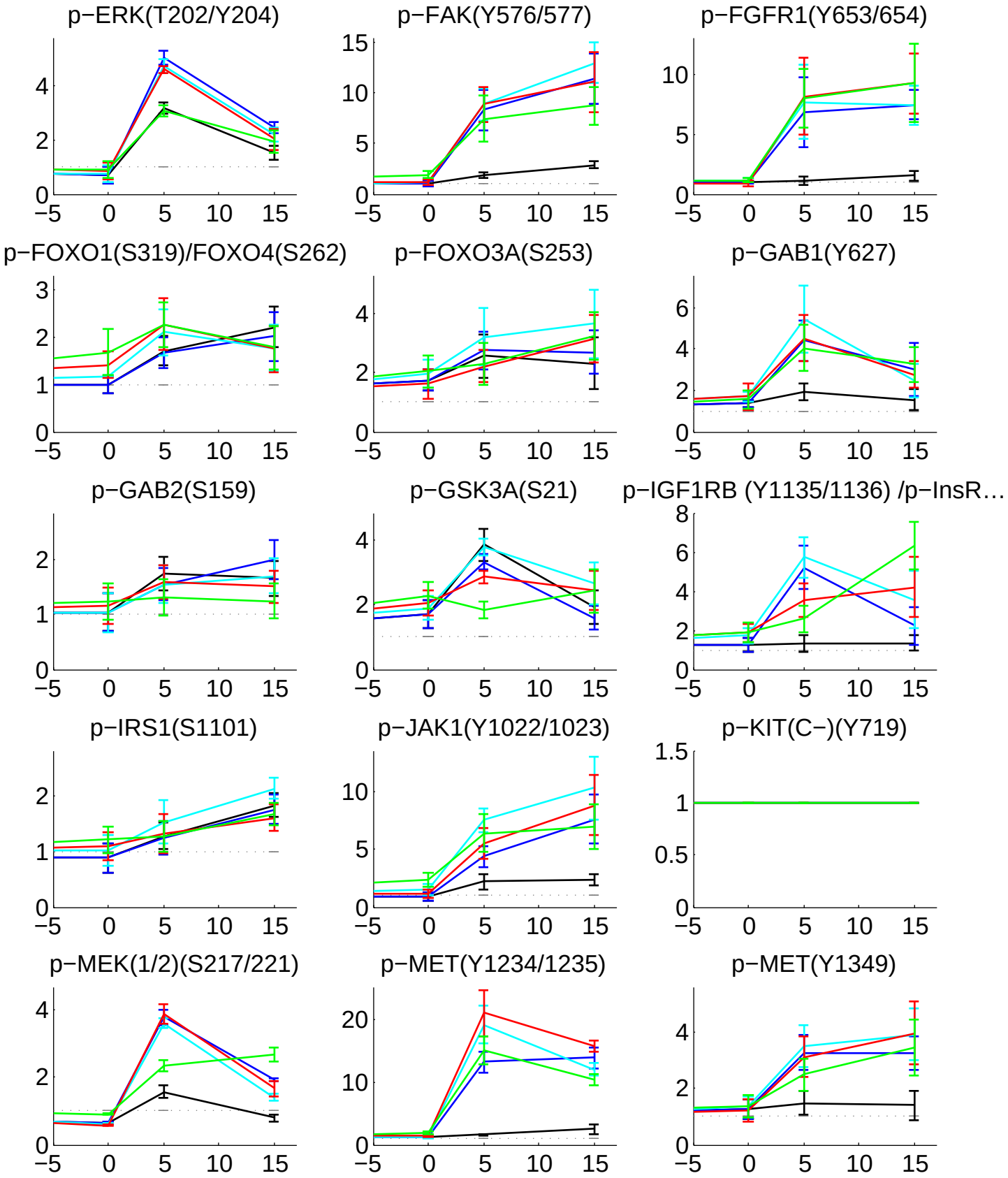
p−ERK(T202/Y204)
p−FAK(Y576/577)
p−FGFR1(Y653/654)
p−FOXO1(S319)/FOXO4(S262)
p−FOXO3A(S253)
p−GAB1(Y627)
p−GAB2(S159)
p−GSK3A(S21)
p−IGF1RB (Y1135/1136) /p−InsR…
p−IRS1(S1101)
p−JAK1(Y1022/1023)
p−KIT(C−)(Y719)
p−MEK(1/2)(S217/221)
p−MET(Y1234/1235)
p−MET(Y1349)

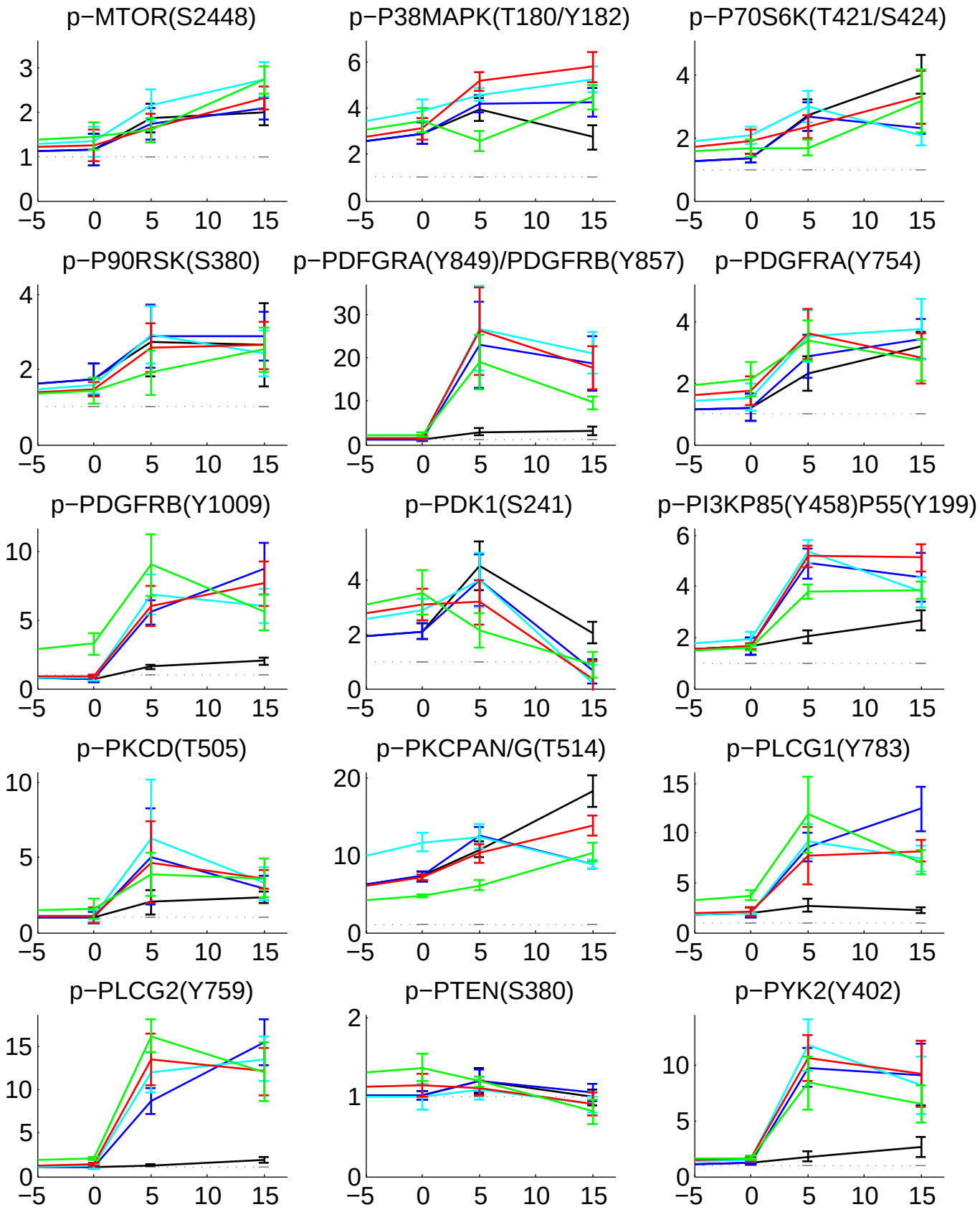
p−MTOR(S2448)
p−P38MAPK(T180/Y182)
p−P70S6K(T421/S424)
p−P90RSK(S380)
p−PDFGRA(Y849)/PDGFRB(Y857)
p−PDGFRA(Y754)
p−PDGFRB(Y1009)
p−PDK1(S241)
p−PI3KP85(Y458)P55(Y199)
p−PKCD(T505)
p−PKCPAN/G(T514)
p−PLCG1(Y783)
p−PLCG2(Y759)
p−PTEN(S380)
p−PYK2(Y402)

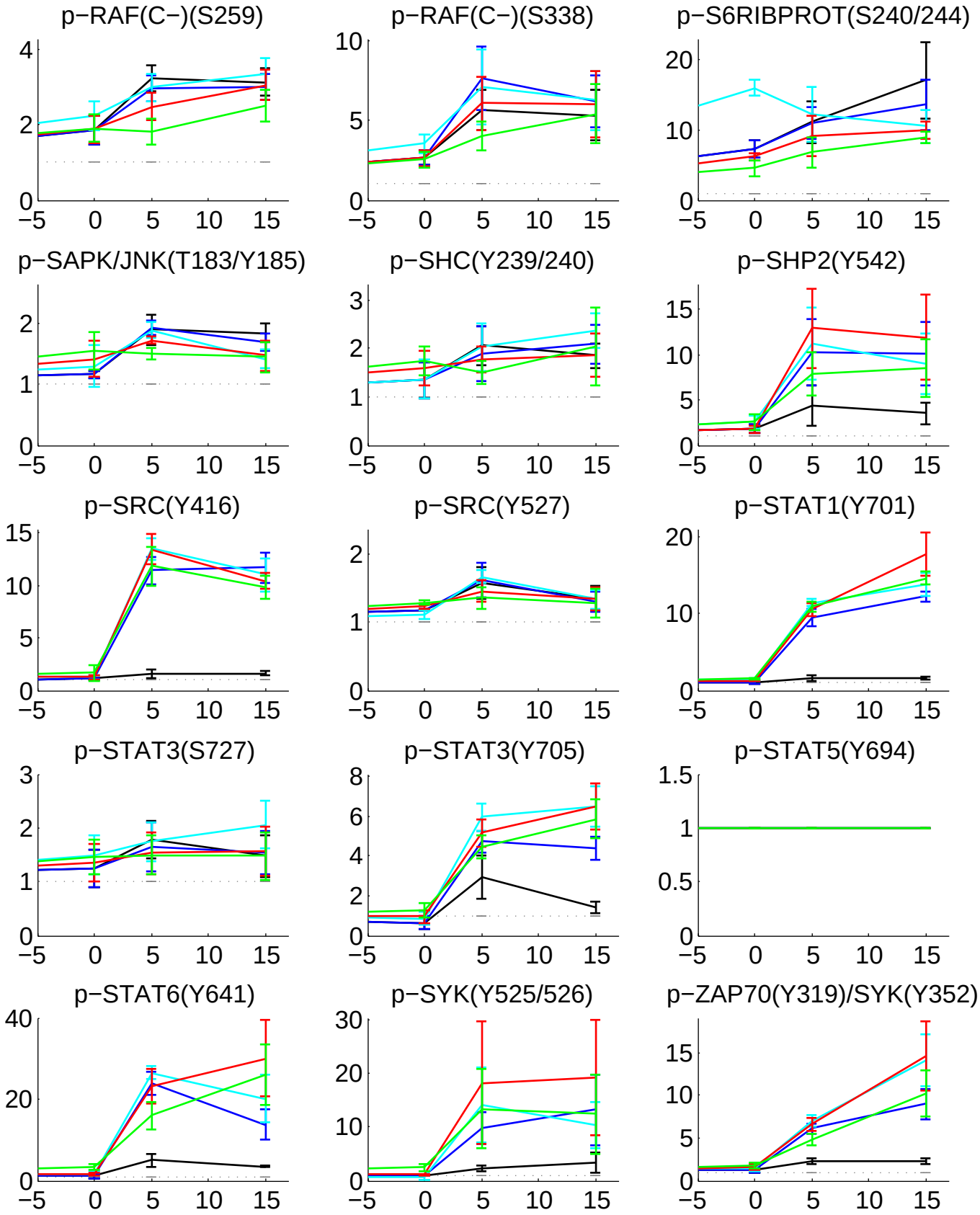
p−RAF(C−)(S259)
p−RAF(C−)(S338)
p−S6RIBPROT(S240/244)
p−SAPK/JNK(T183/Y185)
p−SHC(Y239/240)
p−SHP2(Y542)
p−SRC(Y416)
p−SRC(Y527)
p−STAT1(Y701)
p−STAT3(S727)
p−STAT3(Y705)
p−STAT5(Y694)
p−STAT6(Y641)
p−SYK(Y525/526)
p−ZAP70(Y319)/SYK(Y352)

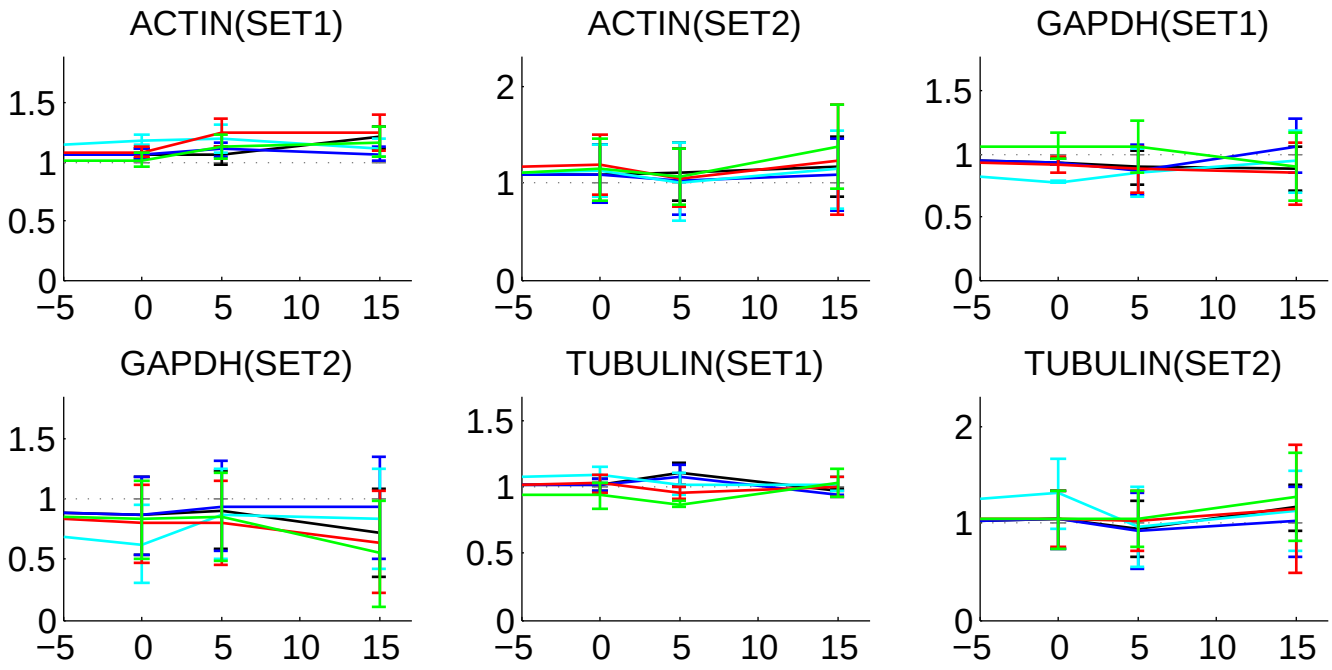
ACTIN(SET1)
ACTIN(SET2)
GAPDH(SET1)
GAPDH(SET2)
TUBULIN(SET1)
TUBULIN(SET2)
−5
0
5
10
15

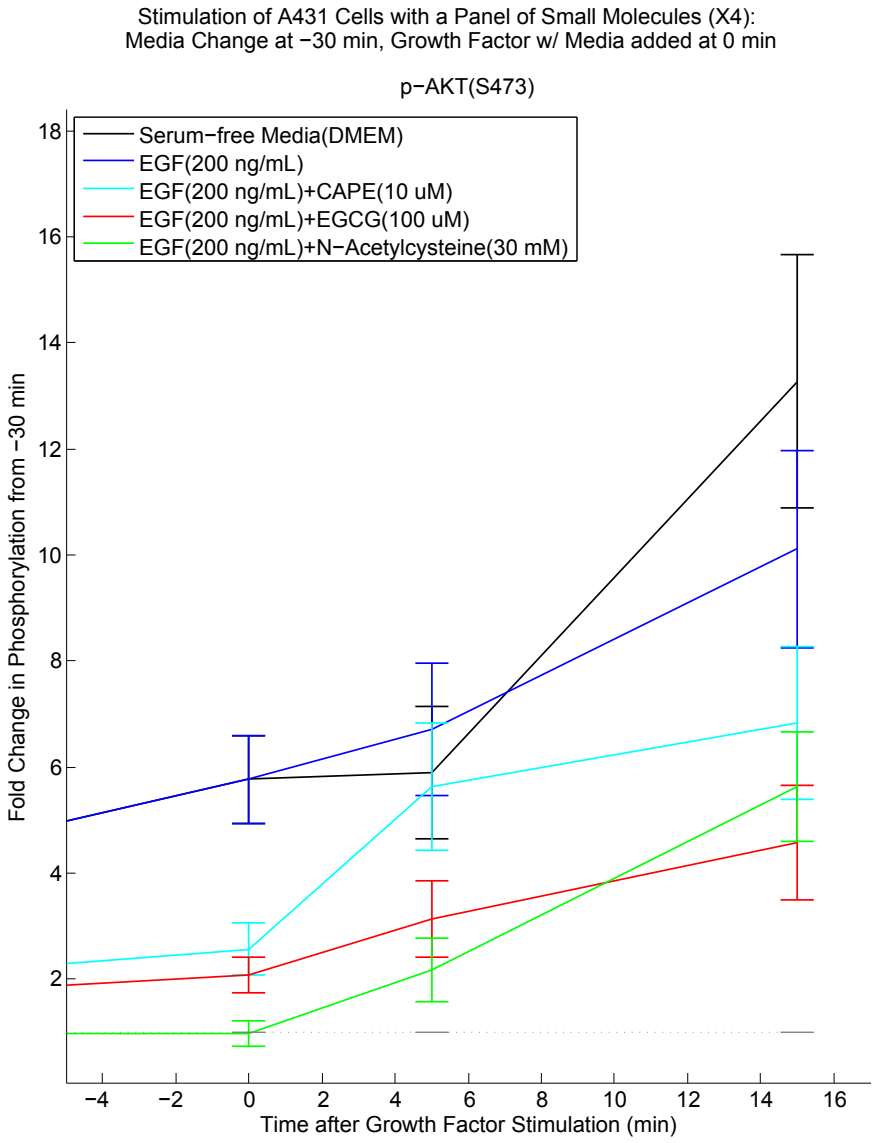

Figure 5: *Serial graphs of phosphorylation kinetics for Panel 4 of small molecules. Subsequent serial graphs are shown on the next 5 pages, where the x-axis reflects time (in minutes) and the y-axis reflects fold change relative to -30 minutes (A fold change of 1 reflects no change from -30 minutes).*

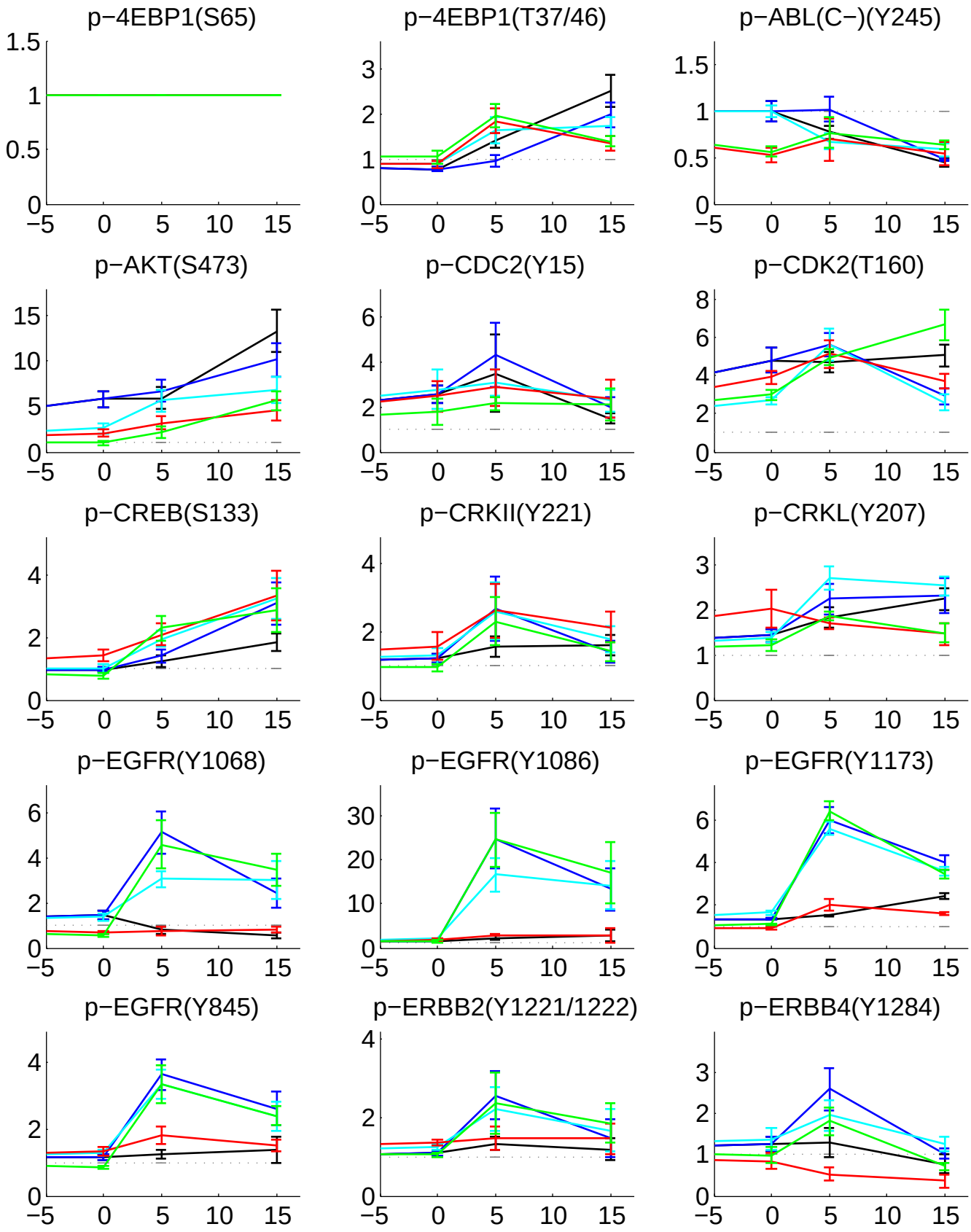
p−4EBP1(S65)
p−4EBP1(T37/46)
p−ABL(C−)(Y245)
p−AKT(S473)
p−CDC2(Y15)
p−CDK2(T160)
p−CREB(S133)
p−CRKII(Y221)
p−CRKL(Y207)
p−EGFR(Y1068)
p−EGFR(Y1086)
p−EGFR(Y1173)
p−EGFR(Y845)
p−ERBB2(Y1221/1222)
p−ERBB4(Y1284)

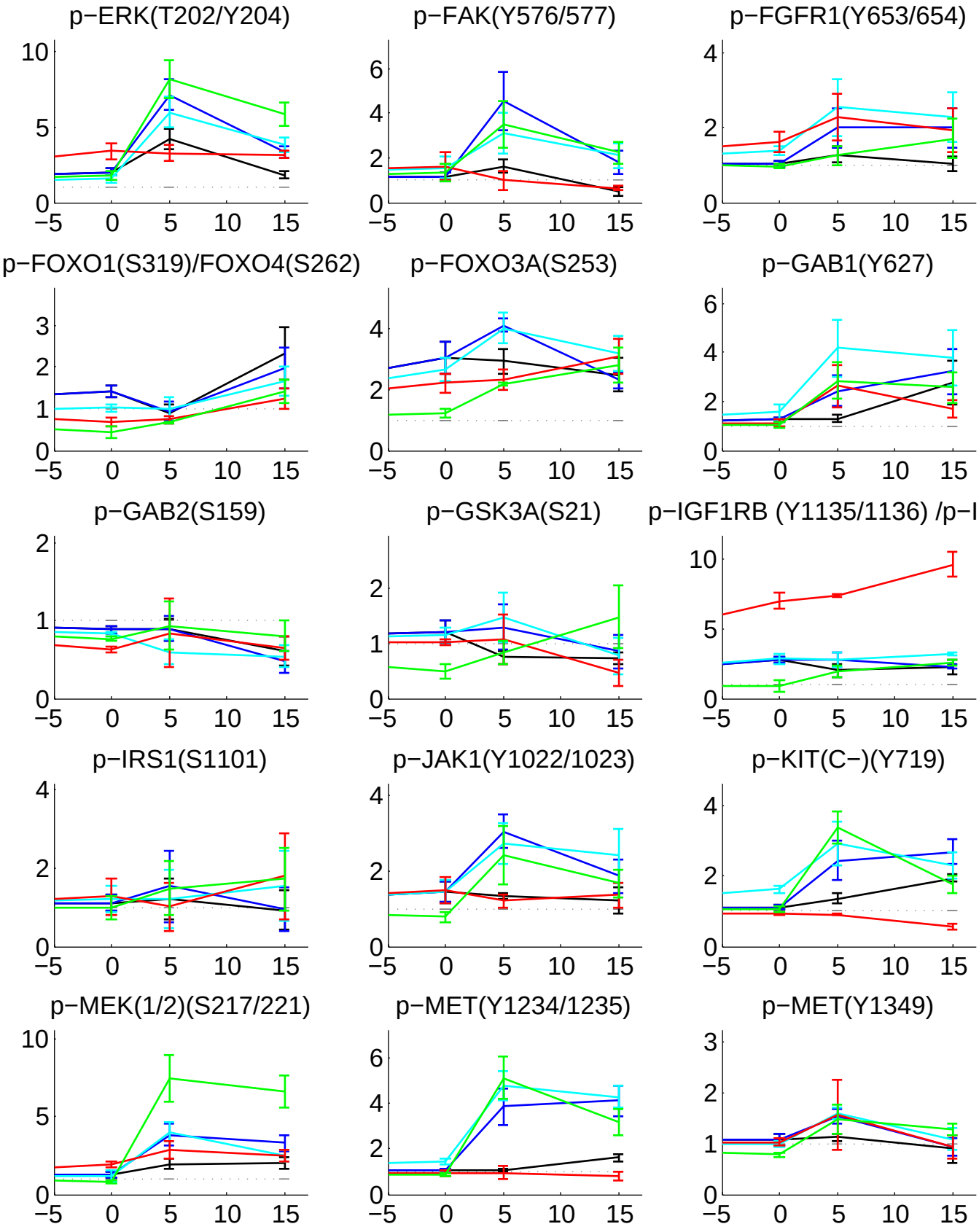
p−ERK(T202/Y204)
p−FAK(Y576/577)
p−FGFR1(Y653/654)
p−FOXO1(S319)/FOXO4(S262)
p−FOXO3A(S253)
p−GAB1(Y627)
p−GAB2(S159)
p−GSK3A(S21)
p−IGF1RB (Y1135/1136) /p−InsR…
p−IRS1(S1101)
p−JAK1(Y1022/1023)
p−KIT(C−)(Y719)
p−MEK(1/2)(S217/221)
p−MET(Y1234/1235)
p−MET(Y1349)

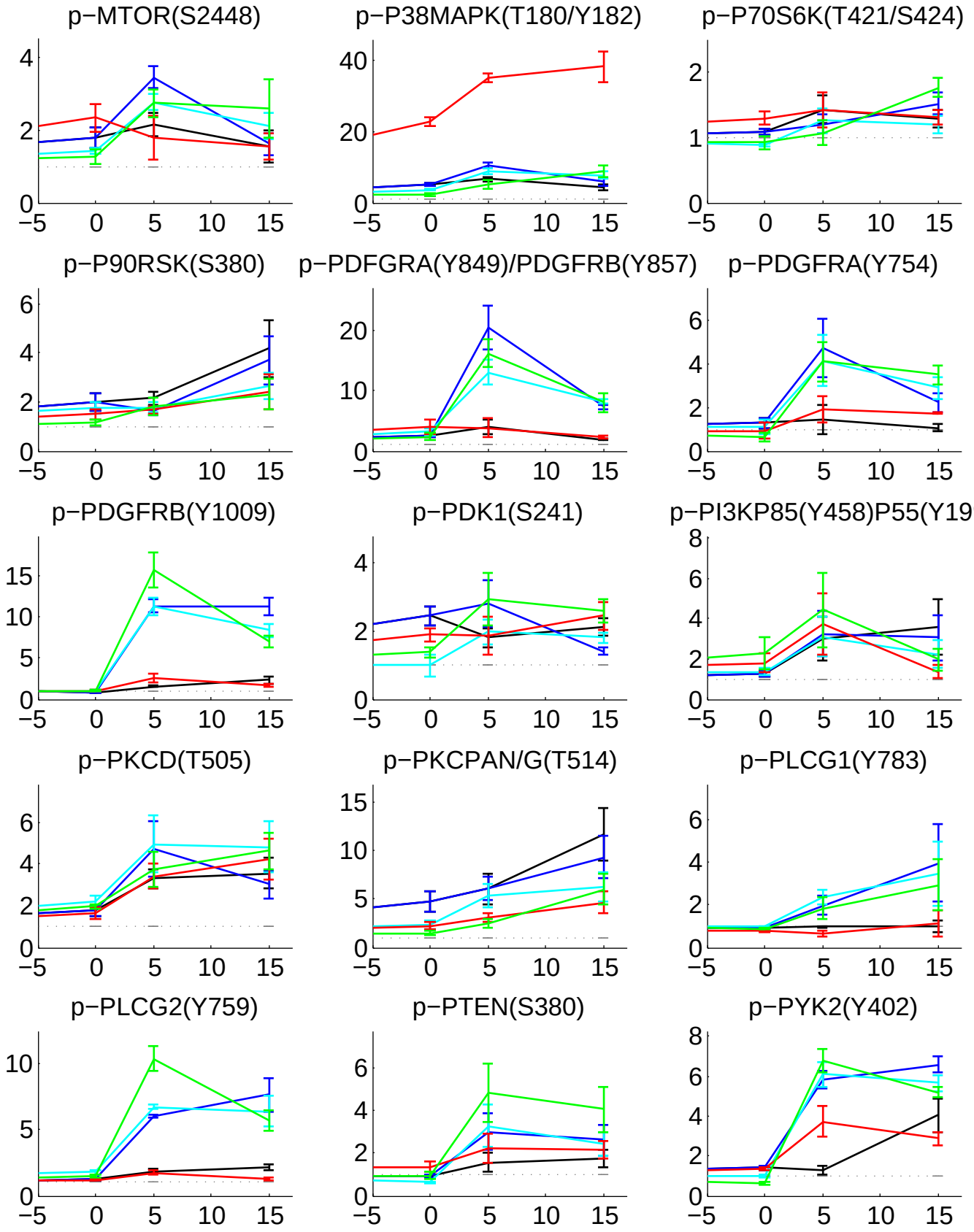
p−MTOR(S2448)
p−P38MAPK(T180/Y182)
p−P70S6K(T421/S424)
p−P90RSK(S380)
p−PDFGRA(Y849)/PDGFRB(Y857)
p−PDGFRA(Y754)
p−PDGFRB(Y1009)
p−PDK1(S241)
p−PI3KP85(Y458)P55(Y199)
p−PKCD(T505)
p−PKCPAN/G(T514)
p−PLCG1(Y783)
p−PLCG2(Y759)
p−PTEN(S380)
p−PYK2(Y402)

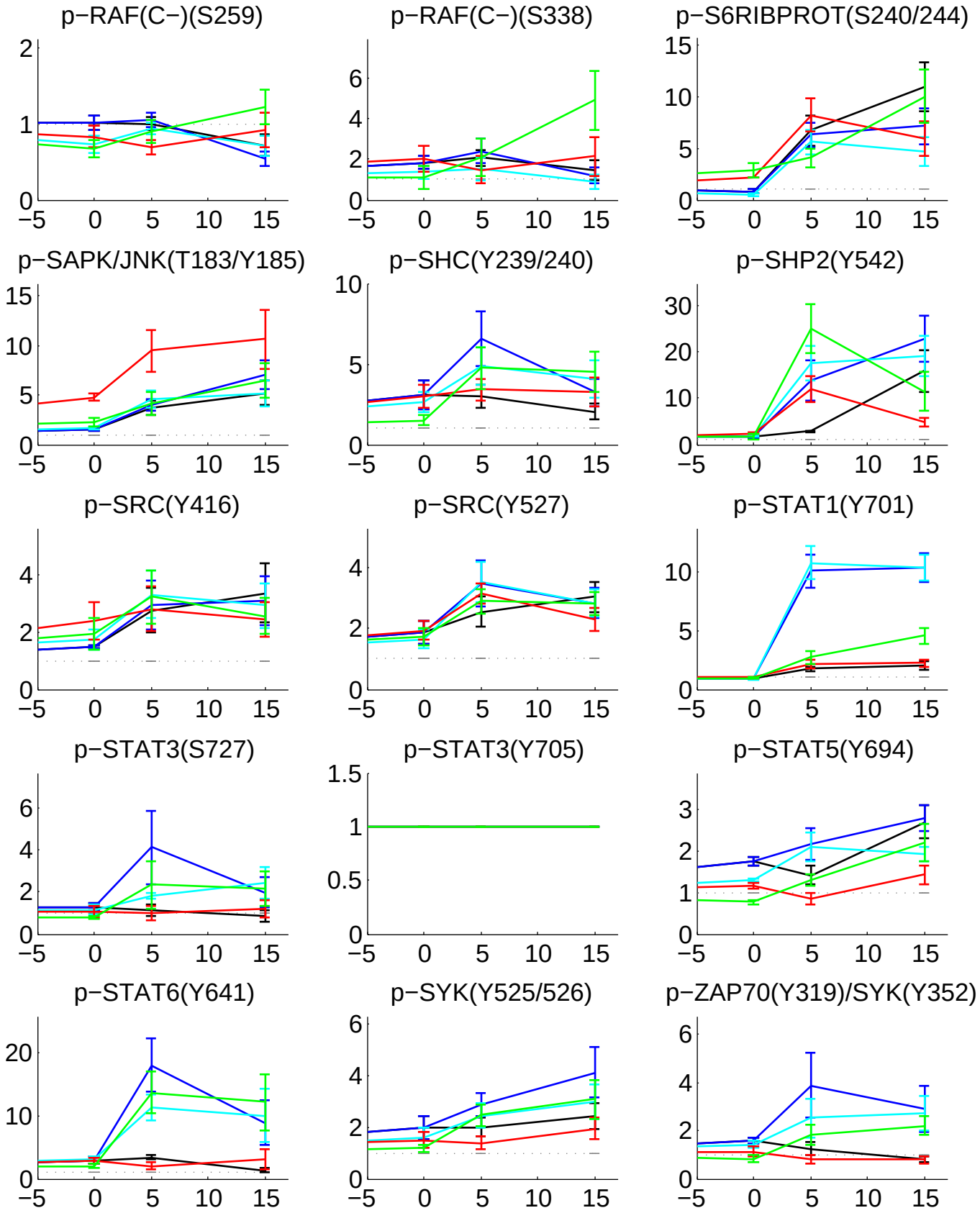
p−RAF(C−)(S259)
p−RAF(C−)(S338)
p−S6RIBPROT(S240/244)
p−SAPK/JNK(T183/Y185)
p−SHC(Y239/240)
p−SHP2(Y542)
p−SRC(Y416)
p−SRC(Y527)
p−STAT1(Y701)
p−STAT3(S727)
p−STAT3(Y705)
p−STAT5(Y694)
p−STAT6(Y641)
p−SYK(Y525/526)
p−ZAP70(Y319)/SYK(Y352)

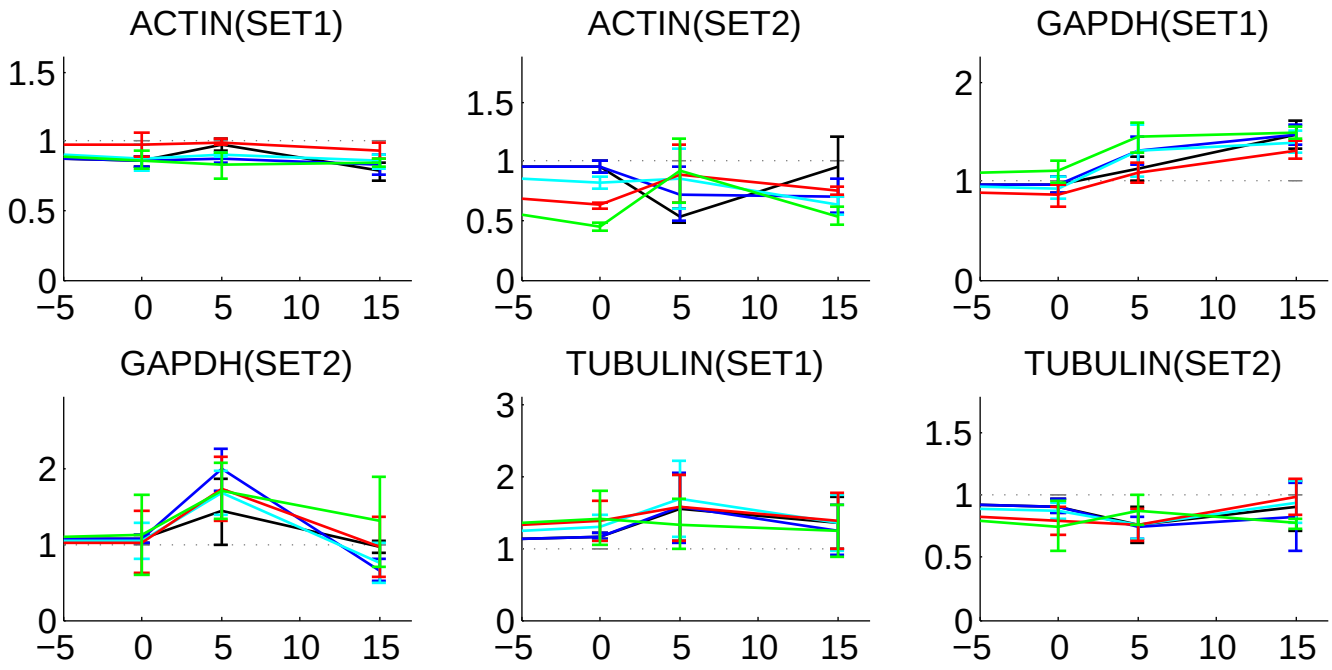
ACTIN(SET1)
ACTIN(SET2)
GAPDH(SET1)
GAPDH(SET2)
TUBULIN(SET1)
TUBULIN(SET2)
−5
0
5
10
15

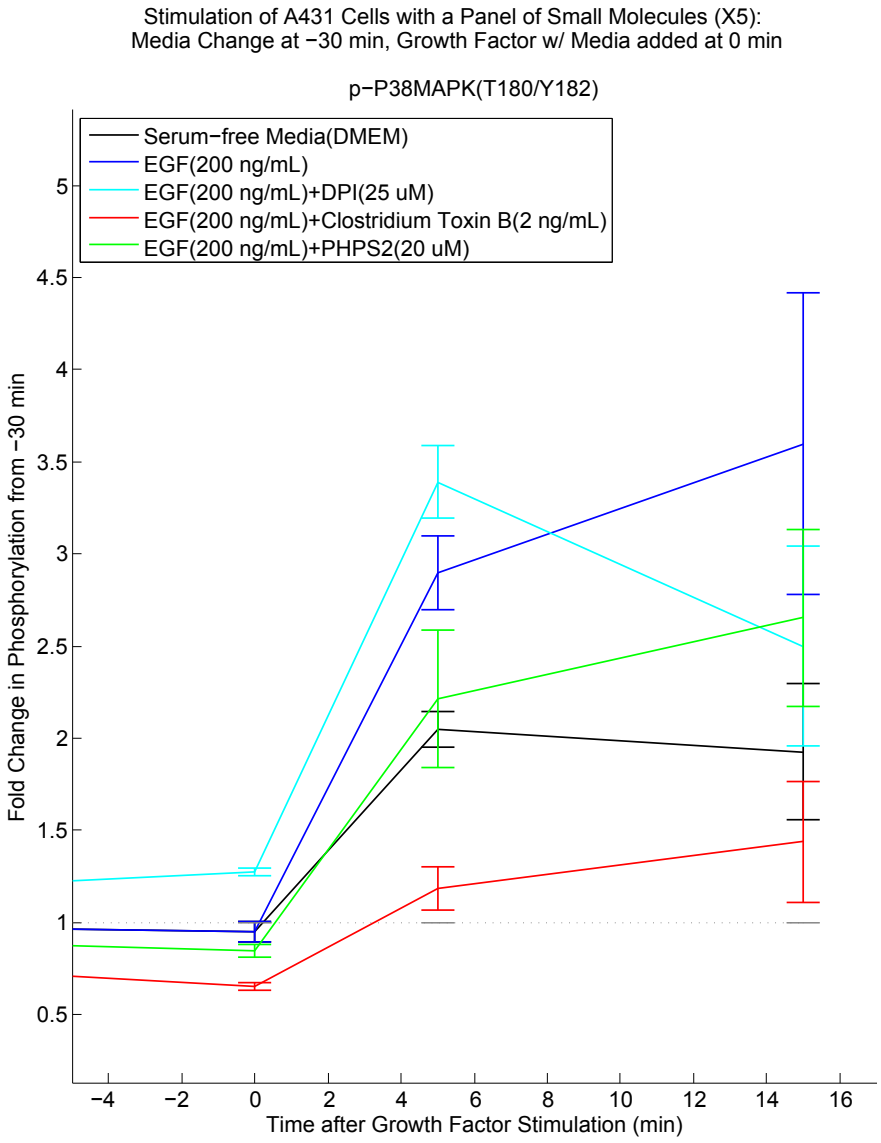

Figure 6: *Serial graphs of phosphorylation kinetics for Panel 5 of small molecules. Subsequent serial graphs are shown on the next 5 pages, where the x-axis reflects time (in minutes) and the y-axis reflects fold change relative to -30 minutes (A fold change of 1 reflects no change from -30 minutes).*

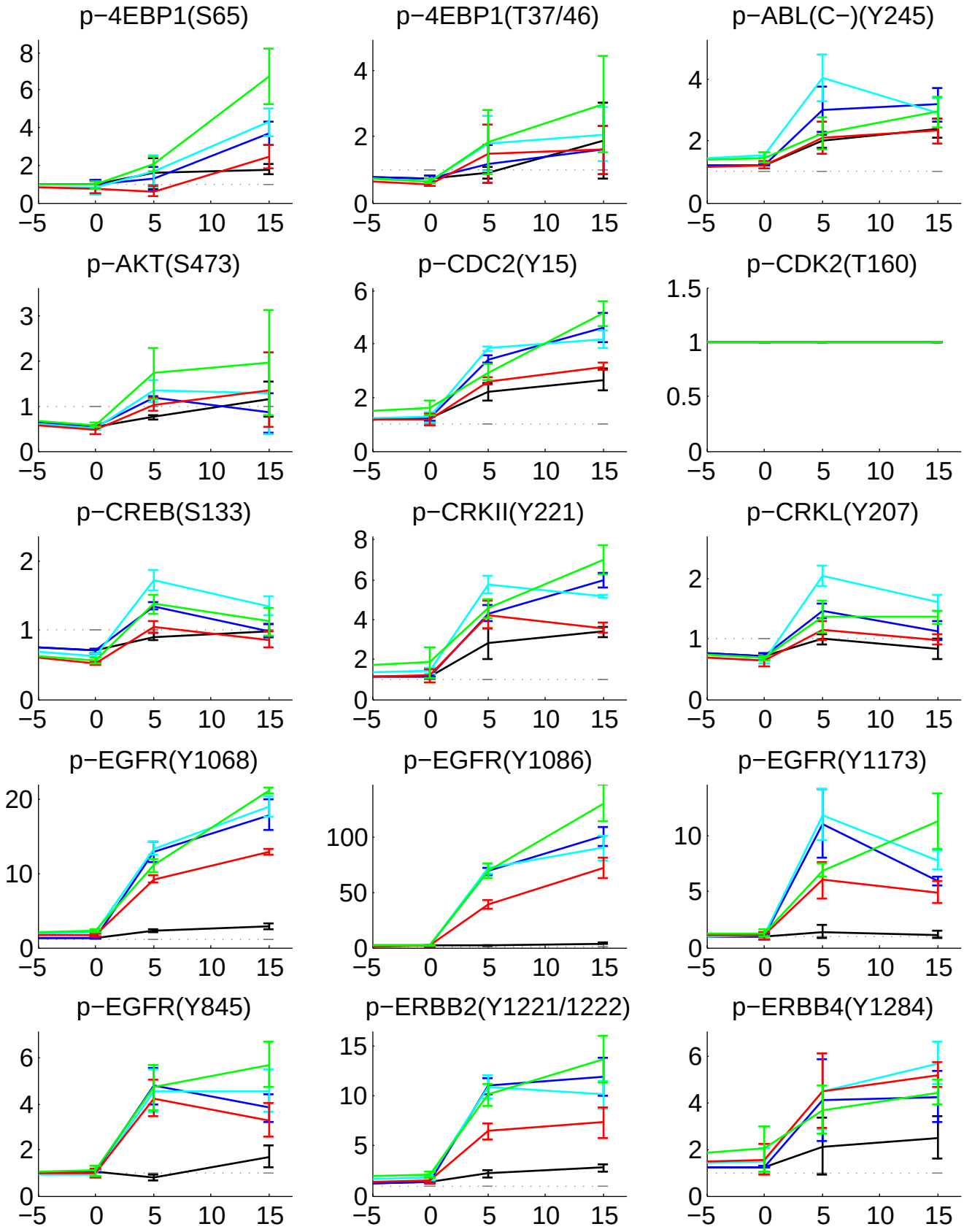
p−4EBP1(S65)
p−4EBP1(T37/46)
p−ABL(C−)(Y245)
p−AKT(S473)
p−CDC2(Y15)
p−CDK2(T160)
p−CREB(S133)
p−CRKII(Y221)
p−CRKL(Y207)
p−EGFR(Y1068)
p−EGFR(Y1086)
p−EGFR(Y1173)
p−EGFR(Y845)
p−ERBB2(Y1221/1222)
p−ERBB4(Y1284)

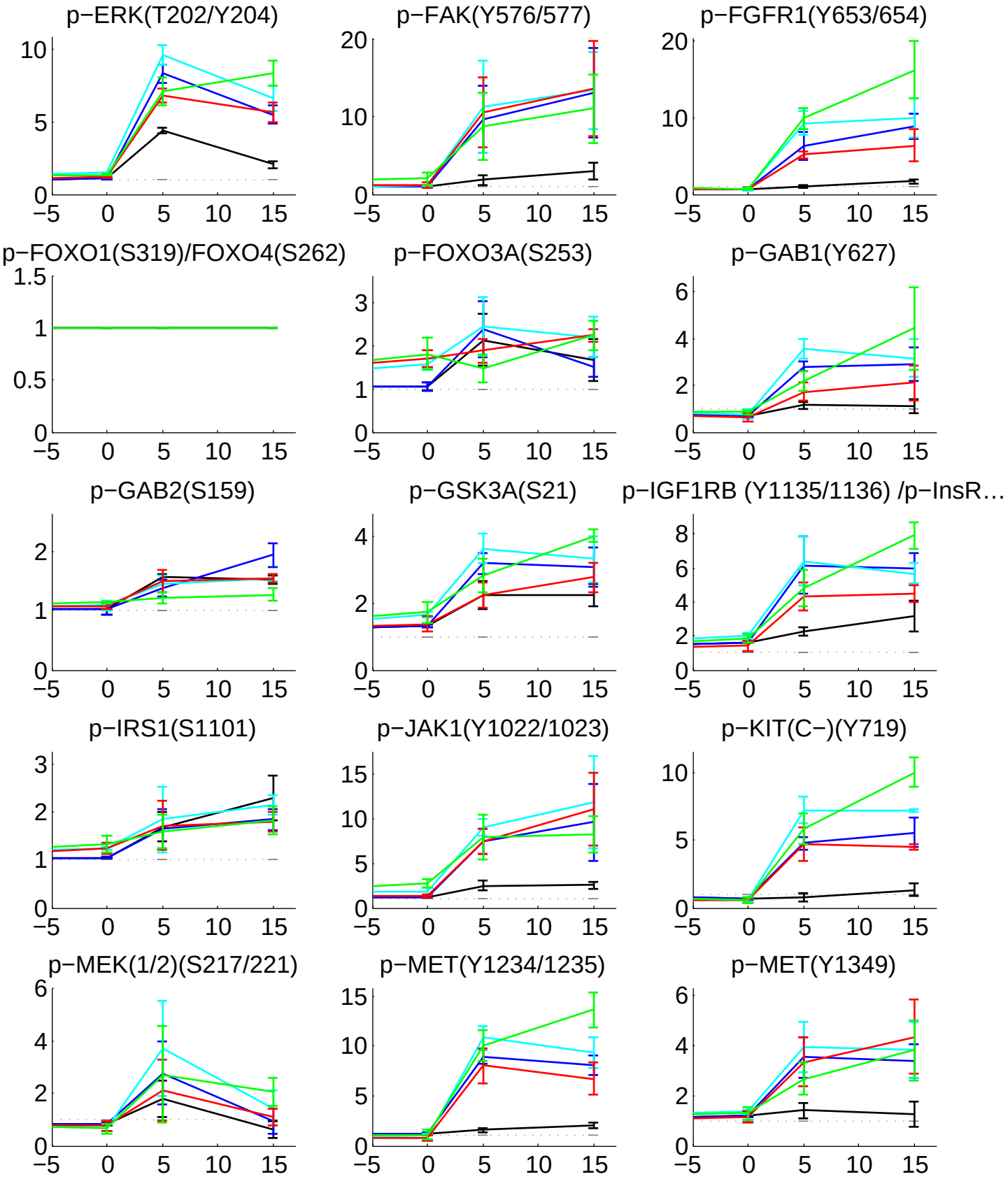
p−ERK(T202/Y204)
p−FAK(Y576/577)
p−FGFR1(Y653/654)
p−FOXO1(S319)/FOXO4(S262)
p−FOXO3A(S253)
p−GAB1(Y627)
p−GAB2(S159)
p−GSK3A(S21)
p−IGF1RB (Y1135/1136) /p−InsR…
p−IRS1(S1101)
p−JAK1(Y1022/1023)
p−KIT(C−)(Y719)
p−MEK(1/2)(S217/221)
p−MET(Y1234/1235)
p−MET(Y1349)

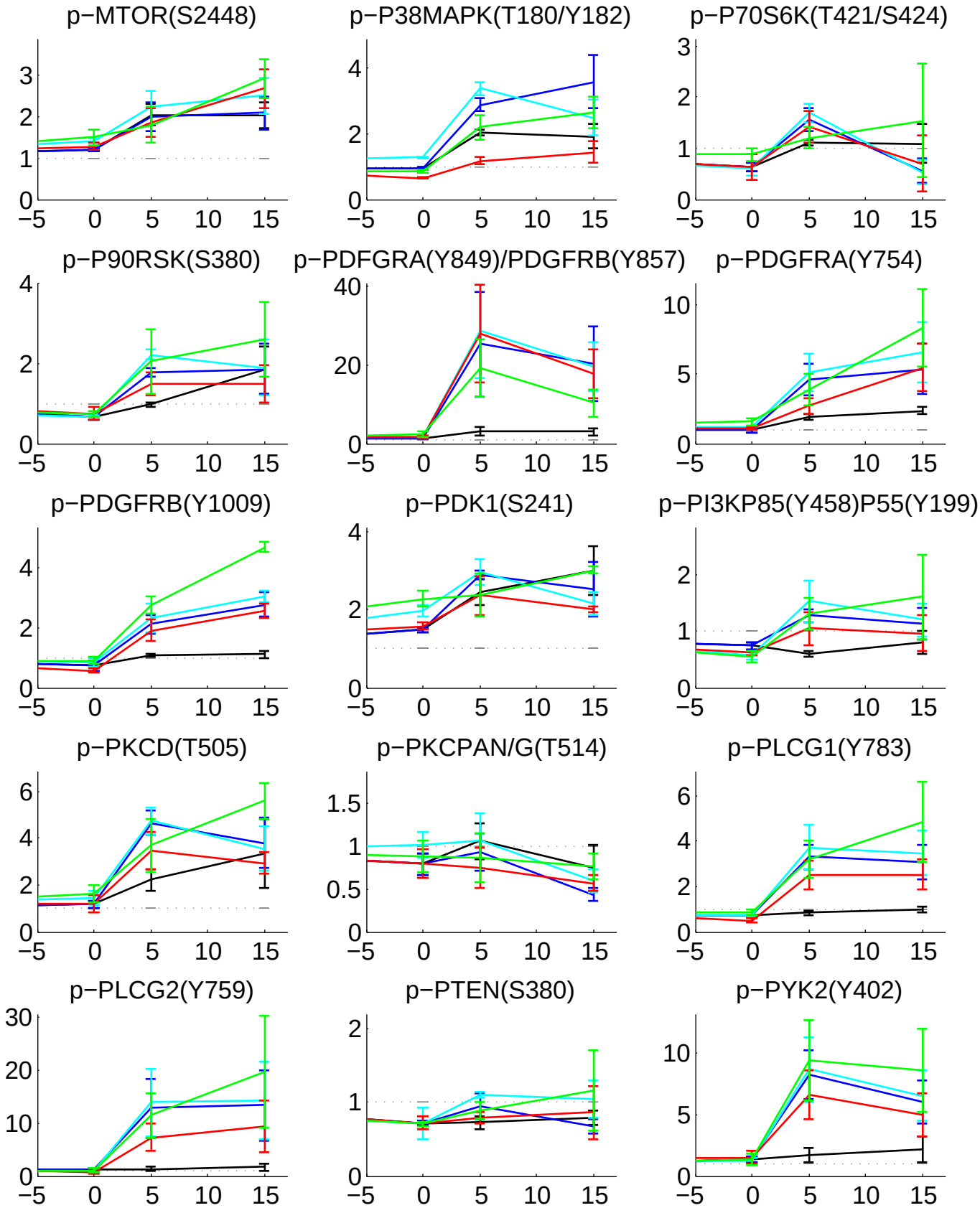
p−MTOR(S2448)
p−P38MAPK(T180/Y182)
p−P70S6K(T421/S424)
p−P90RSK(S380)
p−PDFGRA(Y849)/PDGFRB(Y857)
p−PDGFRA(Y754)
p−PDGFRB(Y1009)
p−PDK1(S241)
p−PI3KP85(Y458)P55(Y199)
p−PKCD(T505)
p−PKCPAN/G(T514)
p−PLCG1(Y783)
p−PLCG2(Y759)
p−PTEN(S380)
p−PYK2(Y402)

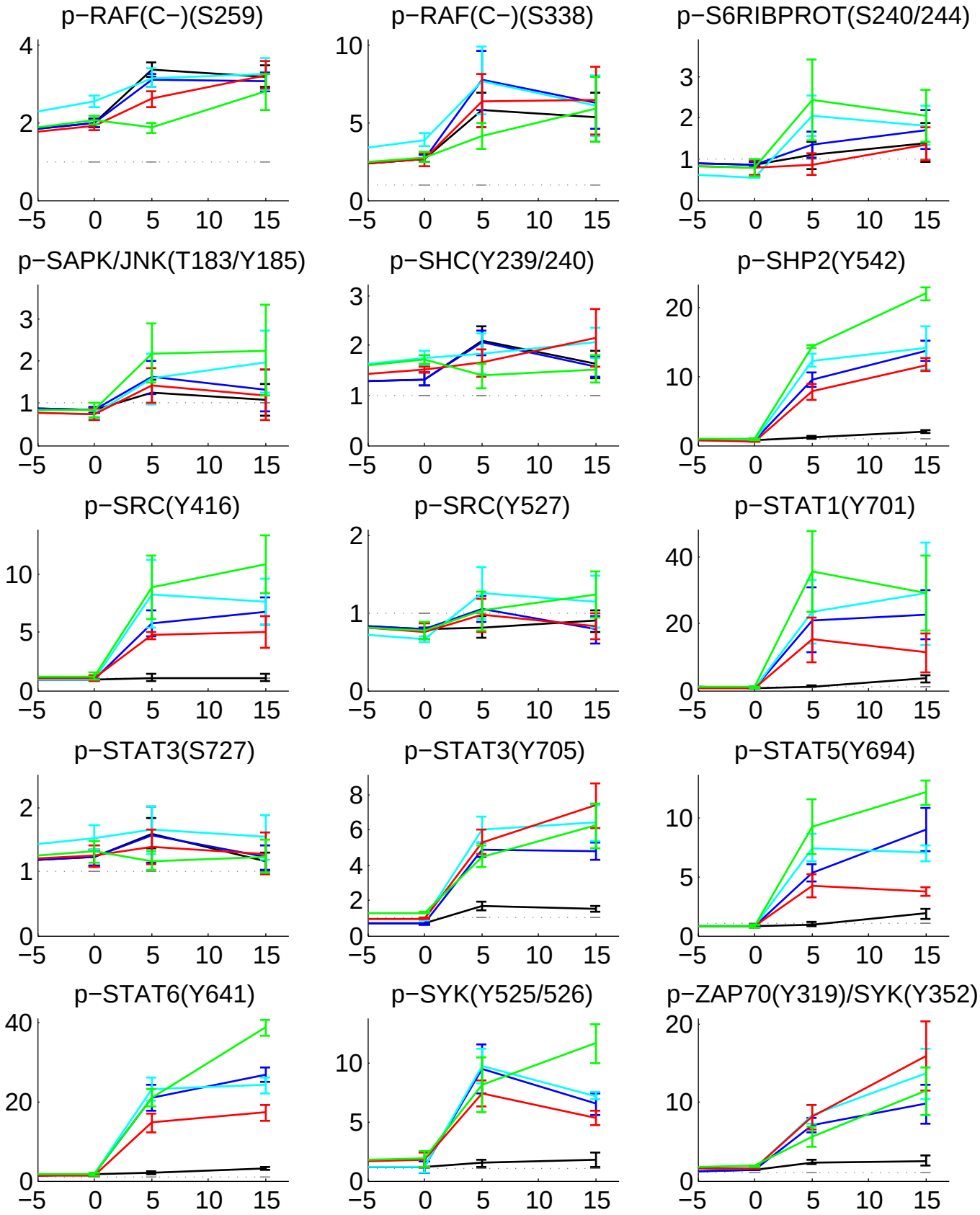
p−RAF(C−)(S259)
p−RAF(C−)(S338)
p−S6RIBPROT(S240/244)
p−SAPK/JNK(T183/Y185)
p−SHC(Y239/240)
p−SHP2(Y542)
p−SRC(Y416)
p−SRC(Y527)
p−STAT1(Y701)
p−STAT3(S727)
p−STAT3(Y705)
p−STAT5(Y694)
p−STAT6(Y641)
p−SYK(Y525/526)
p−ZAP70(Y319)/SYK(Y352)

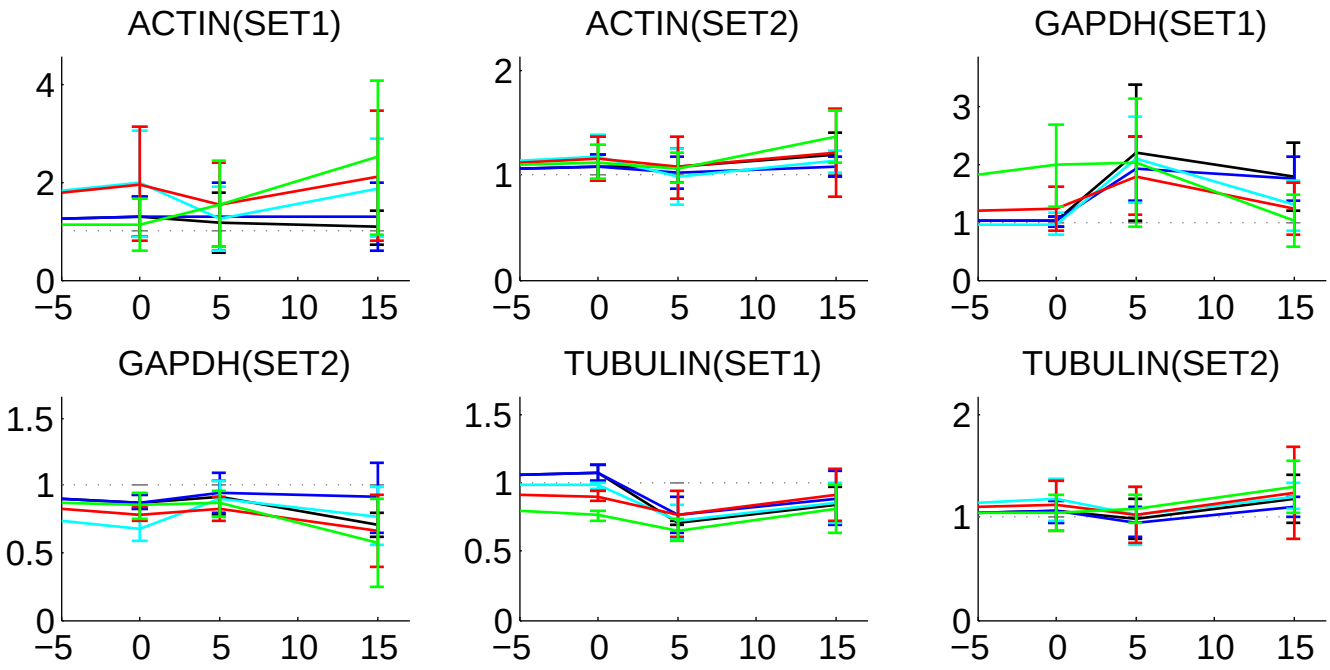
ACTIN(SET1)
ACTIN(SET2)
GAPDH(SET1)
GAPDH(SET2)
TUBULIN(SET1)
TUBULIN(SET2)
−5
0
5
10
15

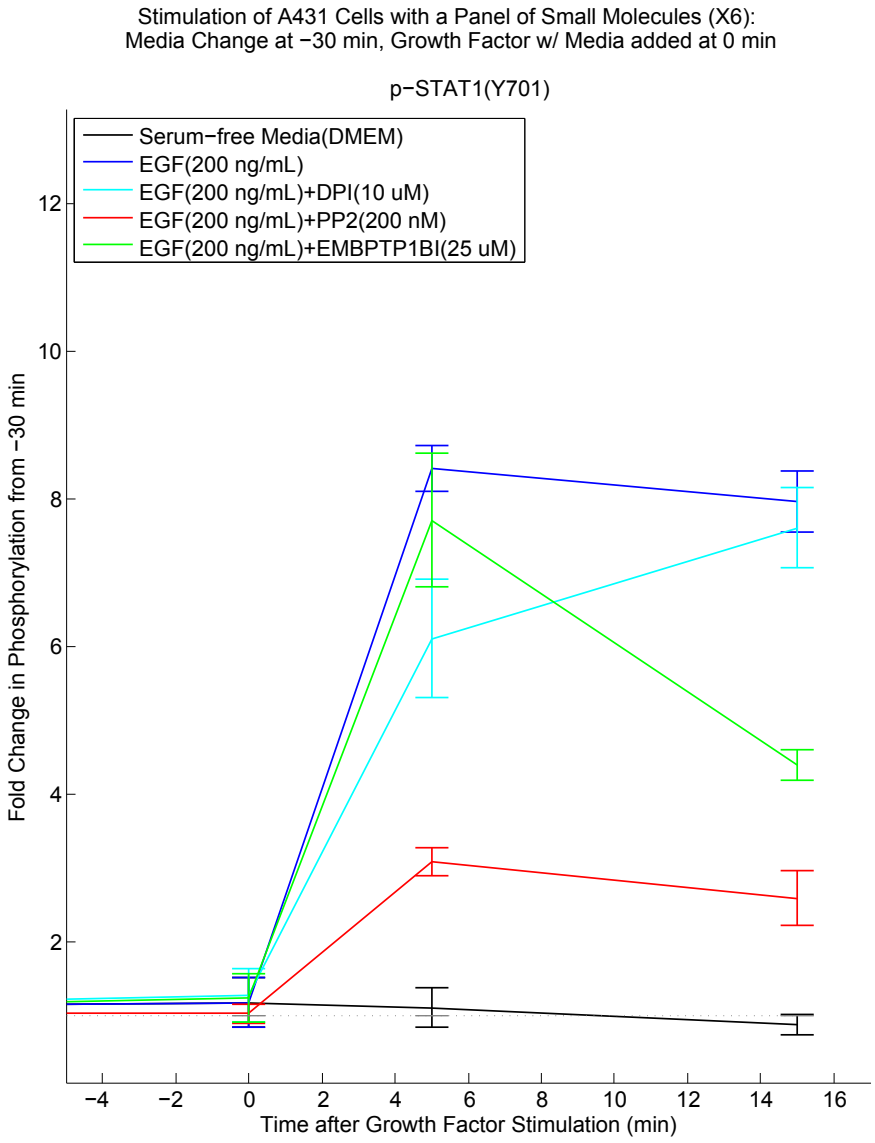

Figure 7: *Serial graphs of phosphorylation kinetics for Panel 6 of small molecules. Subsequent serial graphs are shown on the next 5 pages, where the x-axis reflects time (in minutes) and the y-axis reflects fold change relative to -30 minutes (A fold change of 1 reflects no change from -30 minutes).*

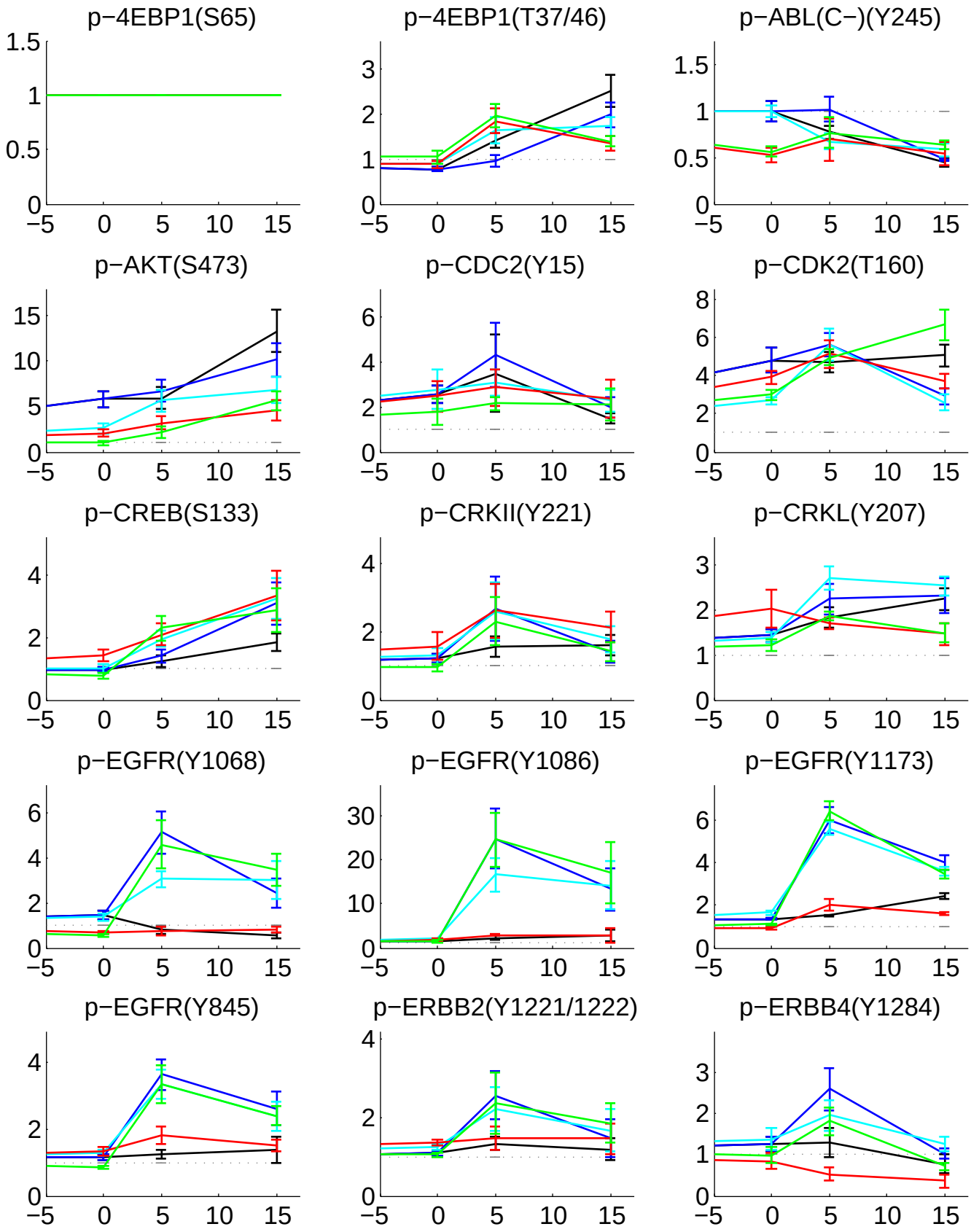
p−4EBP1(S65)
p−4EBP1(T37/46)
p−ABL(C−)(Y245)
p−AKT(S473)
p−CDC2(Y15)
p−CDK2(T160)
p−CREB(S133)
p−CRKII(Y221)
p−CRKL(Y207)
p−EGFR(Y1068)
p−EGFR(Y1086)
p−EGFR(Y1173)
p−EGFR(Y845)
p−ERBB2(Y1221/1222)
p−ERBB4(Y1284)

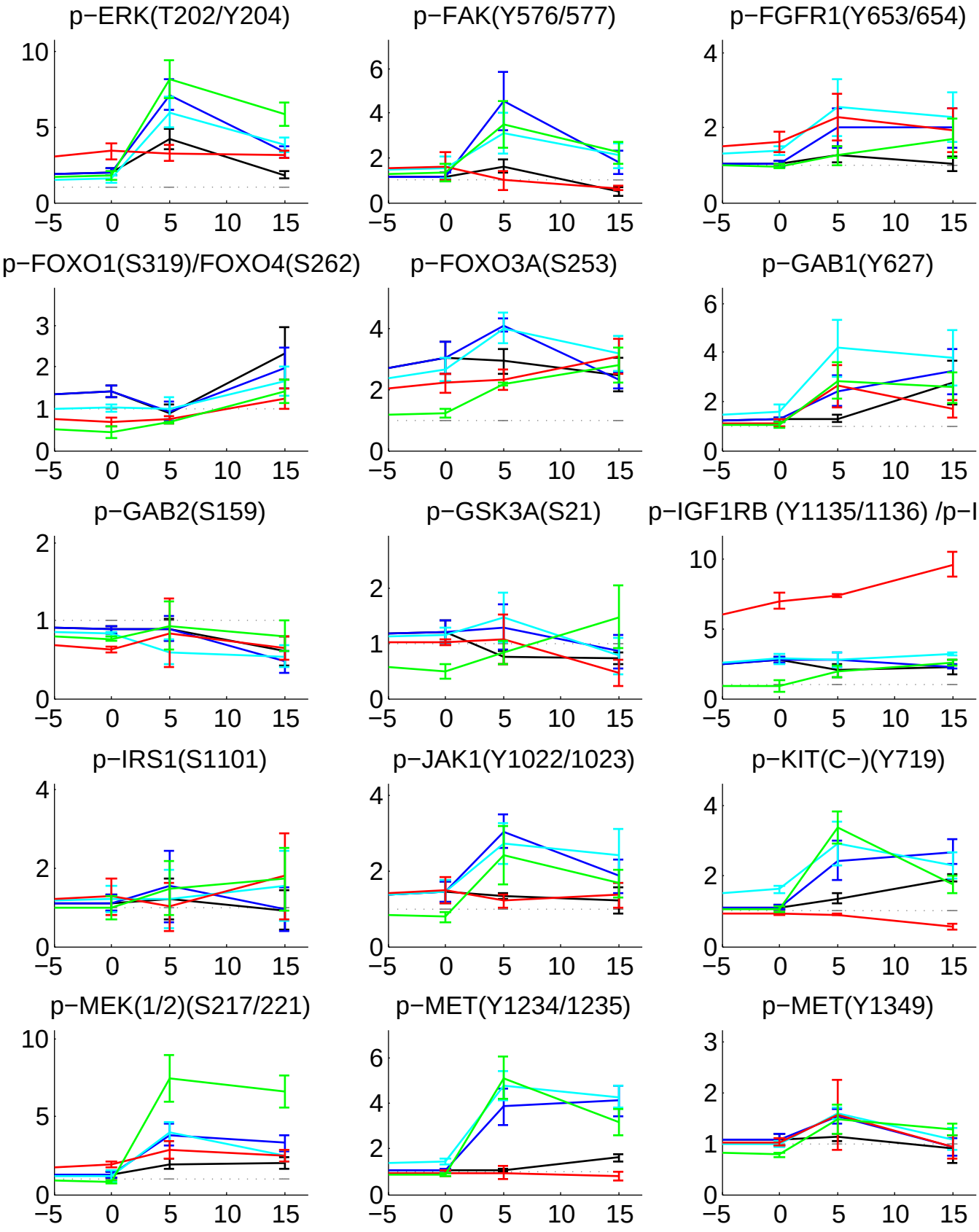
p−ERK(T202/Y204)
p−FAK(Y576/577)
p−FGFR1(Y653/654)
p−FOXO1(S319)/FOXO4(S262)
p−FOXO3A(S253)
p−GAB1(Y627)
p−GAB2(S159)
p−GSK3A(S21)
p−IGF1RB (Y1135/1136) /p−InsR…
p−IRS1(S1101)
p−JAK1(Y1022/1023)
p−KIT(C−)(Y719)
p−MEK(1/2)(S217/221)
p−MET(Y1234/1235)
p−MET(Y1349)

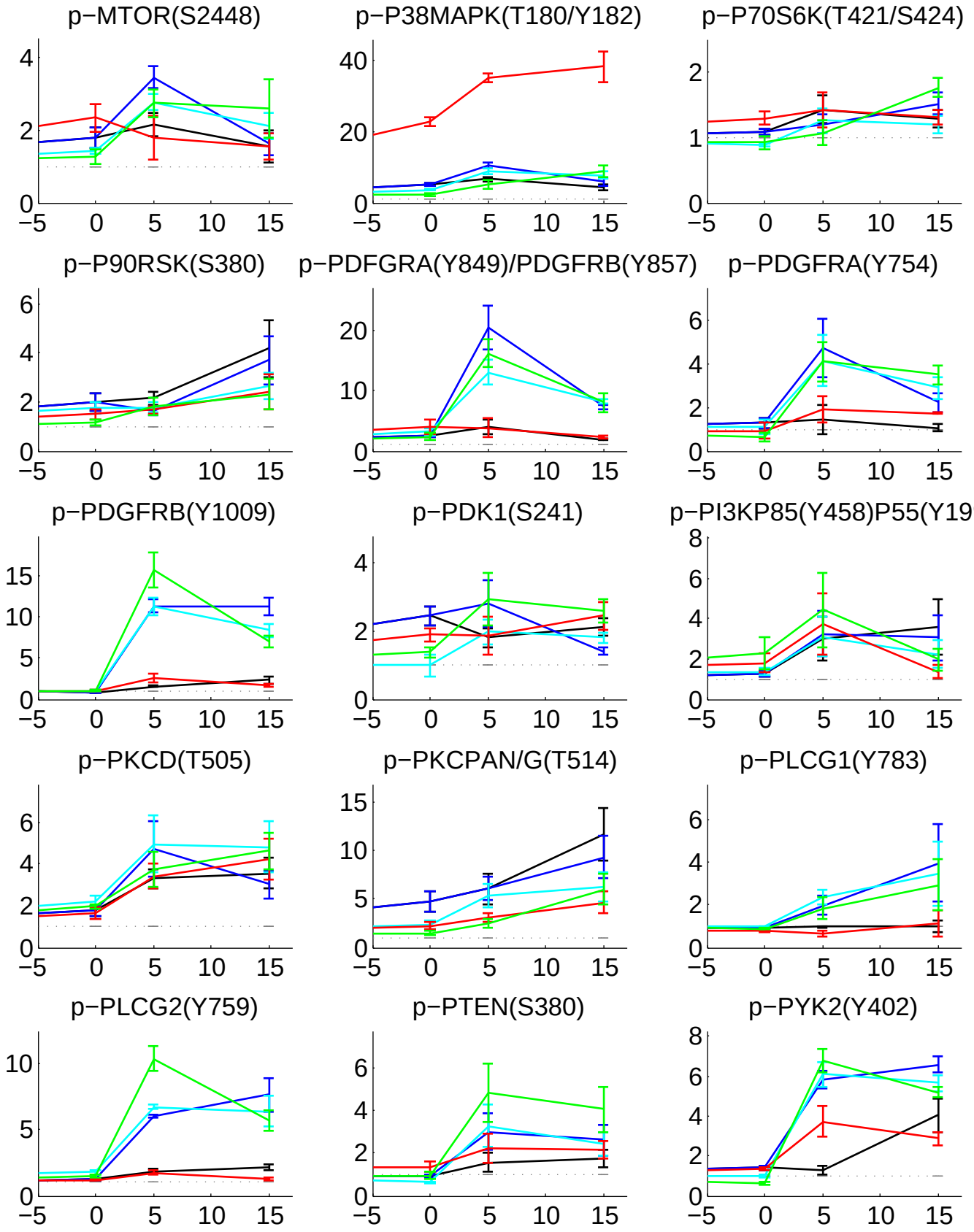
p−MTOR(S2448)
p−P38MAPK(T180/Y182)
p−P70S6K(T421/S424)
p−P90RSK(S380)
p−PDFGRA(Y849)/PDGFRB(Y857)
p−PDGFRA(Y754)
p−PDGFRB(Y1009)
p−PDK1(S241)
p−PI3KP85(Y458)P55(Y199)
p−PKCD(T505)
p−PKCPAN/G(T514)
p−PLCG1(Y783)
p−PLCG2(Y759)
p−PTEN(S380)
p−PYK2(Y402)

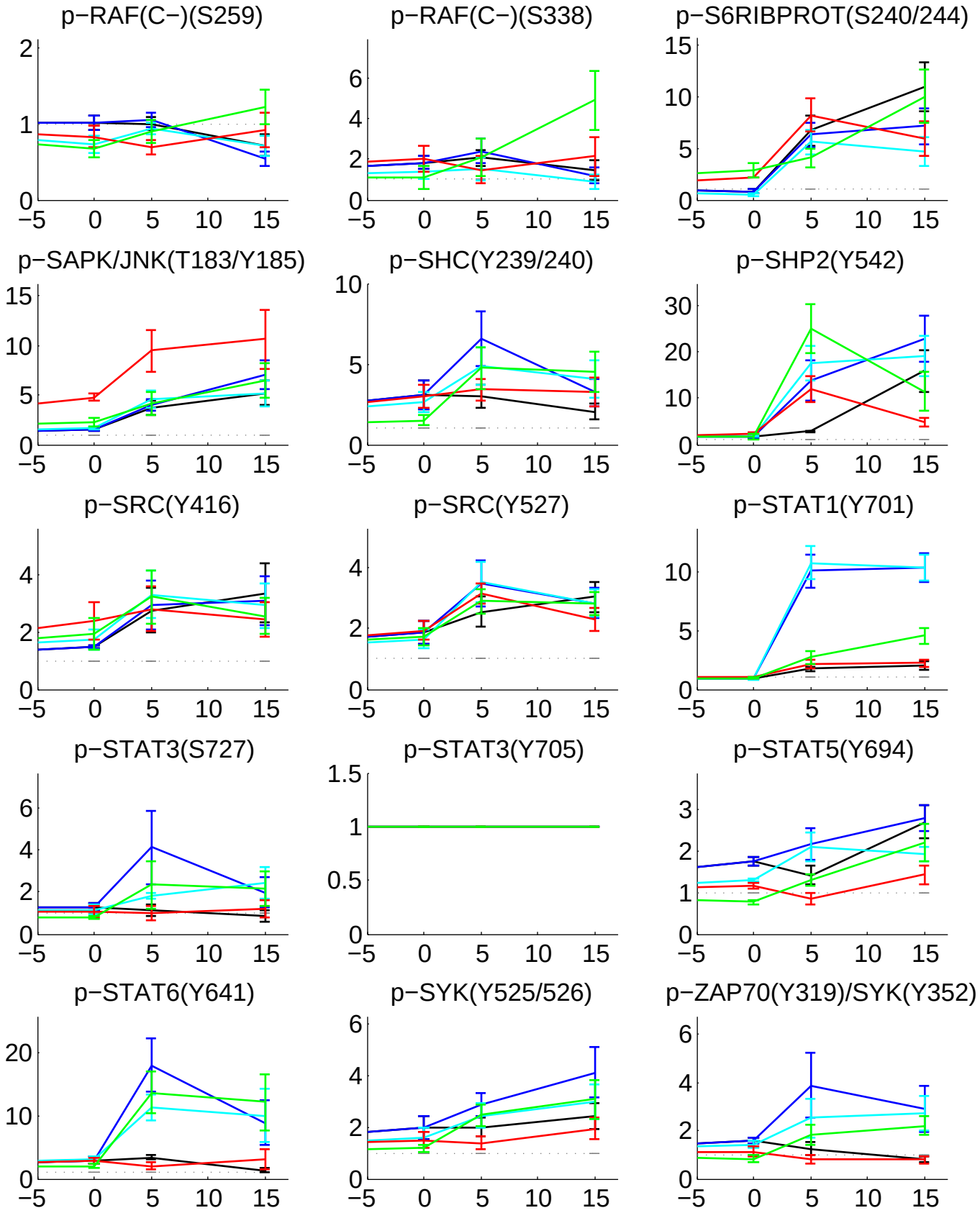
p−RAF(C−)(S259)
p−RAF(C−)(S338)
p−S6RIBPROT(S240/244)
p−SAPK/JNK(T183/Y185)
p−SHC(Y239/240)
p−SHP2(Y542)
p−SRC(Y416)
p−SRC(Y527)
p−STAT1(Y701)
p−STAT3(S727)
p−STAT3(Y705)
p−STAT5(Y694)
p−STAT6(Y641)
p−SYK(Y525/526)
p−ZAP70(Y319)/SYK(Y352)

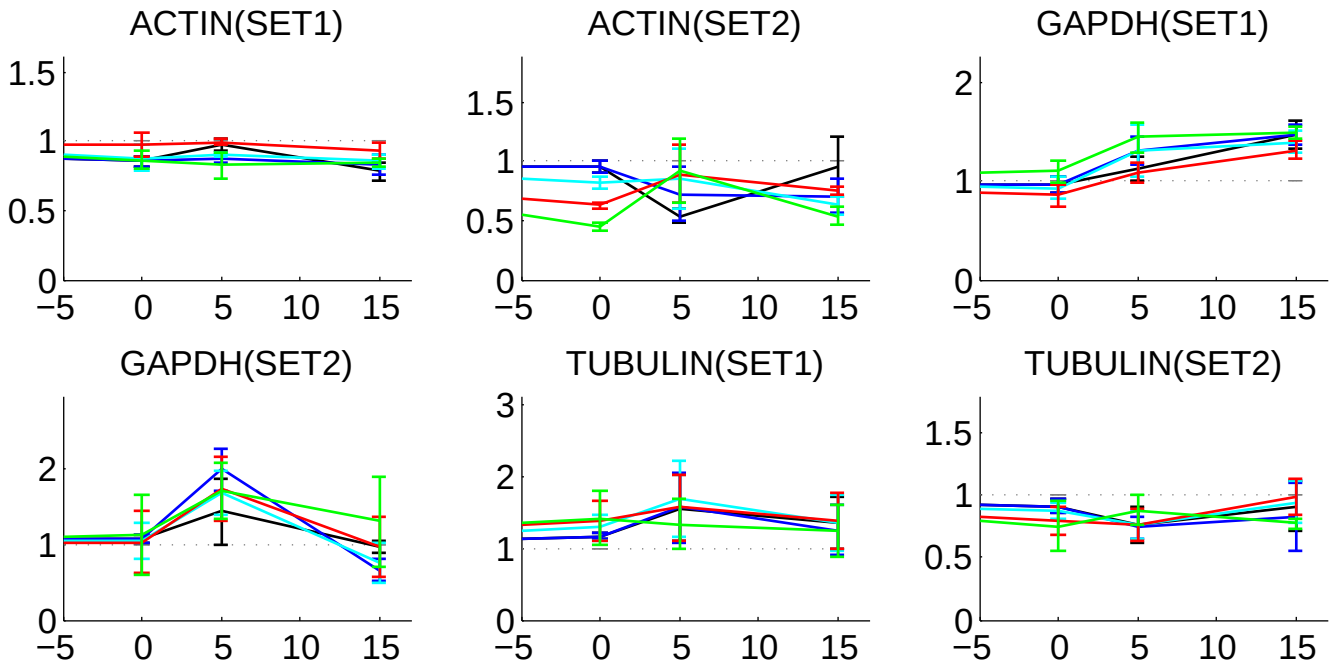
ACTIN(SET1)
ACTIN(SET2)
GAPDH(SET1)
GAPDH(SET2)
TUBULIN(SET1)
TUBULIN(SET2)
−5
0
5
10
15

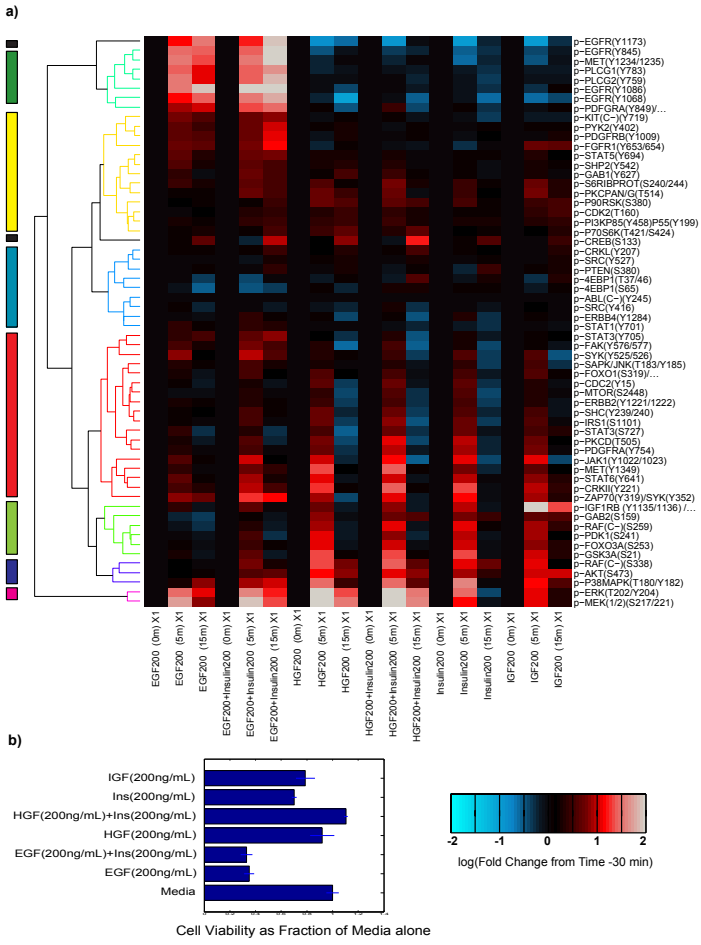

Figure 8: *(a) The clustergram of phosphorylation kinetics is shown for Panel 1 of growth factors. (b) Relative cell viability is shown after 24 hours perturbation, in comparison to media alone.*

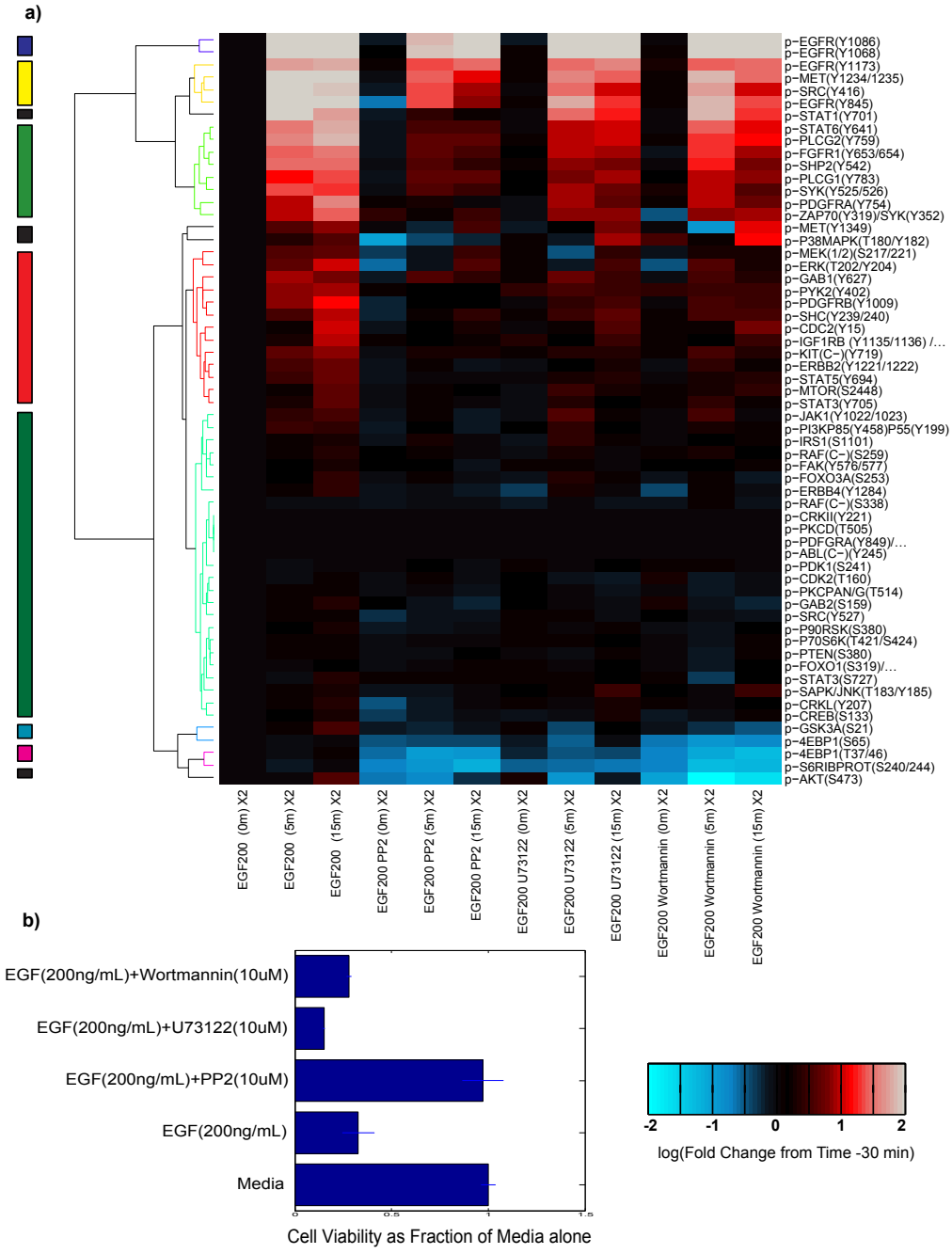

Figure 9: *(a) The clustergram of phosphorylation kinetics is shown for Panel 2 of small molecules. (b) Relative cell viability is shown after 24 hours perturbation, in comparison to media alone.*

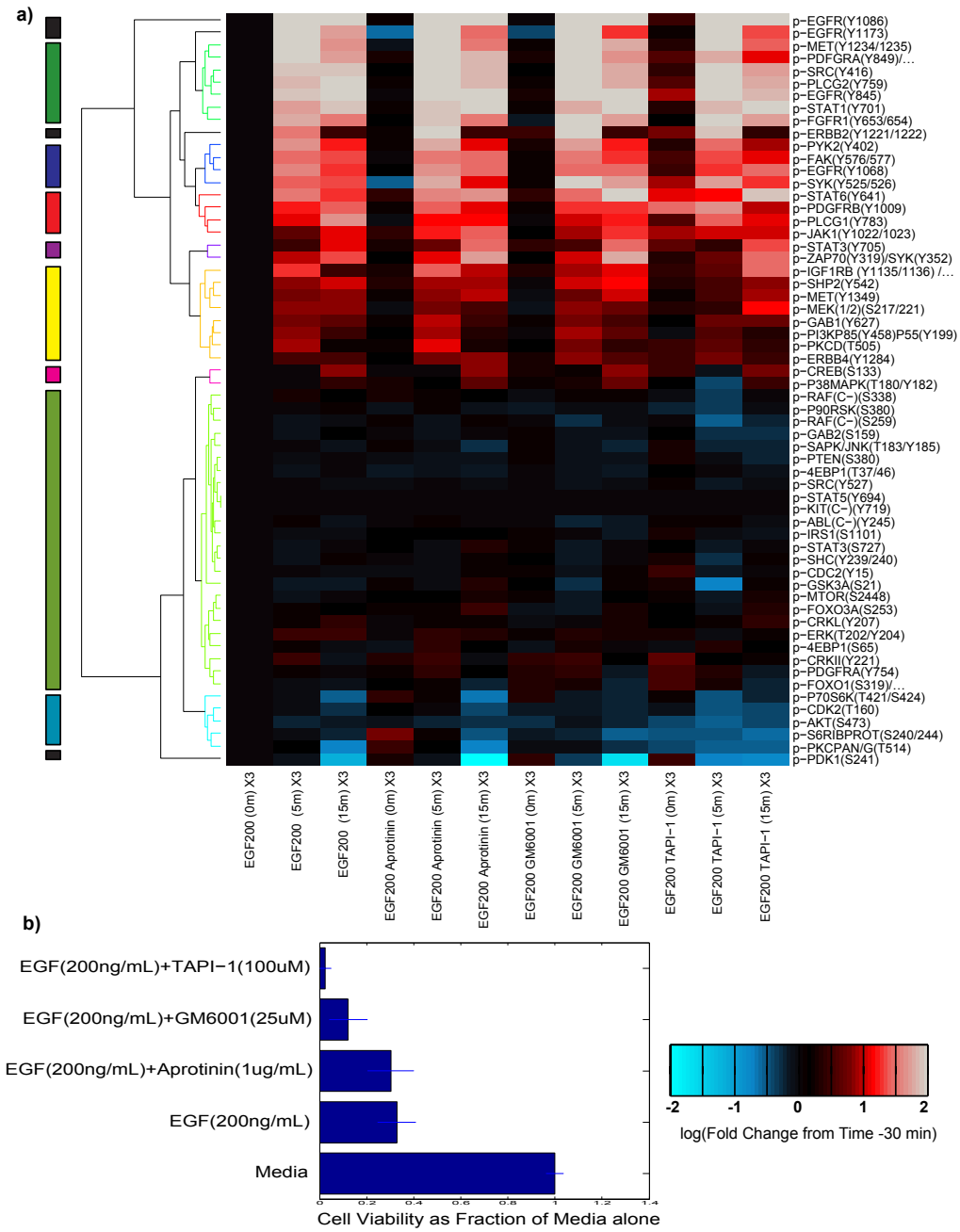

Figure 10: *(a) The clustergram of phosphorylation kinetics is shown for Panel 3 of small molecules. (b) Relative cell viability is shown after 24 hours perturbation, in comparison to media alone.*

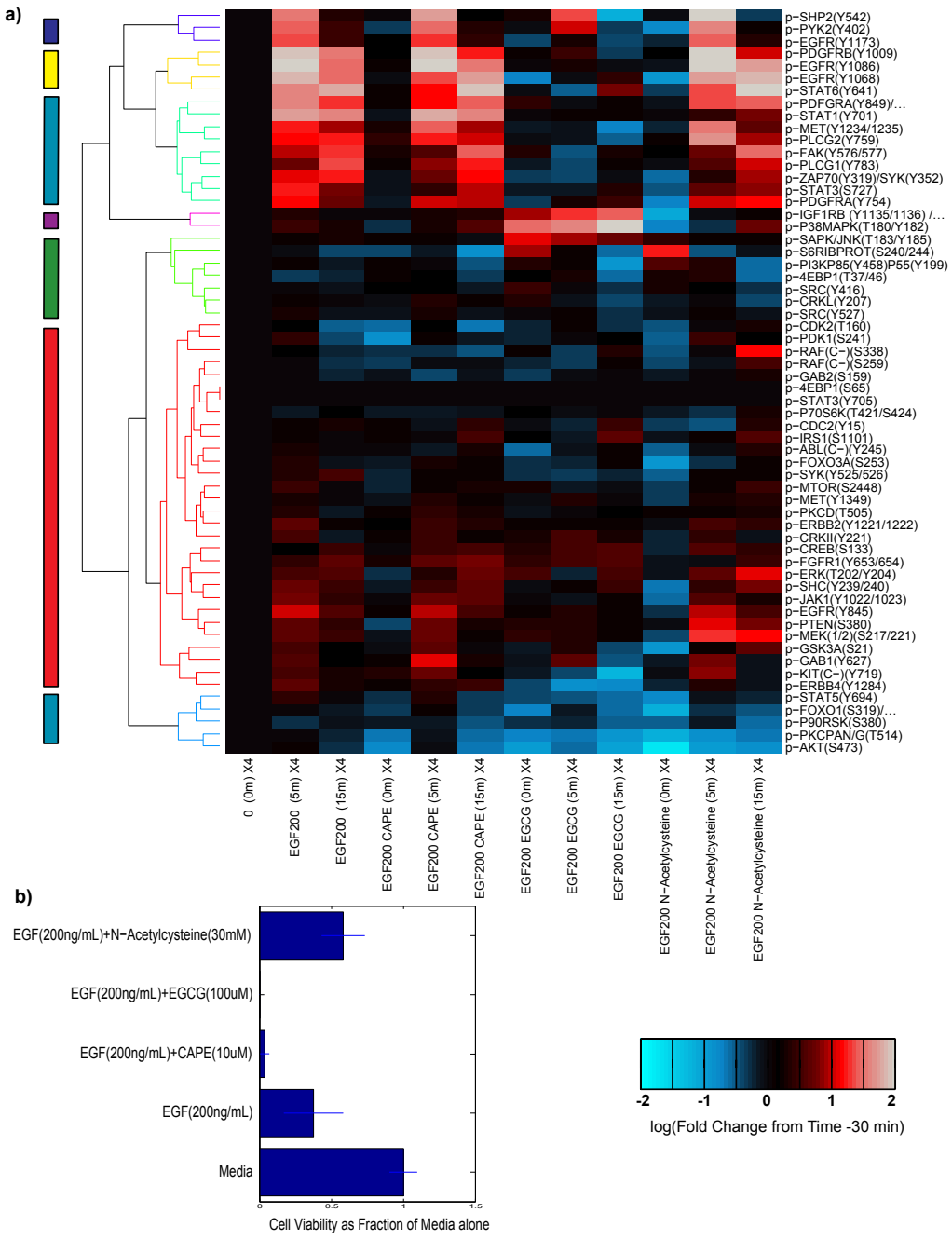

Figure 11: *a) The clustergram of phosphorylation kinetics is shown for Panel 4 of small molecules. b) Relative cell viability is shown after 24 hours perturbation, in comparison to media alone.*

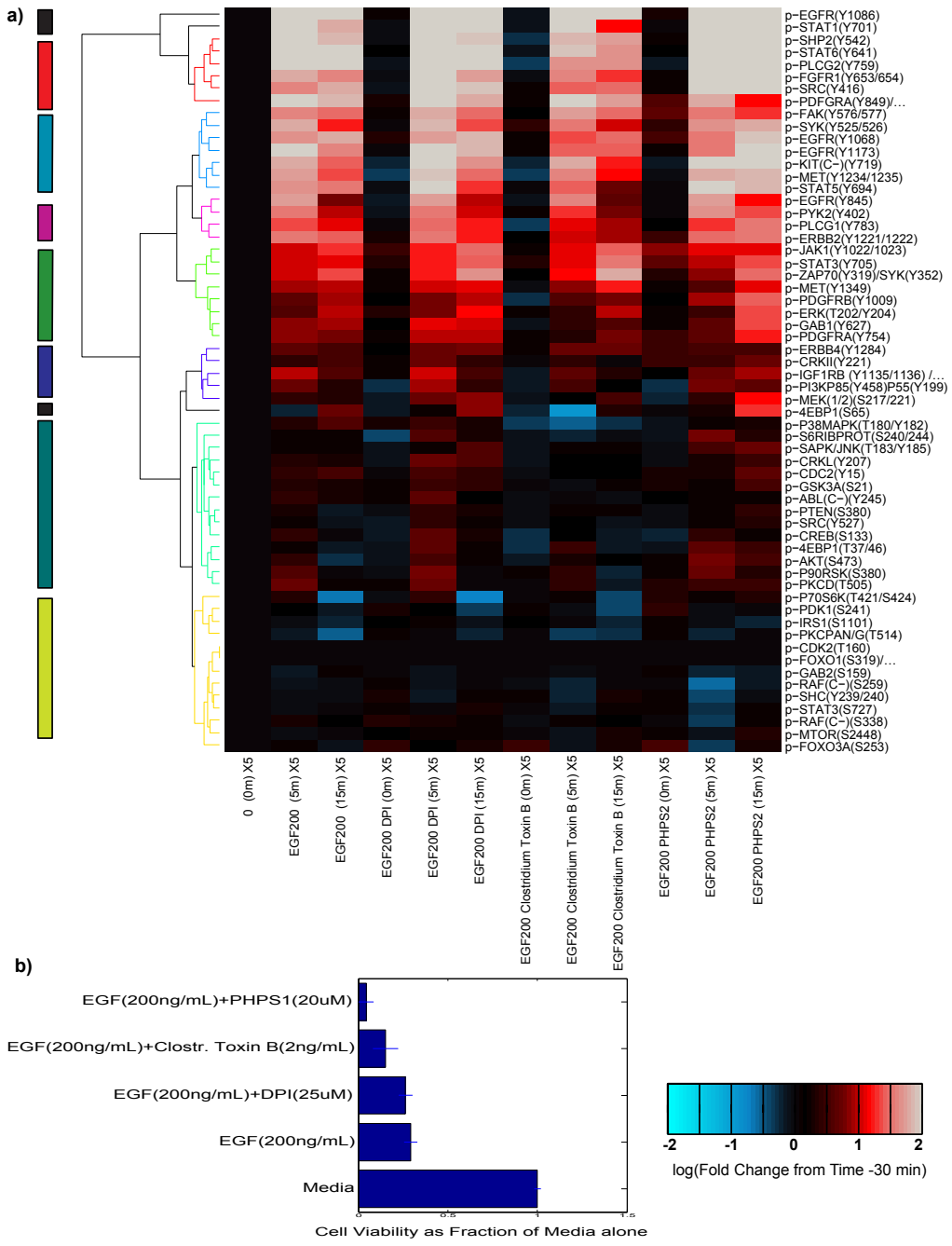

Figure 12: *(a) The clustergram of phosphorylation kinetics is shown for Panel 5 of small molecules. (b) Relative cell viability is shown after 24 hours perturbation, in comparison to media alone.*

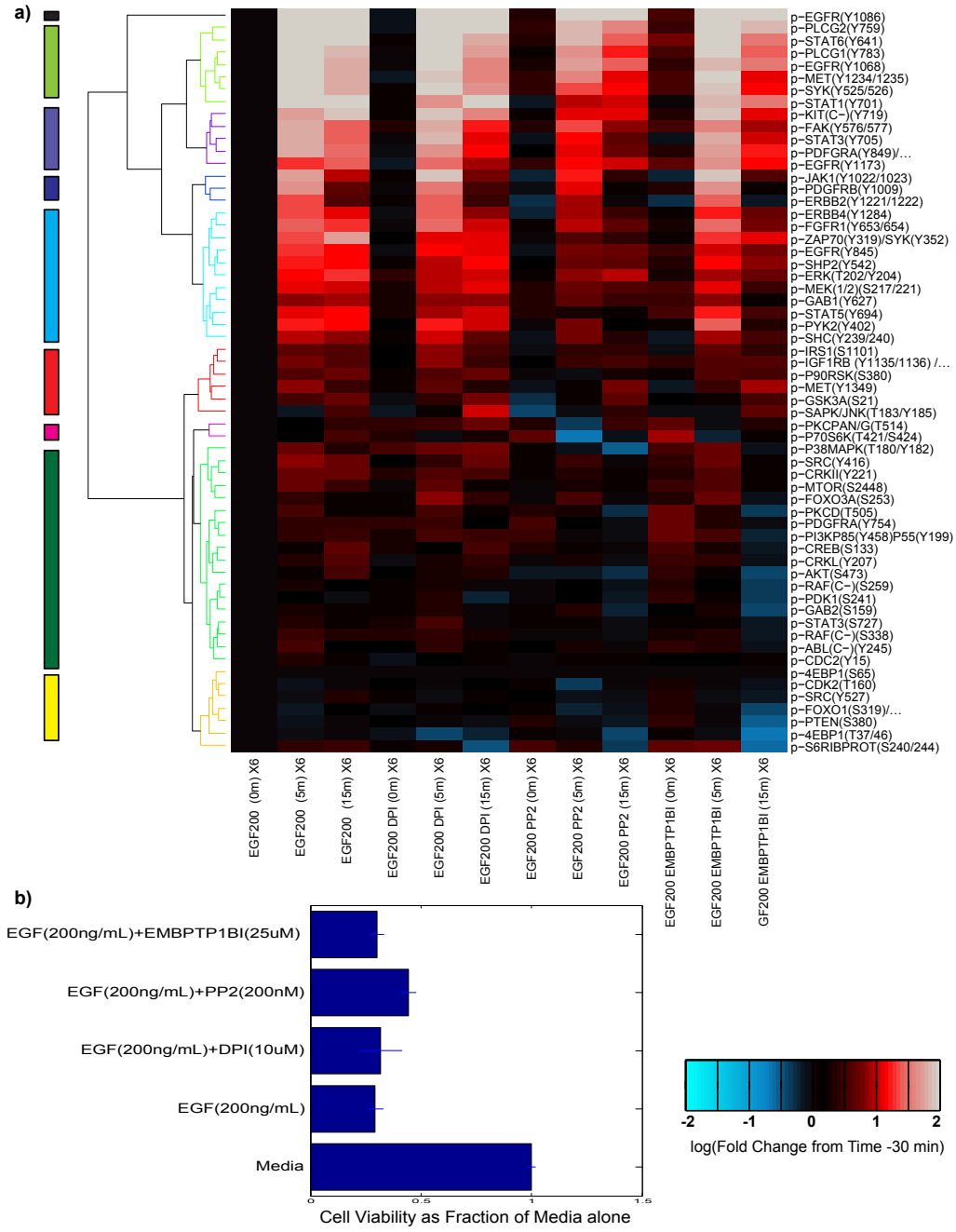

Figure 13: *(a) The clustergram of phosphorylation kinetics is shown for Panel 6 of small molecules. (b) Relative cell viability is shown after 24 hours perturbation, in comparison to media alone.*

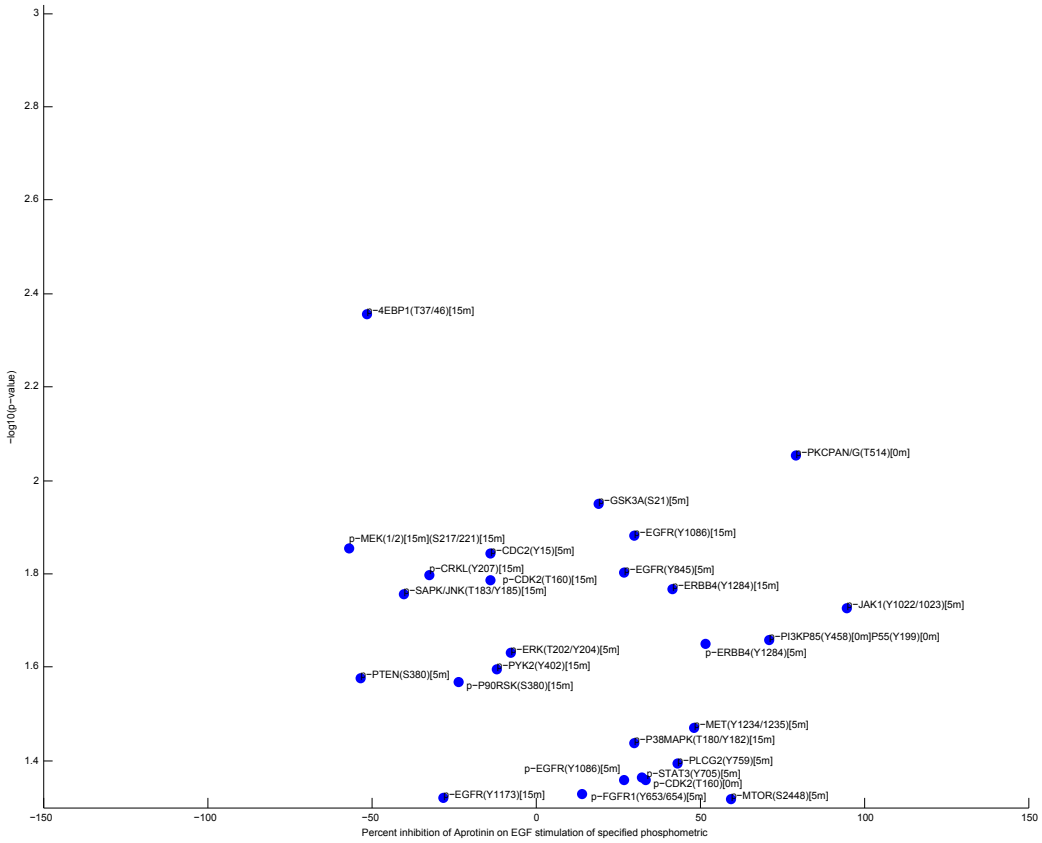

Figure 14: *Volcano plots for each of inhibitor combination. The x-axis reflects the percent inhibition of each phosphometric given the addition of the chemical perturbant. The y-axis reflects the scaled p-value.*

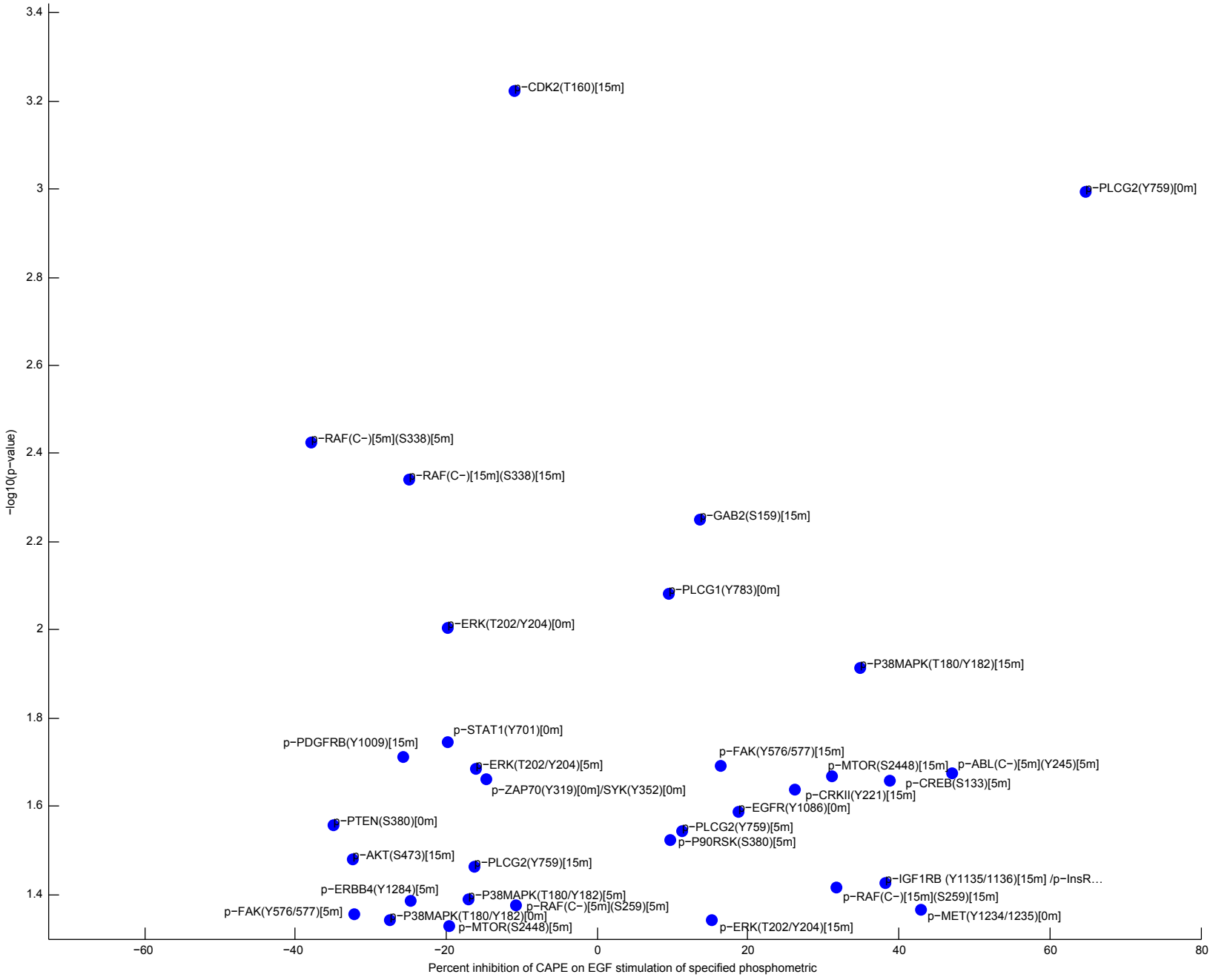
p−CDK2(T160)[15m]
p−PLCG2(Y759)[0m]
p−RAF(C−)[5m](S338)[5m]
p−RAF(C−)[15m](S338)[15m]
p−GAB2(S159)[15m]
p−PLCG1(Y783)[0m]
p−ERK(T202/Y204)[0m]
p−P38MAPK(T180/Y182)[15m]
p−STAT1(Y701)[0m]
p−PDGFRB(Y1009)[15m]
p−FAK(Y576/577)[15m]
p−MTOR(S2448)[15m]
p−ABL(C−)[5m](Y245)[5m]
p−ERK(T202/Y204)[5m]
p−CREB(S133)[5m]
p−ZAP70(Y319)[0m]/SYK(Y352)[0m]
p−CRKII(Y221)[15m]
p−EGFR(Y1086)[0m]
p−PTEN(S380)[0m]
p−PLCG2(Y759)[5m]
p−P90RSK(S380)[5m]
p−AKT(S473)[15m]
p−PLCG2(Y759)[15m]
p−IGF1RB (Y1135/1136)[15m] /p−InsR…
p−ERBB4(Y1284)[5m]
p−P38MAPK(T180/Y182)[5m]
p−RAF(C−)[15m](S259)[15m]
p−FAK(Y576/577)[5m]
p−RAF(C−)[5m](S259)[5m]
p−MET(Y1234/1235)[0m]
p−P38MAPK(T180/Y182)[0m]
p−MTOR(S2448)[5m]
p−ERK(T202/Y204)[15m]
3.4
3.2
3
2.8
2.6
2.4
2.2
2
1.8
1.6
1.4
−log10(p−value)
−60
−40
−20
0
20
40
60
80
Percent inhibition of CAPE on EGF stimulation of specified phosphometric

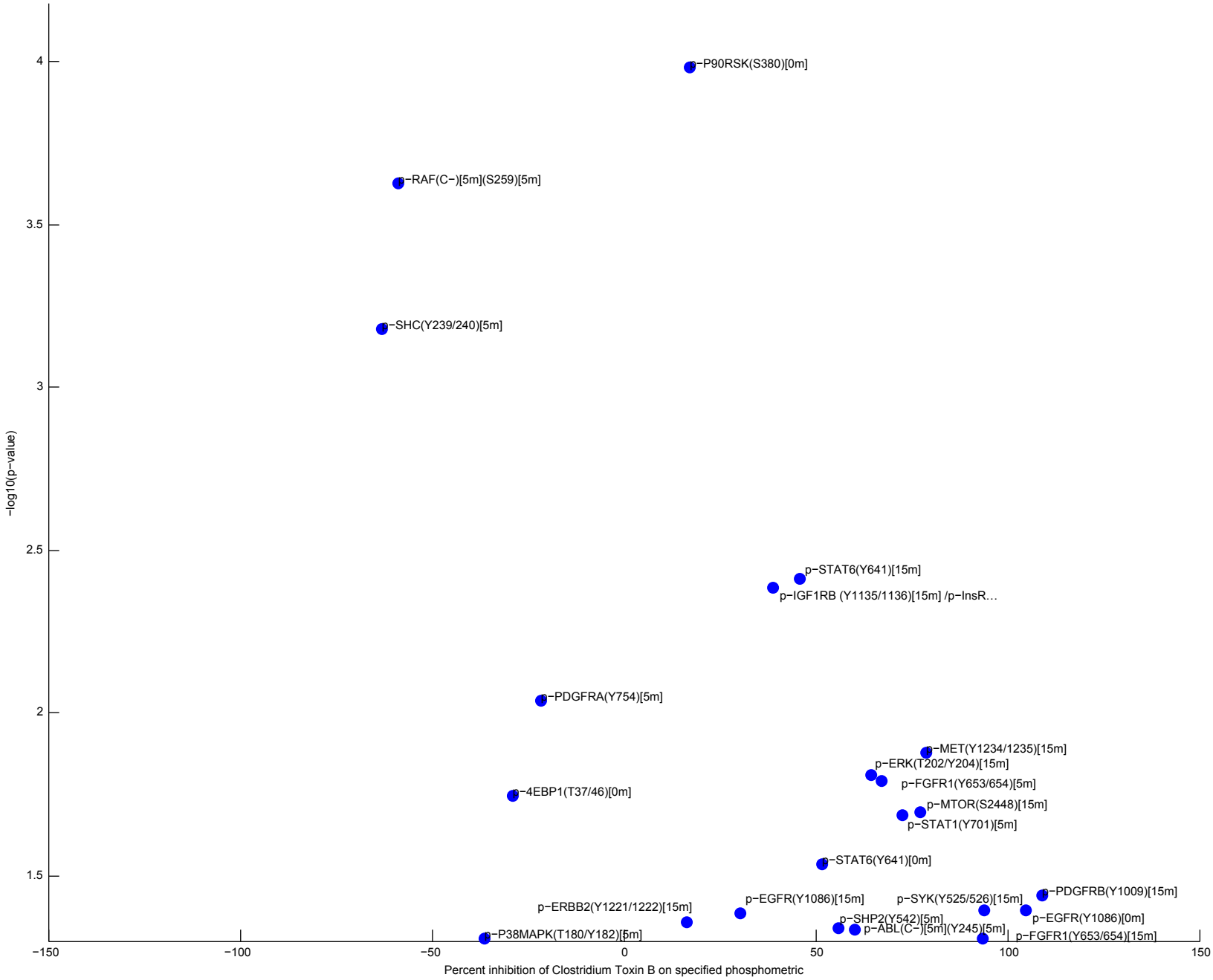
p−P90RSK(S380)[0m]
p−RAF(C−)[5m](S259)[5m]
p−SHC(Y239/240)[5m]
p−STAT6(Y641)[15m]
p−IGF1RB (Y1135/1136)[15m] /p−InsR…
p−PDGFRA(Y754)[5m]
p−MET(Y1234/1235)[15m]
p−ERK(T202/Y204)[15m]
p−FGFR1(Y653/654)[5m]
p−4EBP1(T37/46)[0m]
p−MTOR(S2448)[15m]
p−STAT1(Y701)[5m]
p−STAT6(Y641)[0m]
p−PDGFRB(Y1009)[15m]
p−EGFR(Y1086)[15m]
p−SYK(Y525/526)[15m]
p−ERBB2(Y1221/1222)[15m]
p−SHP2(Y542)[5m]
p−EGFR(Y1086)[0m]
p−ABL(C−)[5m](Y245)[5m]
p−P38MAPK(T180/Y182)[5m]
p−FGFR1(Y653/654)[15m]
4
3.5
3
2.5
2
1.5
−log10(p−value)
−150
−100
−50
0
50
100
150
Percent inhibition of Clostridium Toxin B on specified phosphometric

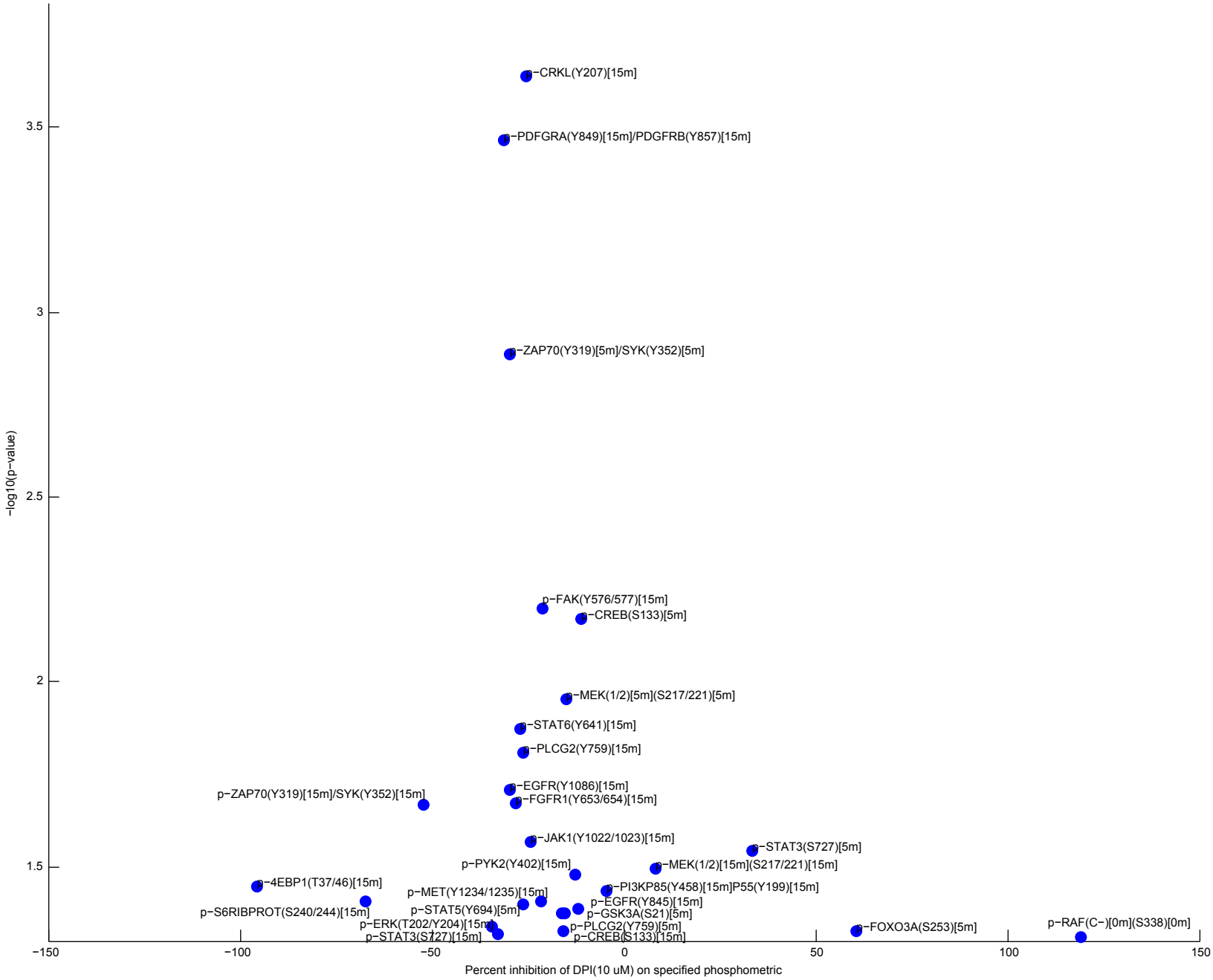
p−CRKL(Y207)[15m]
p−PDFGRA(Y849)[15m]/PDGFRB(Y857)[15m]
p−ZAP70(Y319)[5m]/SYK(Y352)[5m]
p−FAK(Y576/577)[15m]
p−CREB(S133)[5m]
p−MEK(1/2)[5m](S217/221)[5m]
p−STAT6(Y641)[15m]
p−PLCG2(Y759)[15m]
p−EGFR(Y1086)[15m]
p−FGFR1(Y653/654)[15m]
p−ZAP70(Y319)[15m]/SYK(Y352)[15m]
p−JAK1(Y1022/1023)[15m]
p−STAT3(S727)[5m]
p−PYK2(Y402)[15m]
p−MEK(1/2)[15m](S217/221)[15m]
p−4EBP1(T37/46)[15m]
p−PI3KP85(Y458)[15m]P55(Y199)[15m]
p−MET(Y1234/1235)[15m]
p−EGFR(Y845)[15m]
p−S6RIBPROT(S240/244)[15m]
p−STAT5(Y694)[5m]
p−GSK3A(S21)[5m]
p−ERK(T202/Y204)[15m]
p−PLCG2(Y759)[5m]
p−STAT3(S727)[15m]
p−CREB(S133)[15m]
p−FOXO3A(S253)[5m]
p−RAF(C−)[0m](S338)[0m]
3.5
3
2.5
2
1.5
−log10(p−value)
−150
−100
−50
0
50
100
150
Percent inhibition of DPI(10 uM) on specified phosphometric

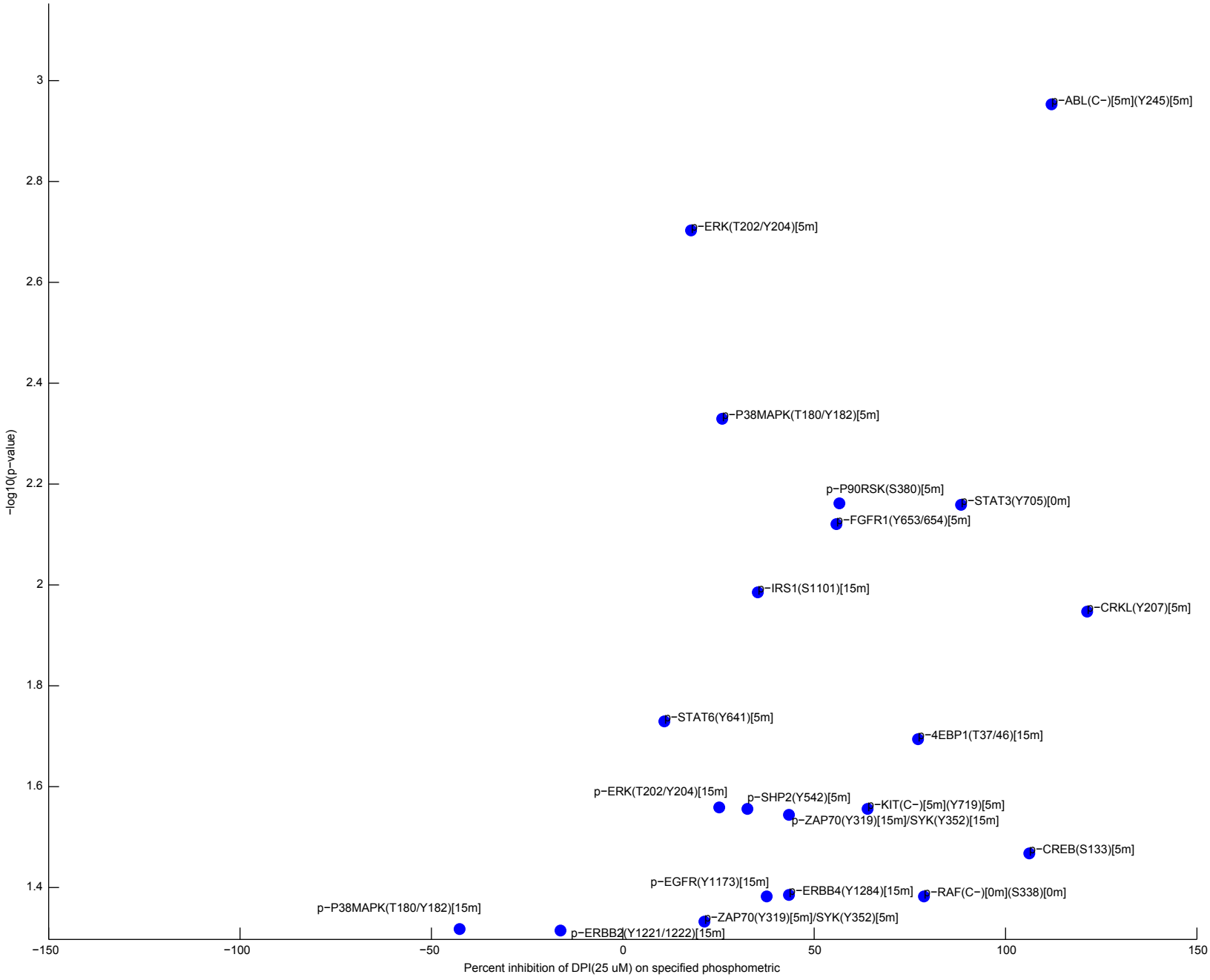
p−ABL(C−)[5m](Y245)[5m]
p−ERK(T202/Y204)[5m]
p−P38MAPK(T180/Y182)[5m]
p−P90RSK(S380)[5m]
p−STAT3(Y705)[0m]
p−FGFR1(Y653/654)[5m]
p−IRS1(S1101)[15m]
p−CRKL(Y207)[5m]
p−STAT6(Y641)[5m]
p−4EBP1(T37/46)[15m]
p−ERK(T202/Y204)[15m]
p−SHP2(Y542)[5m]
p−KIT(C−)[5m](Y719)[5m]
p−ZAP70(Y319)[15m]/SYK(Y352)[15m]
p−CREB(S133)[5m]
p−EGFR(Y1173)[15m]
p−ERBB4(Y1284)[15m]
p−RAF(C−)[0m](S338)[0m]
p−P38MAPK(T180/Y182)[15m]
p−ZAP70(Y319)[5m]/SYK(Y352)[5m]
p−ERBB2(Y1221/1222)[15m]
3
2.8
2.6
2.4
2.2
2
1.8
1.6
1.4
−log10(p−value)
−150
−100
−50
0
50
100
150
Percent inhibition of DPI(25 uM) on specified phosphometric

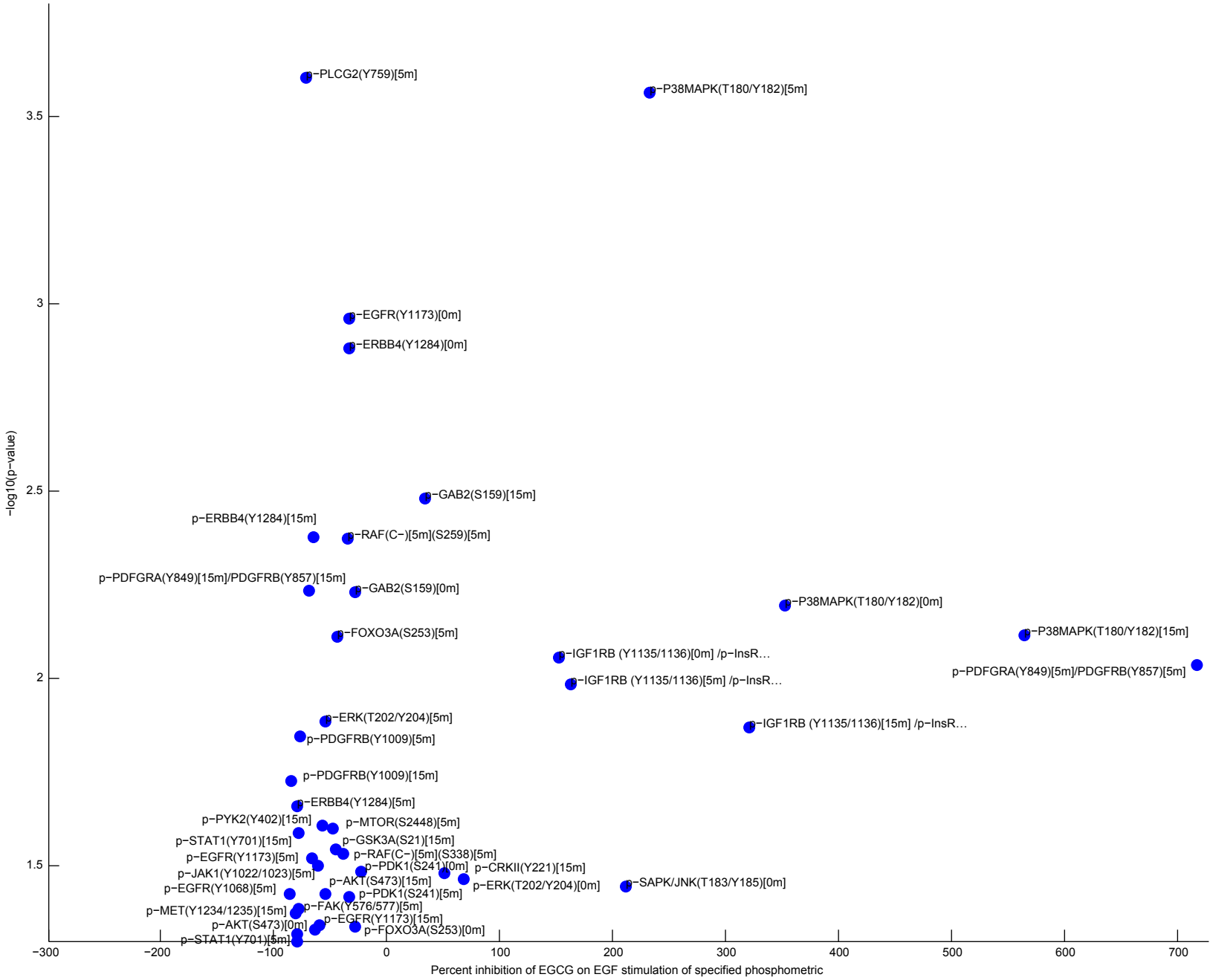
p−PLCG2(Y759)[5m]
p−P38MAPK(T180/Y182)[5m]
p−EGFR(Y1173)[0m]
p−ERBB4(Y1284)[0m]
p−GAB2(S159)[15m]
p−ERBB4(Y1284)[15m]
p−RAF(C−)[5m](S259)[5m]
p−PDGFRA(Y849)[15m]/PDGFRB(Y857)[15m]
p−GAB2(S159)[0m]
p−P38MAPK(T180/Y182)[0m]
p−P38MAPK(T180/Y182)[15m]
p−FOXO3A(S253)[5m]
p−IGF1RB (Y1135/1136)[0m] /p−InsR…
p−PDGFRA(Y849)[5m]/PDGFRB(Y857)[5m]
p−IGF1RB (Y1135/1136)[5m] /p−InsR…
p−ERK(T202/Y204)[5m]
p−IGF1RB (Y1135/1136)[15m] /p−InsR…
p−PDGFRB(Y1009)[5m]
p−PDGFRB(Y1009)[15m]
p−ERBB4(Y1284)[5m]
p−PYK2(Y402)[15m]
p−MTOR(S2448)[5m]
p−STAT1(Y701)[15m]
p−GSK3A(S21)[15m]
p−EGFR(Y1173)[5m]
p−RAF(C−)[5m](S338)[5m]
p−JAK1(Y1022/1023)[5m]
p−PDK1(S241)[0m]
p−CRKII(Y221)[15m]
p−EGFR(Y1068)[5m]
p−AKT(S473)[15m]
p−ERK(T202/Y204)[0m]
p−SAPK/JNK(T183/Y185)[0m]
p−PDK1(S241)[5m]
p−MET(Y1234/1235)[15m]
p−FAK(Y576/577)[5m]
p−AKT(S473)[0m]
p−EGFR(Y1173)[15m]
p−STAT1(Y701)[5m]
p−FOXO3A(S253)[0m]
3.5
3
2.5
2
1.5
−log10(p−value)
−300
−200
−100
0
100
200
300
400
500
600
700
Percent inhibition of EGCG on EGF stimulation of specified phosphometric

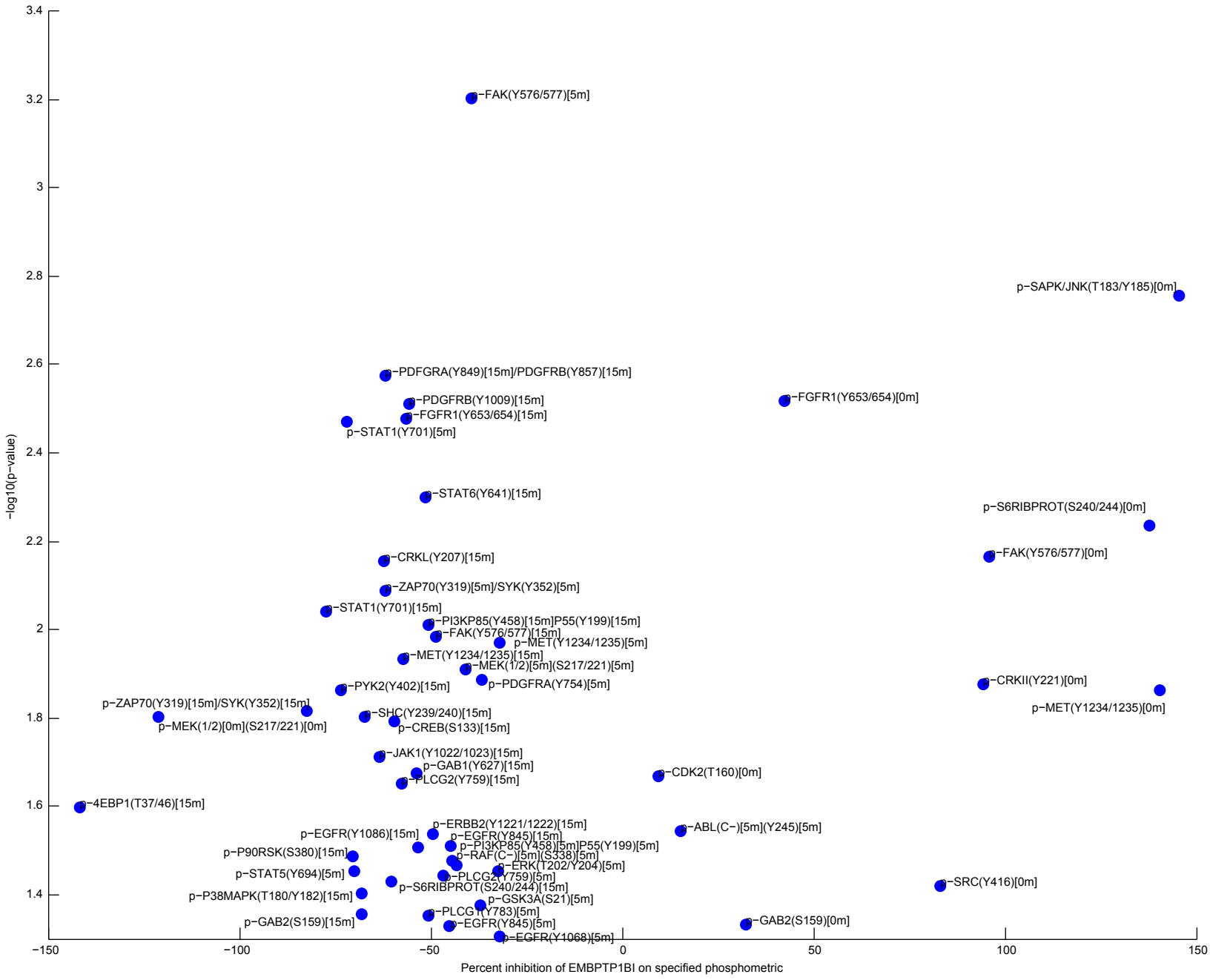
3.4
3.2
3
2.8
2.6
2.4
2.2
2
1.8
1.6
1.4
−log10(p−value)
−150
−100
−50
0
50
100
150
Percent inhibition of EMBPTP1BI on specified phosphometric
p−FAK(Y576/577)[5m]
p−SAPK/JNK(T183/Y185)[0m]
p−PDFGRA(Y849)[15m]/PDGFRB(Y857)[15m]
p−PDGFRB(Y1009)[15m]
p−FGFR1(Y653/654)[15m]
p−STAT1(Y701)[5m]
p−FGFR1(Y653/654)[0m]
p−STAT6(Y641)[15m]
p−S6RIBPROT(S240/244)[0m]
p−CRKL(Y207)[15m]
p−FAK(Y576/577)[0m]
p−ZAP70(Y319)[5m]/SYK(Y352)[5m]
p−STAT1(Y701)[15m]
p−PI3KP85(Y458)[15m]P55(Y199)[15m]
p−FAK(Y576/577)[15m]
p−MET(Y1234/1235)[5m]
p−MET(Y1234/1235)[15m]
p−MEK(1/2)[5m](S217/221)[5m]
p−PDGFRA(754)[5m]
p−CRKII(Y221)[0m]
p−PYK2(Y402)[15m]
p−ZAP70(Y319)[15m]/SYK(Y352)[15m]
p−MET(Y1234/1235)[0m]
p−SHC(Y239/240)[15m]
p−MEK(1/2)[0m](S217/221)[0m]
p−CREB(S133)[15m]
p−JAK1(Y1022/1023)[15m]
p−GAB1(Y627)[15m]
p−CDK2(T160)[0m]
p−PLCG2(Y759)[15m]
p−4EBP1(T37/46)[15m]
p−ERBB2(Y1221/1222)[15m]
p−ABL(C−)[5m](Y245)[5m]
p−EGFR(Y1086)[15m]
p−EGFR(Y845)[15m]
p−PI3KP85(Y458)[5m]P55(Y199)[5m]
p−P90RSK(S380)[15m]
p−RAF(C−)[5m](S338)[5m]
p−ERK(T202/Y204)[5m]
p−STAT5(Y694)[5m]
p−PLCG2(Y759)[5m]
p−SRC(Y416)[0m]
p−S6RIBPROT(S240/244)[15m]
p−P38MAPK(T180/Y182)[15m]
p−GSK3A(S21)[5m]
p−PLCG1(Y783)[5m]
p−GAB2(S159)[15m]
p−EGFR(Y845)[5m]
p−GAB2(S159)[0m]
p−EGFR(Y1068)[5m]

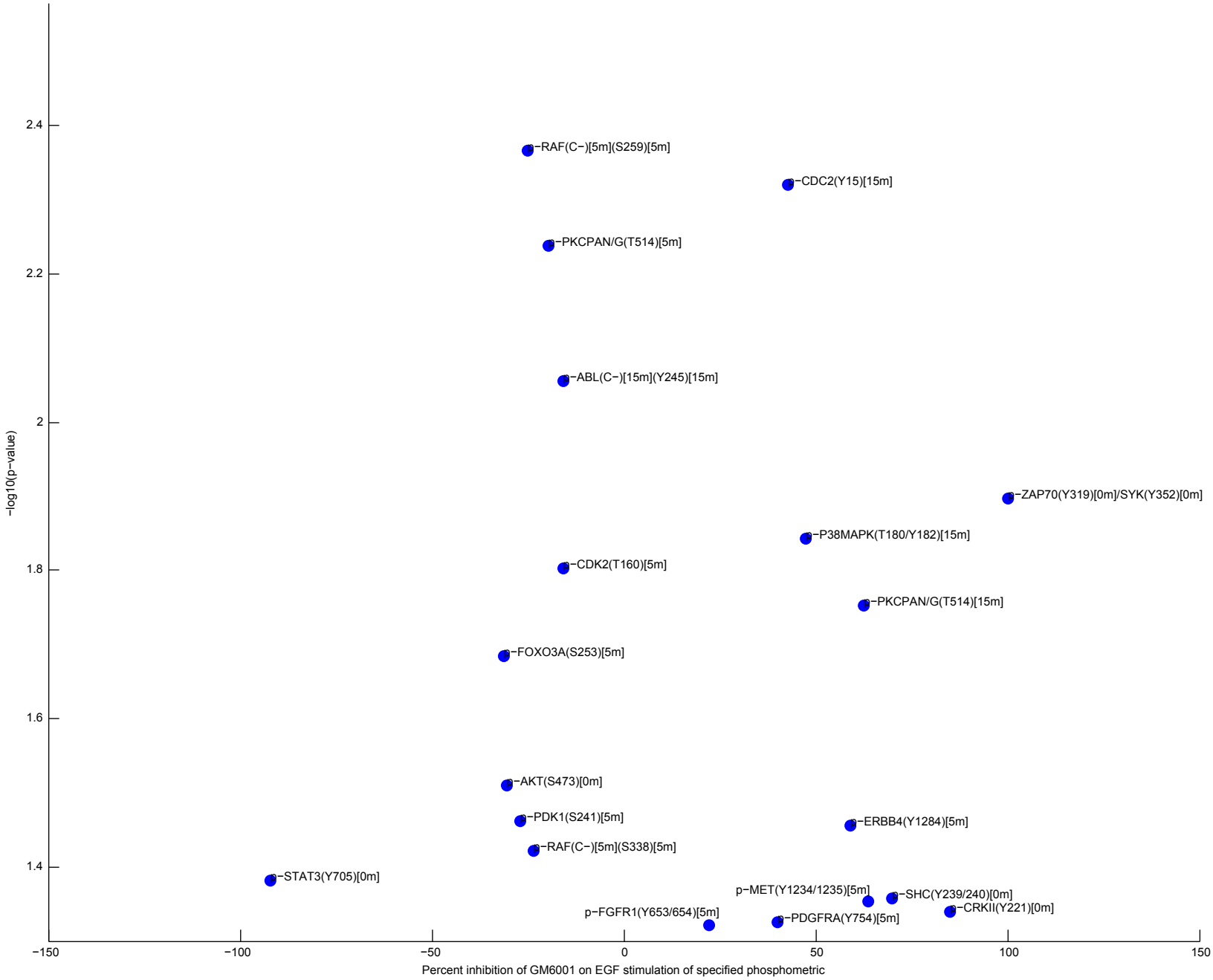
p−RAF(C−)[5m](S259)[5m]
p−CDC2(Y15)[15m]
p−PKCPAN/G(T514)[5m]
p−ABL(C−)[15m](Y245)[15m]
p−ZAP70(Y319)[0m]/SYK(Y352)[0m]
p−P38MAPK(T180/Y182)[15m]
p−CDK2(T160)[5m]
p−PKCPAN/G(T514)[15m]
p−FOXO3A(S253)[5m]
p−AKT(S473)[0m]
p−PDK1(S241)[5m]
p−ERBB4(Y1284)[5m]
p−RAF(C−)[5m](S338)[5m]
p−STAT3(Y705)[0m]
p−MET(Y1234/1235)[5m]
p−SHC(Y239/240)[0m]
p−CRKII(Y221)[0m]
p−FGFR1(Y653/654)[5m]
p−PDGFRA(Y754)[5m]
2.4
2.2
2
1.8
1.6
1.4
−log10(p−value)
−150
−100
−50
0
50
100
150
Percent inhibition of GM6001 on EGF stimulation of specified phosphometric

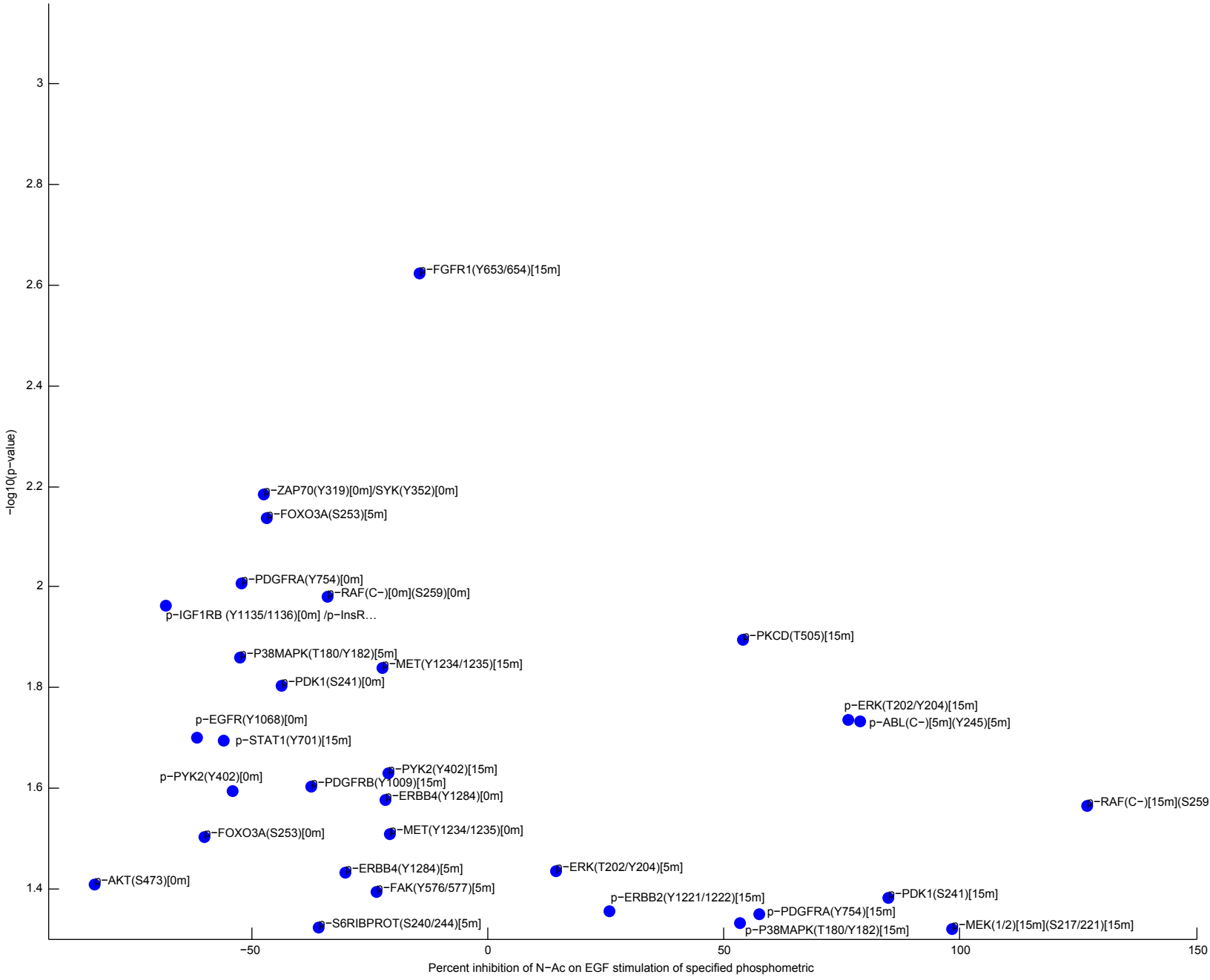
−log10(p−value)
3
2.8
2.6
2.4
2.2
2
1.8
1.6
1.4
p−FGFR1(Y653/654)[15m]
p−ZAP70(Y319)[0m]/SYK(Y352)[0m]
p−FOXO3A(S253)[5m]
p−PDGFRA(Y754)[0m]
p−RAF(C−)[0m](S259)[0m]
p−IGF1RB (Y1135/1136)[0m] /p−InsR…
p−PKCD(T505)[15m]
p−P38MAPK(T180/Y182)[5m]
p−MET(Y1234/1235)[15m]
p−PDK1(S241)[0m]
p−ERK(T202/Y204)[15m]
p−EGFR(Y1068)[0m]
p−ABL(C−)[5m](Y245)[5m]
p−STAT1(Y701)[15m]
p−PYK2(Y402)[15m]
p−PYK2(Y402)[0m]
p−PDGFRB(Y1009)[15m]
p−ERBB4(Y1284)[0m]
p−RAF(C−)[15m](S259
p−FOXO3A(S253)[0m]
p−MET(Y1234/1235)[0m]
p−ERBB4(Y1284)[5m]
p−ERK(T202/Y204)[5m]
p−AKT(S473)[0m]
p−FAK(Y576/577)[5m]
p−PDK1(S241)[15m]
p−ERBB2(Y1221/1222)[15m]
p−PDGFRA(Y754)[15m]
p−S6RIBPROT(S240/244)[5m]
p−P38MAPK(T180/Y182)[15m]
p−MEK(1/2)[15m](S217/221)[15m]
−50
0
50
100
150
Percent inhibition of N−Ac on EGF stimulation of specified phosphometric

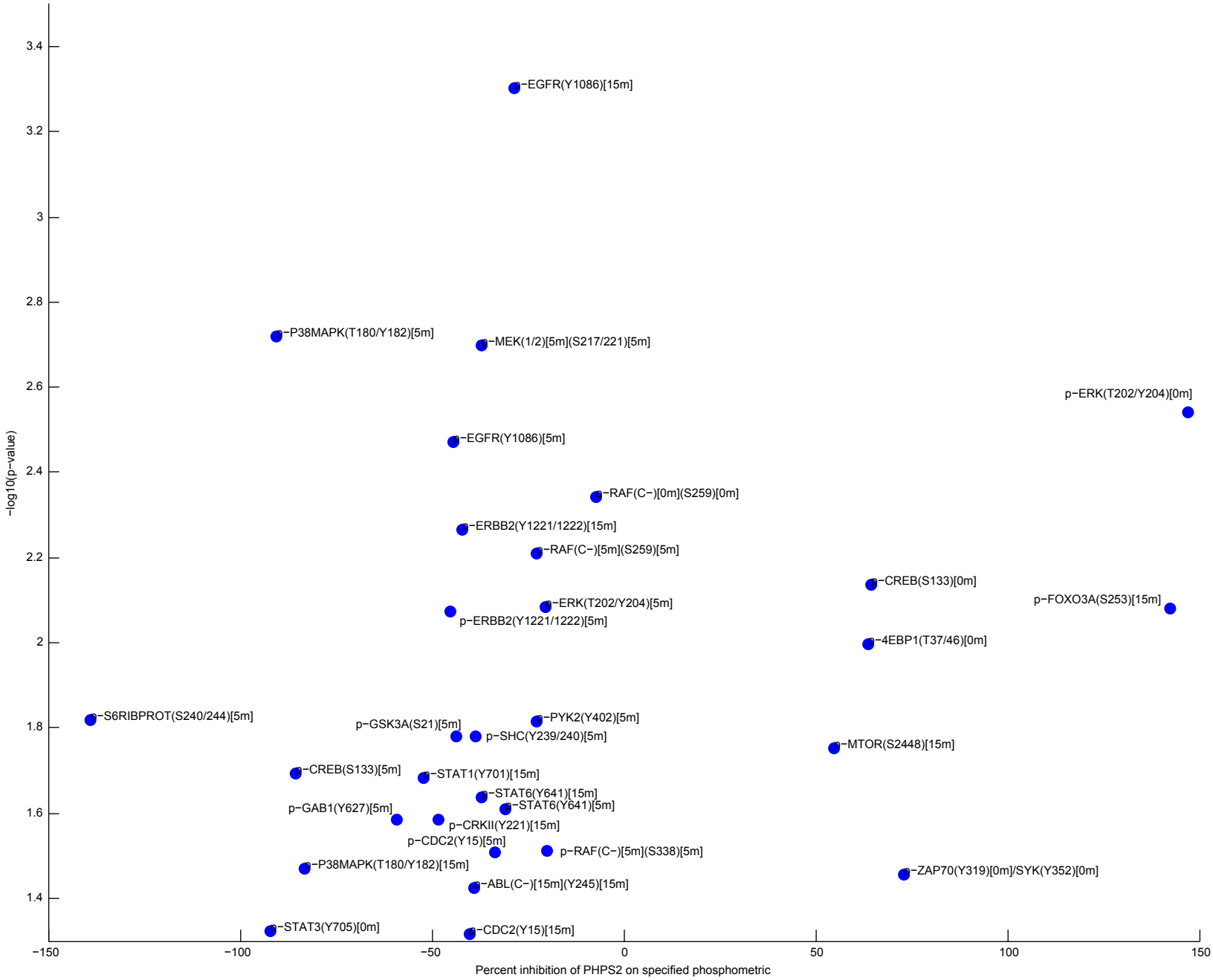
p−EGFR(Y1086)[15m]
p−P38MAPK(T180/Y182)[5m]
p−MEK(1/2)[5m](S217/221)[5m]
p−ERK(T202/Y204)[0m]
p−EGFR(Y1086)[5m]
p−RAF(C−)[0m](S259)[0m]
p−ERBB2(Y1221/1222)[15m]
p−RAF(C−)[5m](S259)[5m]
p−CREB(S133)[0m]
p−FOXO3A(S253)[15m]
p−ERK(T202/Y204)[5m]
p−ERBB2(Y1221/1222)[5m]
p−4EBP1(T37/46)[0m]
p−S6RIBPROT(S240/244)[5m]
p−GSK3A(S21)[5m]
p−PYK2(Y402)[5m]
p−SHC(Y239/240)[5m]
p−MTOR(S2448)[15m]
p−CREB(S133)[5m]
p−STAT1(Y701)[15m]
p−STAT6(Y641)[15m]
p−GAB1(Y627)[5m]
p−STAT6(Y641)[5m]
p−CRKII(Y221)[15m]
p−CDC2(Y15)[5m]
p−RAF(C−)[5m](S338)[5m]
p−P38MAPK(T180/Y182)[15m]
p−ZAP70(Y319)[0m]/SYK(Y352)[0m]
p−ABL(C−)[15m](Y245)[15m]
p−STAT3(Y705)[0m]
p−CDC2(Y15)[15m]
3.4
3.2
3
2.8
2.6
2.4
2.2
2
1.8
1.6
1.4
−log10(p−value)
−150
−100
−50
0
50
100
150
Percent inhibition of PHPS2 on specified phosphometric

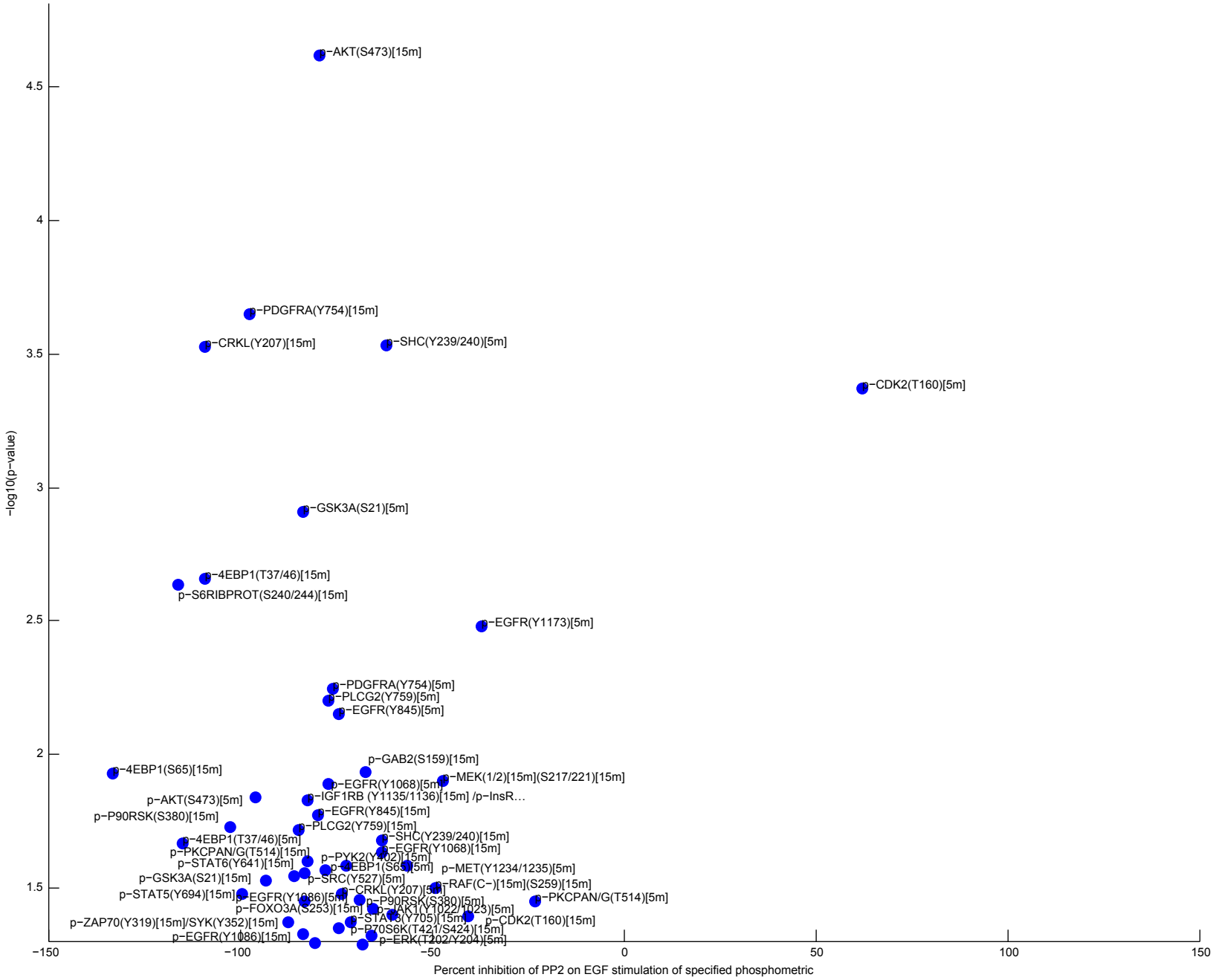
p−AKT(S473)[15m]
p−PDGFRA(Y754)[15m]
p−CRKL(Y207)[15m]
p−SHC(Y239/240)[5m]
p−CDK2(T160)[5m]
p−GSK3A(S21)[5m]
p−4EBP1(T37/46)[15m]
p−S6RIBPROT(S240/244)[15m]
p−EGFR(Y1173)[5m]
p−PDGFRA(Y754)[5m]
p−PLCG2(Y759)[5m]
p−EGFR(Y845)[5m]
p−GAB2(S159)[15m]
p−4EBP1(S65)[15m]
p−MEK(1/2)[15m](S217/221)[15m]
p−EGFR(Y1068)[5m]
p−AKT(S473)[5m]
p−IGF1RB (Y1135/1136)[15m] /p−InsR…
p−P90RSK(S380)[15m]
p−EGFR(Y845)[15m]
p−PLCG2(Y759)[15m]
p−4EBP1(T37/46)[5m]
p−SHC(Y239/240)[15m]
p−PKCPAN/G(T514)[15m]
p−EGFR(Y1068)[15m]
p−STAT6(Y641)[15m]
p−PYK2(Y402)[15m]
p−4EBP1(S65)[5m]
p−MET(Y1234/1235)[5m]
p−GSK3A(S21)[15m]
p−SRC(Y527)[5m]
p−RAF(C−)[15m](S259)[15m]
p−STAT5(Y694)[15m]
p−CRKL(Y207)[5m]
p−EGFR(Y1086)[5m]
p−P90RSK(S380)[5m]
p−PKCPAN/G(T514)[5m]
p−FOXO3A(S253)[15m]
p−JAK1(Y1022/1023)[5m]
p−ZAP70(Y319)[15m]/SYK(Y352)[15m]
p−STAT3(Y705)[15m]
p−CDK2(T160)[15m]
p−P70S6K(T421/S424)[15m]
p−EGFR(Y1086)[15m]
p−ERK(T202/Y204)[5m]
−log10(p−value)
4.5
4
3.5
3
2.5
2
1.5
−150
−100
−50
0
50
100
150
Percent inhibition of PP2 on EGF stimulation of specified phosphometric

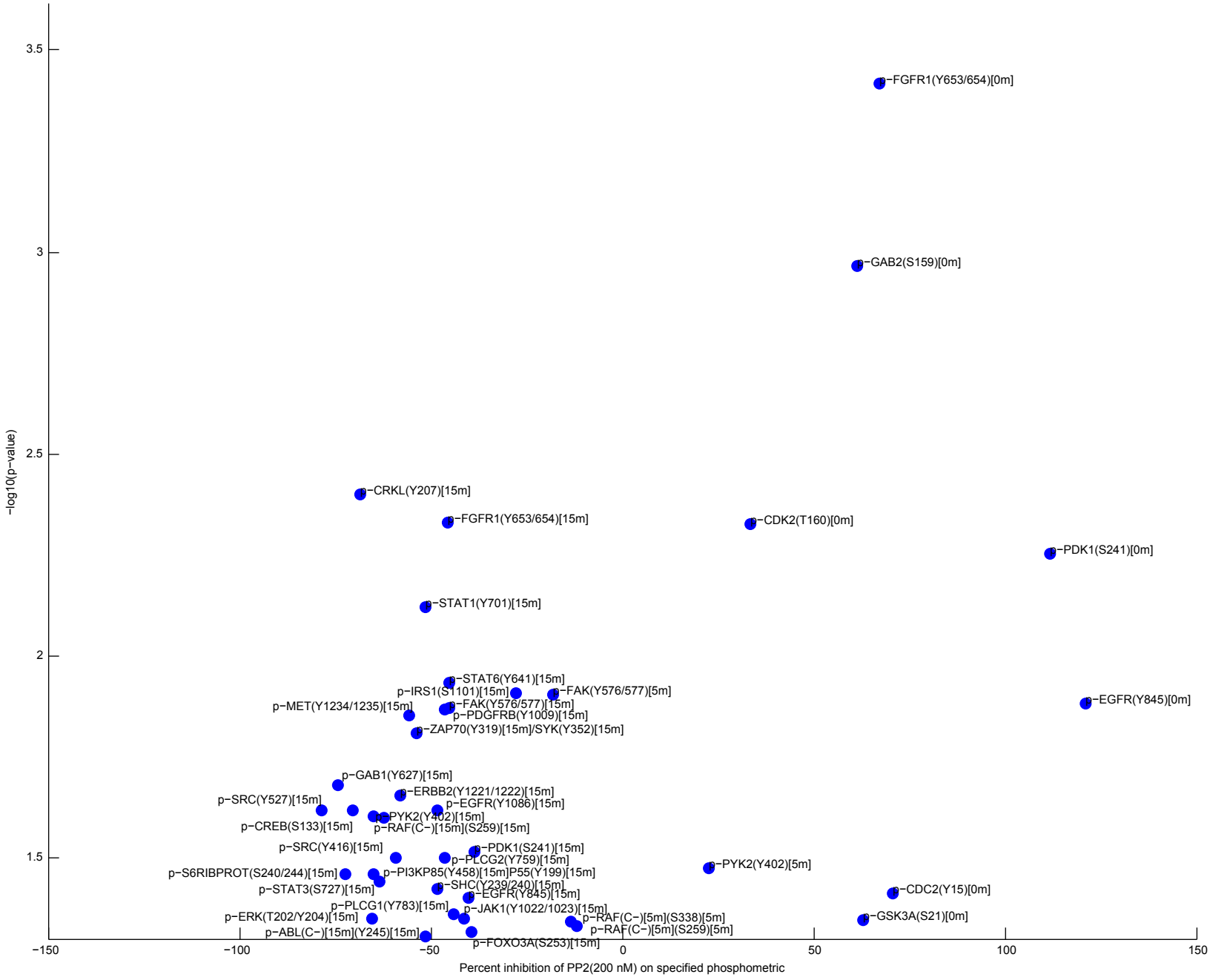
3.5
3
2.5
2
1.5
−log10(p−value)
p−FGFR1(Y653/654)[0m]
p−GAB2(S159)[0m]
p−CRKL(Y207)[15m]
p−FGFR1(Y653/654)[15m]
p−CDK2(T160)[0m]
p−PDK1(S241)[0m]
p−STAT1(Y701)[15m]
p−STAT6(Y641)[15m]
p−IRS1(S1101)[15m]
p−FAK(Y576/577)[5m]
p−EGFR(Y845)[0m]
p−MET(Y1234/1235)[15m]
p−FAK(Y576/577)[15m]
p−PDGFRB(Y1009)[15m]
p−ZAP70(Y319)[15m]/SYK(Y352)[15m]
p−GAB1(Y627)[15m]
p−ERBB2(Y1221/1222)[15m]
p−SRC(Y527)[15m]
p−EGFR(Y1086)[15m]
p−PYK2(Y402)[15m]
p−CREB(S133)[15m]
p−RAF(C−)[15m](S259)[15m]
p−SRC(Y416)[15m]
p−PDK1(S241)[15m]
p−PLCG2(Y759)[15m]
p−PYK2(Y402)[5m]
p−S6RIBPROT(S240/244)[15m]
p−PI3KP85(Y458)[15m]P55(Y199)[15m]
p−STAT3(S727)[15m]
p−SHC(Y239/240)[15m]
p−CDC2(Y15)[0m]
p−EGFR(Y845)[15m]
p−PLCG1(Y783)[15m]
p−JAK1(Y1022/1023)[15m]
p−ERK(T202/Y204)[15m]
p−RAF(C−)[5m](S338)[5m]
p−GSK3A(S21)[0m]
p−ABL(C−)[15m](Y245)[15m]
p−RAF(C−)[5m](S259)[5m]
p−FOXO3A(S253)[15m]
−150
−100
−50
0
50
100
150
Percent inhibition of PP2(200 nM) on specified phosphometric

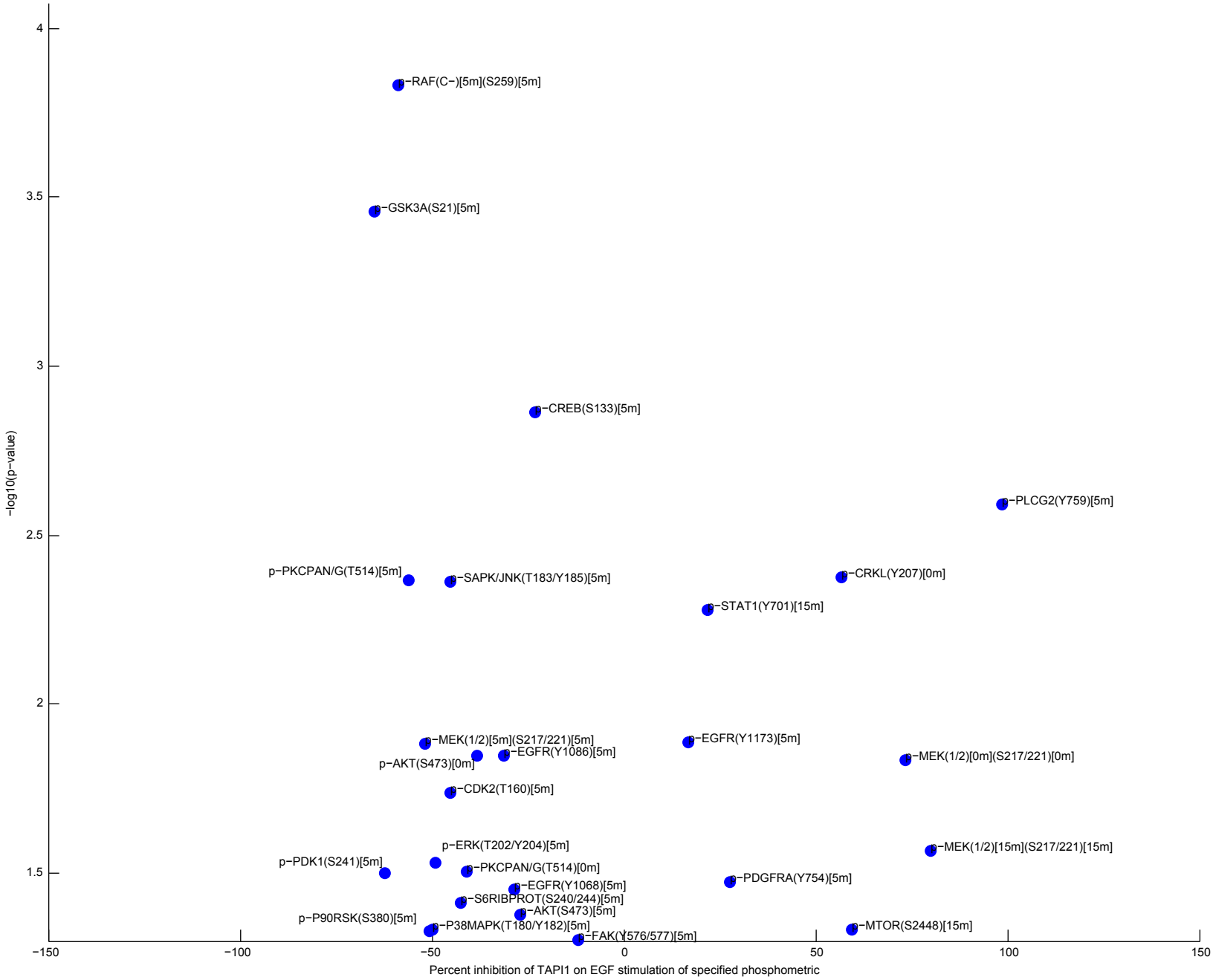
p−RAF(C−)[5m](S259)[5m]
p−GSK3A(S21)[5m]
p−CREB(S133)[5m]
p−PLCG2(Y759)[5m]
p−PKCPAN/G(T514)[5m]
p−SAPK/JNK(T183/Y185)[5m]
p−CRKL(Y207)[0m]
p−STAT1(Y701)[15m]
p−MEK(1/2)[5m](S217/221)[5m]
p−EGFR(Y1173)[5m]
p−EGFR(Y1086)[5m]
p−AKT(S473)[0m]
p−MEK(1/2)[0m](S217/221)[0m]
p−CDK2(T160)[5m]
p−ERK(T202/Y204)[5m]
p−MEK(1/2)[15m](S217/221)[15m]
p−PDK1(S241)[5m]
p−PKCPAN/G(T514)[0m]
p−PDGFRA(Y754)[5m]
p−EGFR(Y1068)[5m]
p−S6RIBPROT(S240/244)[5m]
p−P90RSK(S380)[5m]
p−AKT(S473)[5m]
p−P38MAPK(T180/Y182)[5m]
p−MTOR(S2448)[15m]
p−FAK(Y576/577)[5m]
4
3.5
3
2.5
2
1.5
−log10(p−value)
−150
−100
−50
0
50
100
150
Percent inhibition of TAPI1 on EGF stimulation of specified phosphometric

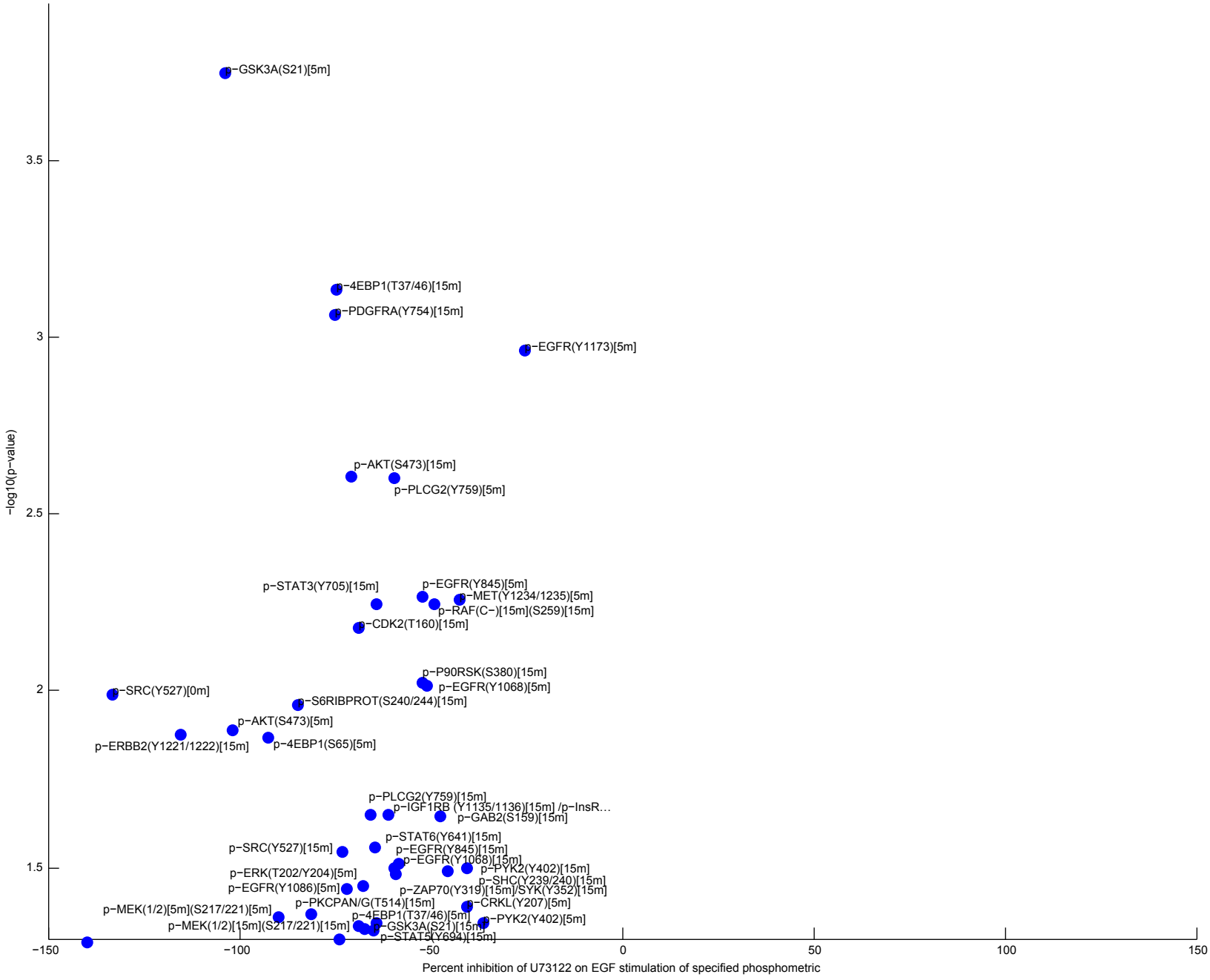
p−GSK3A(S21)[5m]
p−4EBP1(T37/46)[15m]
p−PDGFRA(Y754)[15m]
p−EGFR(Y1173)[5m]
p−AKT(S473)[15m]
p−PLCG2(Y759)[5m]
p−STAT3(Y705)[15m]
p−EGFR(Y845)[5m]
p−MET(Y1234/1235)[5m]
p−RAF(C−)[15m](S259)[15m]
p−CDK2(T160)[15m]
p−P90RSK(S380)[15m]
p−EGFR(Y1068)[5m]
p−SRC(Y527)[0m]
p−S6RIBPROT(S240/244)[15m]
p−AKT(S473)[5m]
p−ERBB2(Y1221/1222)[15m]
p−4EBP1(S65)[5m]
p−PLCG2(Y759)[15m]
p−IGF1RB (Y1135/1136)[15m] /p−InsR…
p−GAB2(S159)[15m]
p−STAT6(Y641)[15m]
p−SRC(Y527)[15m]
p−EGFR(Y845)[15m]
p−EGFR(Y1068)[15m]
p−PYK2(Y402)[15m]
p−ERK(T202/Y204)[5m]
p−SHC(Y239/240)[15m]
p−EGFR(Y1086)[5m]
p−ZAP70(Y319)[15m]/SYK(Y352)[15m]
p−MEK(1/2)[5m](S217/221)[5m]
p−PKCPAN/G(T514)[15m]
p−CRKL(Y207)[5m]
p−4EBP1(T37/46)[5m]
p−PYK2(Y402)[5m]
p−MEK(1/2)[15m](S217/221)[15m]
p−GSK3A(S21)[15m]
p−STAT5(Y694)[15m]
3.5
3
2.5
2
1.5
−log10(p−value)
−150
−100
−50
0
50
100
150
Percent inhibition of U73122 on EGF stimulation of specified phosphometric

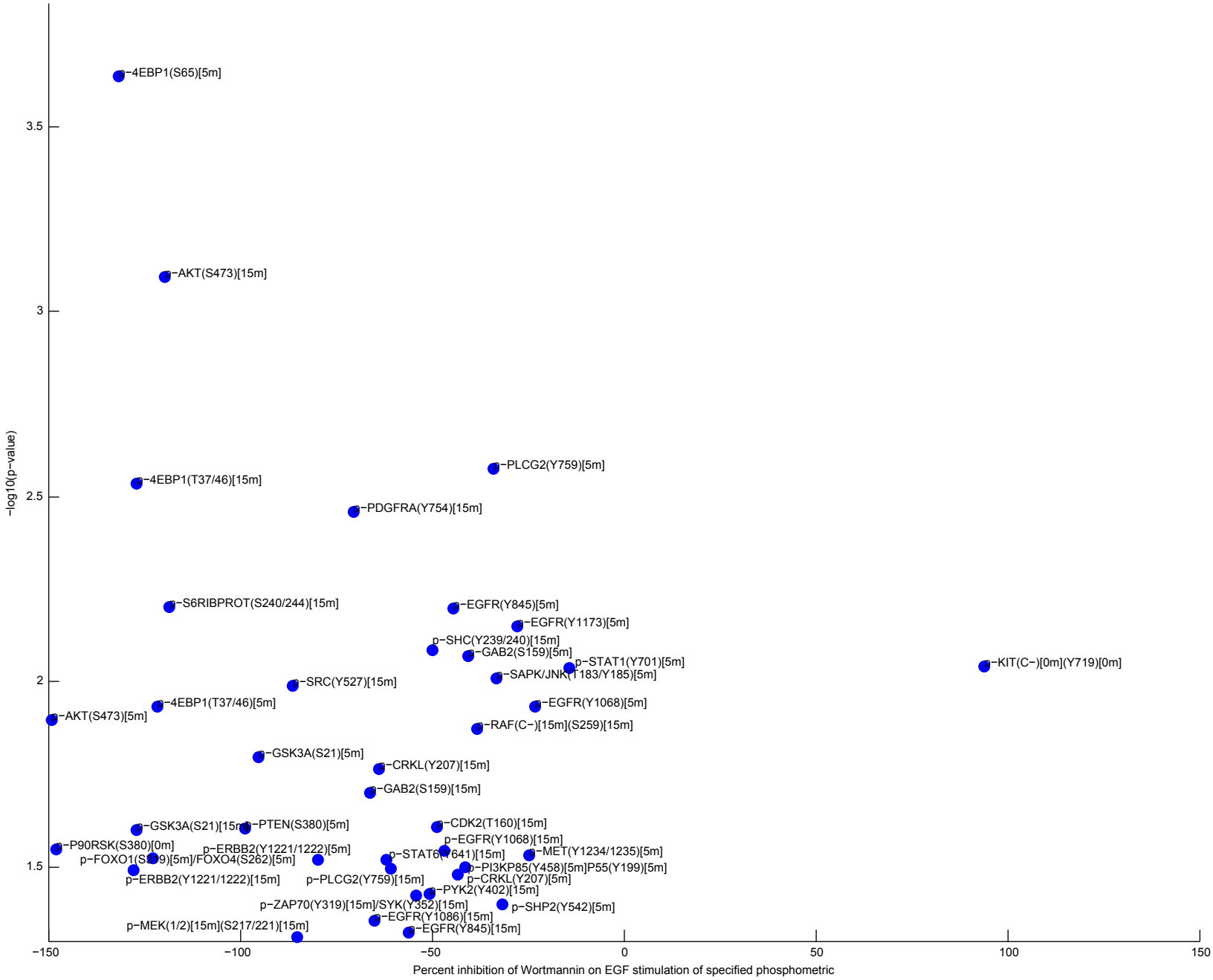
p−4EBP1(S65)[5m]
p−AKT(S473)[15m]
p−PLCG2(Y759)[5m]
p−4EBP1(T37/46)[15m]
p−PDGFRA(Y754)[15m]
p−S6RIBPROT(S240/244)[15m]
p−EGFR(Y845)[5m]
p−EGFR(Y1173)[5m]
p−SHC(Y239/240)[15m]
p−GAB2(S159)[5m]
p−STAT1(Y701)[5m]
p−KIT(C−)[0m](Y719)[0m]
p−SAPK/JNK(T183/Y185)[5m]
p−SRC(Y527)[15m]
p−4EBP1(T37/46)[5m]
p−EGFR(Y1068)[5m]
p−AKT(S473)[5m]
p−RAF(C−)[15m](S259)[15m]
p−GSK3A(S21)[5m]
p−CRKL(Y207)[15m]
p−GAB2(S159)[15m]
p−GSK3A(S21)[15m]
p−PTEN(S380)[5m]
p−CDK2(T160)[15m]
p−EGFR(Y1068)[15m]
p−P90RSK(S380)[0m]
p−ERBB2(Y1221/1222)[5m]
p−MET(Y1234/1235)[5m]
p−FOXO1(S319)[5m]/FOXO4(S262)[5m]
p−STAT6(Y641)[15m]
p−PI3KP85(Y458)[5m]P55(Y199)[5m]
p−ERBB2(Y1221/1222)[15m]
p−PLCG2(Y759)[15m]
p−CRKL(Y207)[5m]
p−PYK2(Y402)[15m]
p−ZAP70(Y319)[15m]/SYK(Y352)[15m]
p−SHP2(Y542)[5m]
p−EGFR(Y1086)[15m]
p−MEK(1/2)[15m](S217/221)[15m]
p−EGFR(Y845)[15m]
−log10(p−value)
3.5
3
2.5
2
1.5
−150
−100
−50
0
50
100
150
Percent inhibition of Wortmannin on EGF stimulation of specified phosphometric

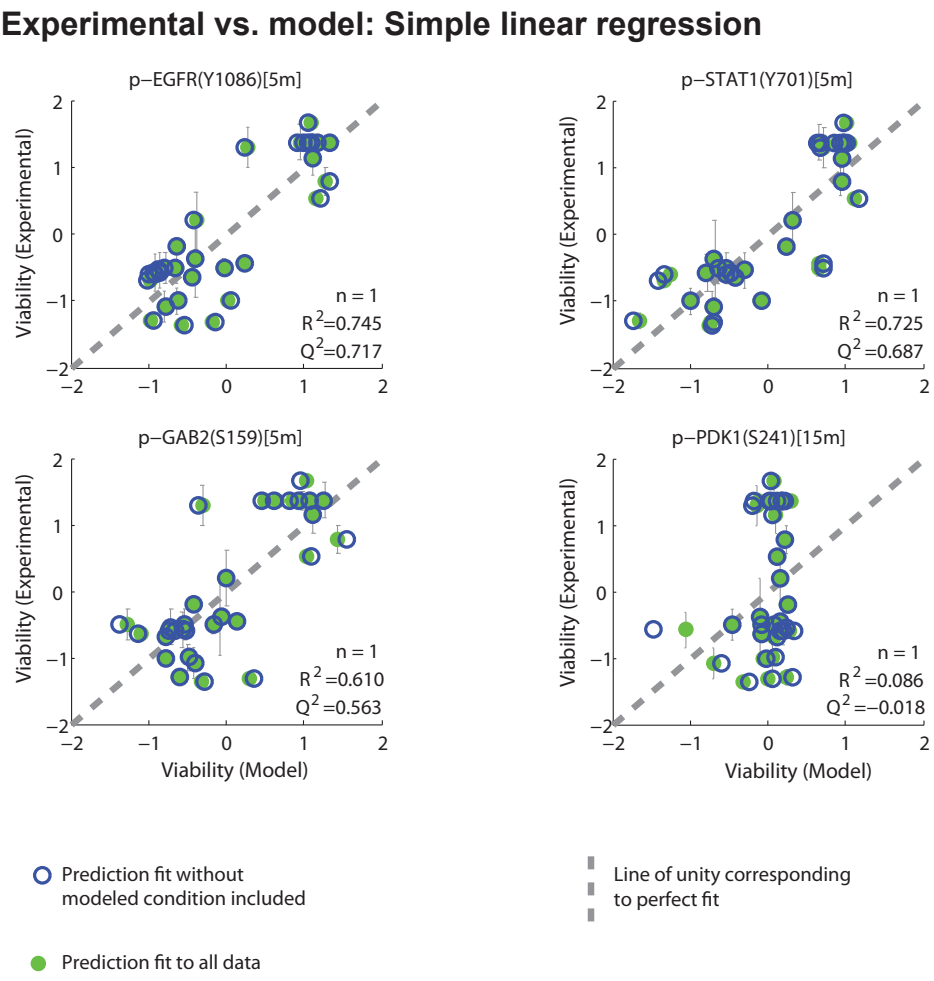

Figure 15: ***Comparison of simple linear regression models.*** *A comparison of simple linear regression models reveals significant predictors for explaining cell viability. The R^2 and Q^2_{LOO} metrics are given for each optimized regression method to quantify its fitness and predictive capacity, respectively. The number of predictors used in each algorithm is depicted by n. Simple least squares regression was implemented using four highly-correlated phosphoprotein signaling metrics. Solid green circles show predicted response for conditions that are trained on the complete data set. Open blue circles show predictions that were trained on data omitting the predicted condition.*

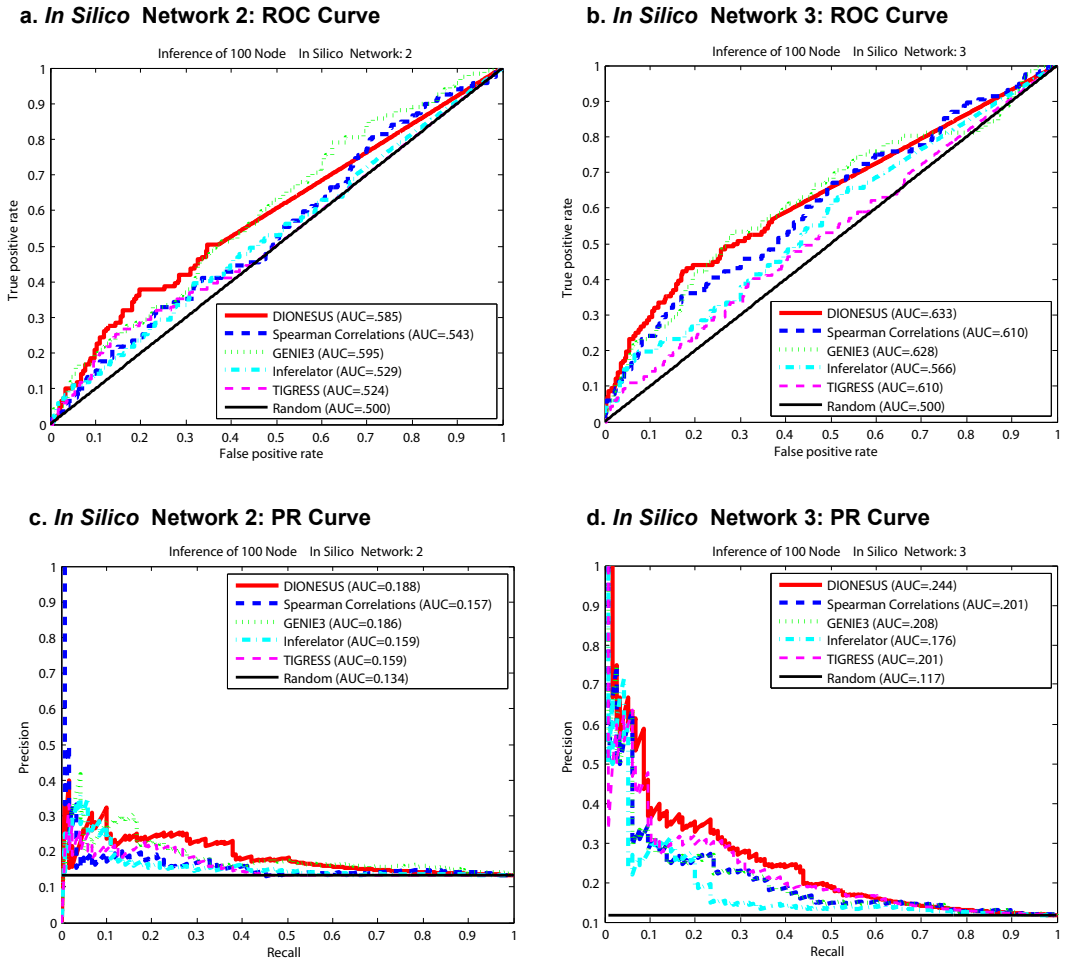

Figure 16: ***DIONESUS accurately reconstructs a signaling network from a kinetic model derived from two one-hundred node in silico networks .*** *(a and b) The receiving-operating characteristic (ROC) curves for DIONESUS and top-performing inference algorithms for the reconstruction of two 100-node in silico network from kinetic time-course data. Higher accuracy of inference corresponds to a higher Area Under the ROC curve (AUROC). (c and d) The precision-recall (PR) curves corresponding to the same analyses displayed in part d are shown. A higher area under the PR curve (AUPR) corresponds to a more accurate algorithm.*

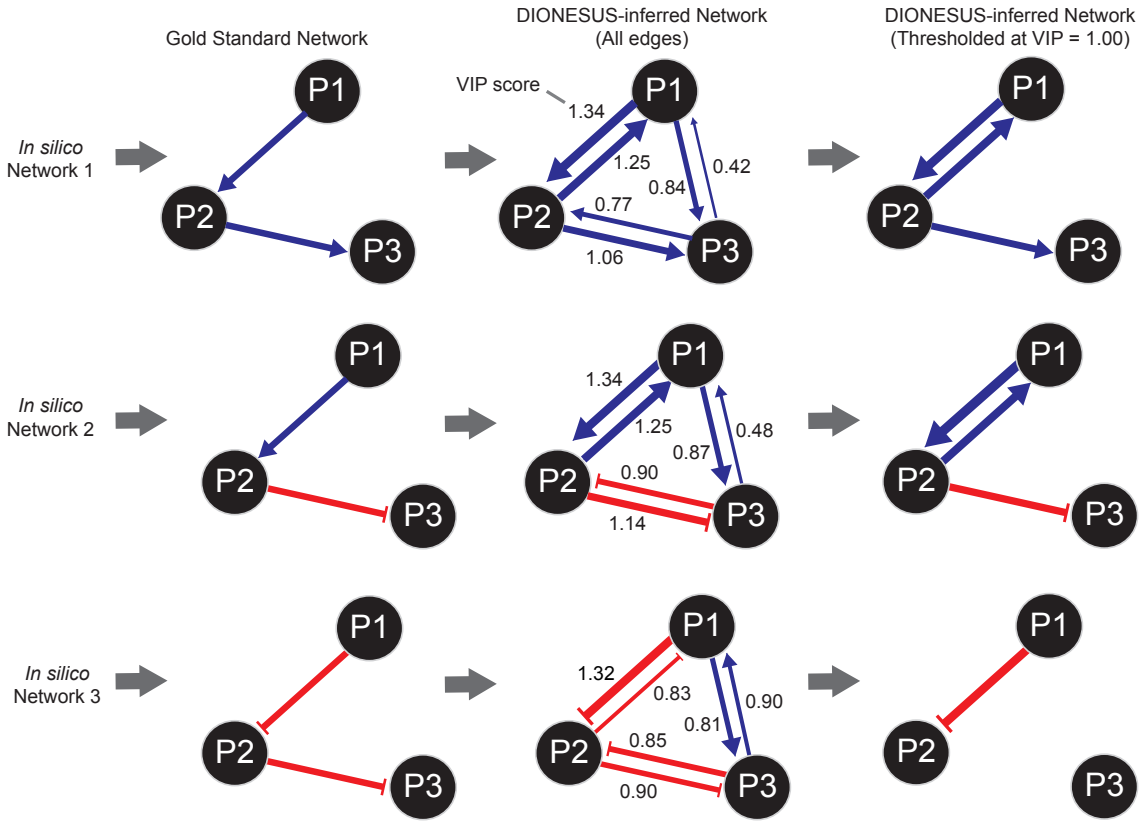

Figure 17: ***Three separate 3-node in silico toy models were constructed using GeneNetWeaver to demonstrate the strengths and limitations of inferring the directionality and the activating or inhibitory nature of each inferred edge using DIONESUS.*** *Each model was created from a linear cascade motif of the structure: P1→P2→P3. While none of these networks were inferred with 100% accuracy, in each case, the algorithm correctly inferred whether each real edge was activating or inhibitory. In addition, the real edges (e.g. P1→P2) always reflected higher confidence (indicated by the VIP score) than the reverse, false positive edge (e.g. P2→P1). Furthermore, the indirect edge from P1→P3 reflected the least confidence and was consistently below the edge threshold in all three examples. Taken together, the DIONESUS algorithm was able to uncover the most salient features of the in silico models.*

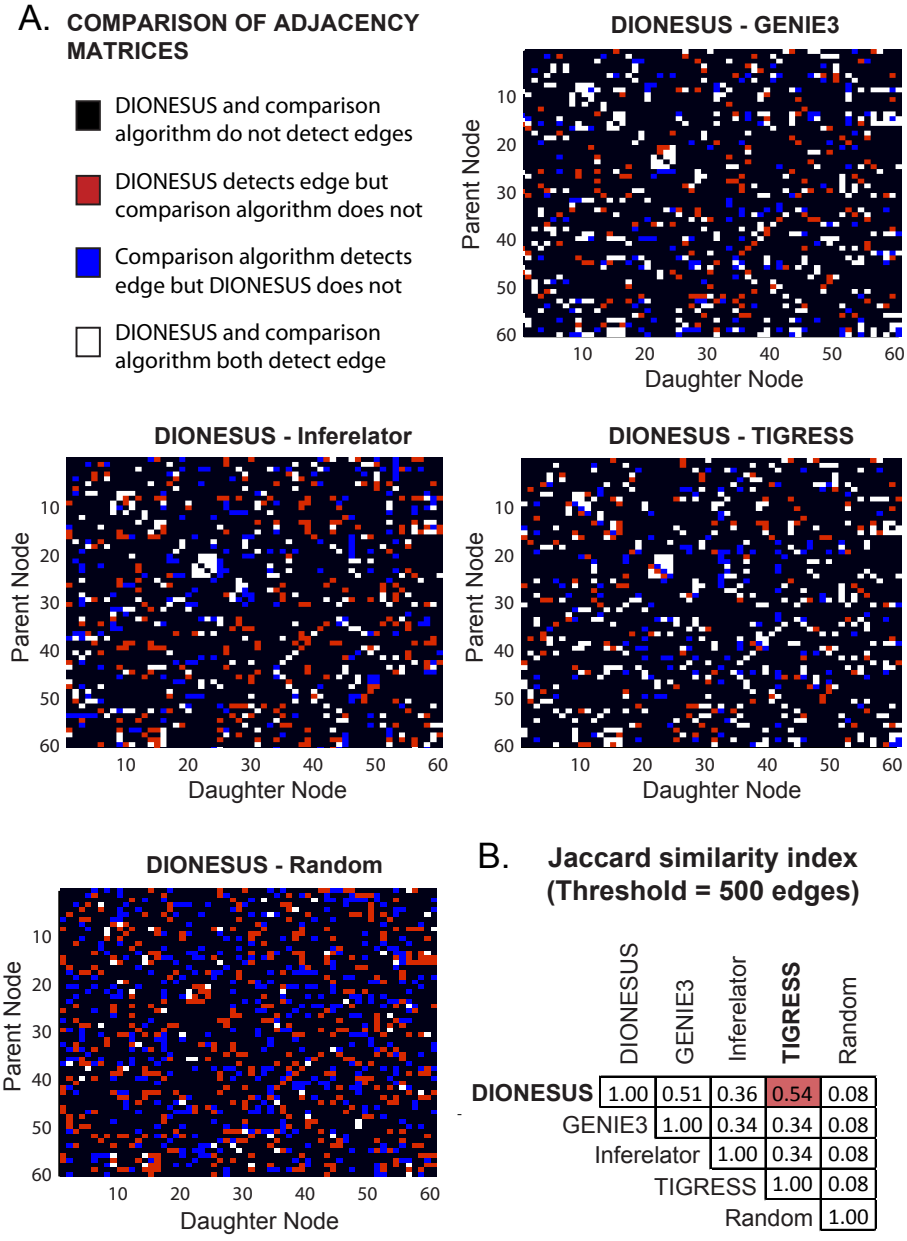

Figure 18: ***DIONESUS performs similarly to top-performing network inference algorithms with a fraction of the computational expense.*** *a) The adjacency matrix between all 60 phosphosites was calculated for the DIONESUS, GENIE3, Inferelator, and TIGRESS algorithms using default parameters. Each algorithm was thresholded at 500 edges to provide a sufficient edge count for comparison. As a negative control, a single random matrix was created by assigning 500 edges with equal probability to each position in the matrix (excluding self-edges). A comparison of the overlap for each adjacency matrix is shown. b) The Jaccard similarity index, a measure of adjacency matrix similarity, between two algorithms are listed in the table. DIONESUS and TIGRESS shared the most edges in common suggesting similar preferences in edge detection.*

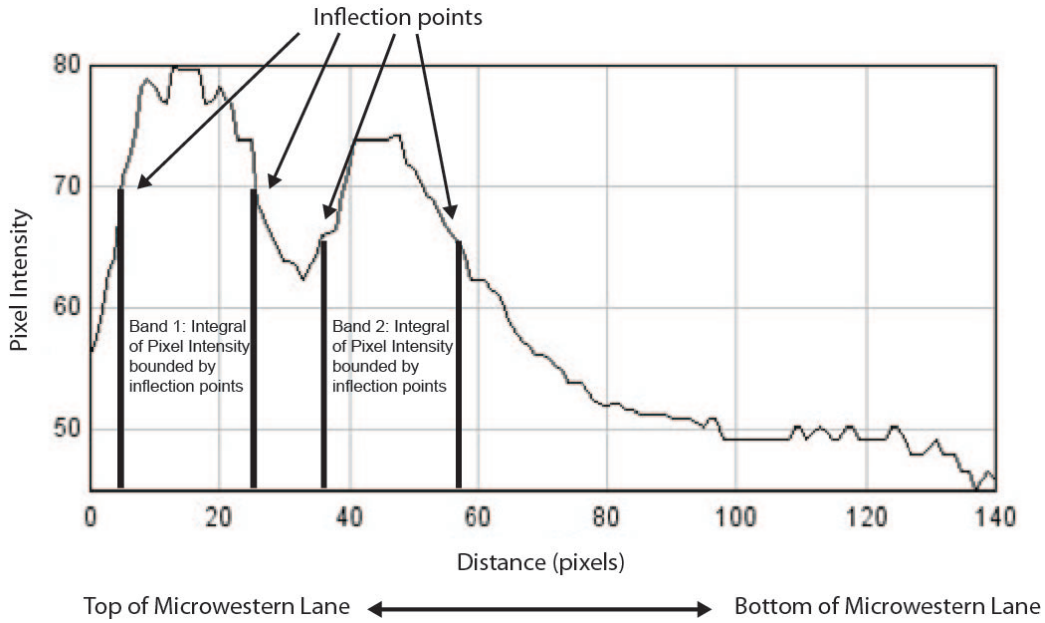

Figure 19: ***ImageJ software was used to quantify microwestern arrays where bands were difficult to differentiate by visual examination.*** *In cases where there were multiple bands in close proximity in a lane of the microwestern array, the intensity of pixels from the top to the bottom of the microwestern lane was assessed using the ImageJ software. A line was manually drawn from the top to the bottom of the lane and the 'Plot Intensity' tool was used to create a plot of the pixel intensity across the length of the line. This figure reflects the microwestern array lane of A431 cell treated with EGF+INS stimulation and blotted with the p-c-MET(Y1349) antibody. The value for each band is the integral of the pixel intensities between inflection points on each side of a peak. This method removes human variability in the quantification of band intensities.*